CAPACITY OF HUMAN OPERATOR USING SMART STICK CONTROLLER

THESIS

Adolfo Cozzone
Captain, USAF

AFIT/GE/ENG/88D-7

DEPARTMENT OF THE AIR FORCE
AIR UNIVERSITY
AIR FORCE INSTITUTE OF TECHNOLOGY

Wright-Patterson Air Force Base, Ohio

CAPACITY OF HUMAN OPERATOR USING SMART STICK CONTROLLER

THESIS

Adolfo Cozzone
Captain, USAF

AFIT/GE/ENG/88D-7

AFIT/GE/ENG/88D-7

CAPACITY OF A HUMAN OPERATOR USING THE SMART STICK CONTROLLER

THESIS

Presented to the Faculty of the School of Engineering
of the Air Force Institute of Technology
Air University
In Partial Fulfillment of the
Requirements for the Degree of
Master of Science in Electrical Engineering

Adolfo Cozzone, B.S.E.E.
Captain, USAF

December 1988

Acknowledgements

A debt of gratitude is owed to my advisor, Major David M. Norman of the Air Force Institute of Technology without whose confidence and constant enthusiasm this work would have not been possible.

A debt of gratitude is also owed to Dr. Repperger, Armstrong Aeronautical Medical Laboratory, who proposed this research topic. His confidence in my work is greatly appreciated. Thanks are also extended to my thesis readers Major Prescott, and Dr. Kabrisky, AFIT.

I am also indebted to Mr. Frazier, Lt. Scarborough, and Amn. Hutton who participated as test subjects for this project, and to Mr. Roark, Raytheon, for maintaining the various computers used for this project.

Finally, I am indebted to my wife [redacted] and my daughters [redacted] without whose patience and cooperation this work would have not been possible.

Adolfo Cozzone

Table of Contents

List of Figures

List of Tables

Abstract

This thesis ~~research~~ provides an analysis of transinformation rate and capacity for six subjects using the smart stick controller. The subjects were tested in both a passive and active stick mode using three different forcing functions. The smart stick controller is an aircraft stick actively controlled by an algorithm developed by the Armstrong Aerospace Medical Research Laboratory (AAMRL) at Wright-Patterson AFB, OH to improve pilot tracking performance. In the passive mode, the stick behaves as any other stick used to control aircraft. However, in the active mode, the stick exerts a force in the direction opposite to the desired motion.

This thesis reviews the literature, develops and analyzes a compensatory tracking task using classical control theory, and applies information theory results to the human quasi-linear model to determine the transinformation rate and capacity of the human operator. Finally, the results for both the active and passive mode are compared. Power spectral densities of the forcing functions, display error, and human response are used to calculate the human transfer function, noise remnant, transinformation rate and capacity. Initial results indicate that there is an increase in the

capacity of the operator between passive and active stick mode. The results indicate that, for four of the six subjects, the capacity increases under all three forcing functions. The highest capacity achieved was 11.34 bits/sec using the stick in the active mode. When information on capacity is used in conjunction with noise remnant, and human transfer function, it is evident that a significant change in performance occurs when the stick is operated in the active mode.

CAPACITY OF A HUMAN OPERATOR USING THE SMART STICK CONTROLLER

I. Introduction

1.1 Background

Modern high performance aircraft place great demands on the operator in terms of precise control of the aircraft while at the same time requiring the pilot to attend to a multitude of other tasks. Additionally, each aircraft has different handling capabilities often requiring the pilot years of practice to master. In an effort to reduce this length of time and increase the efficiency of the human operator in controlling the aircraft, the Armstrong Aerospace Medical Research Laboratory (AAMRL) has performed studies on human performance. The intent was to develop techniques to increase the efficiency of operators in piloting aircraft, and to reduce the time required to learn these skills.

While conducting centrifuge experiments to characterize pilot tracking performance using different stick controllers, AAMRL personnel observed a marked improvement in performance when the G-force acted in the direction

opposite to the desired stick motion. The improvement was attributed to the fact that the force, when directed in the opposite direction of the stick motion, acted as a damping force on the pilot's stick motion which reduced overshoot and increased tracking efficiency. (10:2-3) This observation led to the design of the "smart" stick controller.

In the current configuration, the stick can be operated either in a passive or active (assistive) mode. The smart stick is basically an electro-mechanical device whose characteristics can be controlled by a computer. In the passive mode all forces are supplied by the operator, and the stick behaves as a displacement stick controller. However, in the assistive mode, the stick exerts a force that is proportional to that exerted by the operator but in the opposite direction. The intent is to mimic the conditions that occurred in the centrifuge experiment without subjecting the operator to G-forces. (9:719-721)

Experimental observations indicate that tracking performance is significantly improved using the smart stick in the active mode. However, the reasons for the improvement are not fully understood. Two explanations are offered for this improvement. First, the smart stick provides the operator with additional information. This information is in the form of forces exerted by the computer

controlled hydraulics on the stick. Thus, the operator senses both force feedback from the stick and position feedback by observing the output of the stick on a video monitor. Now, since the operator has more information available, he is able to make more accurate responses than he would make had he only the visual stimuli available. The second reason given is that the forces exerted by the stick in the active mode help dampen forces exerted by the operator, thus preventing large overshoots. These forces then smooth the operator's performance resulting in less error and increased performance.

1.2 Problem Statement

The purpose of this thesis is to develop the information theory needed to support the AAMRL smart stick experiment, and using that theory and experimental apparatus, to measure the capacity of several operators while performing compensatory tracking tasks using the stick in both the passive and assistive mode.

1.3 Scope

This research is part of a larger effort pursed by AAMRL to improve human performance though a combination of information theory and classical control techniques. This thesis is concerned with determining whether the stick,

operated in the assistive mode, improves the information capacity of the human operator.

1.4 Approach

The purpose of this study is to measure the capacity in bits per second of a human operator. To accomplish this task both the bandwidth and signal-to-noise ratio must be determined. Using information theory and appropriate assumptions the information theory model of a human operator performing a compensatory tracking task is developed. The "smart" stick apparatus is used to train and test subjects who will perform the tracking task. Each subject is tested in both the active and passive mode. Since the human operator is the only element where noise is introduced into the system, a change in stick mode should produce a change in performance.

A measure of this noise is used to calculate the operator's capacity using the stick in both the passive and active modes. The passive device will be used to determine a baseline for the human operator. These results will then be compared to those obtained by using the device in the active mode to determine whether the assistive device improves the capacity of the human operator.

1.5 Overview of Remaining Chapters

This report consists of five additional chapters. In Chapter II a brief historical background regarding the evolution of information theory in human performance is explored. Chapter III details the information theory model of the human operator. Chapter IV describes the experimental set up. In Chapter V, the data collected during the experiment is analyzed. A detailed analysis is performed for one subject and the results are tabulated and graphically presented. A summary of the experimental results for all the subjects who participated in the experiment is provided in appendices A through E. Chapter VI contains the conclusion and recommended areas for further research.

II. Background

2.1 Introduction

A branch of psychology called human performance is used to analyze the processes involved in developing skilled performance. It studies how the skills are developed and identifies the factors which may limit skilled performance. The overall objective of this branch of experimental psychology is to predict human performance in specific situations and acting under specialized constraints. More specifically, human performance is devoted to the study of skilled performance. (4:1)

All humans react to external stimuli. However, these reactions can be differentiated by the process which takes place between the time the stimulus is received and the time the response is provided. If the response to a stimulus is automatically generated by the central nervous system without any cognizant action on the part of the subject, then this response is called a reflective action. On the other hand, skilled performance requires that some processing take place. That is, the response is not automatically generated, but the subject analyzes the stimulus and chooses an appropriate response among a number of possible alternatives. (4:1-5)

2.2 Information Processing

Fitts defined Human Performance Theory as the study of how the internal processing of information is accomplished, and how the human central nervous system communicates with the environment. He theorized that there are three tasks performed by the central nervous system to process stimuli. They are the process by which information is transmitted, the process to reduce input information, and the process of elaboration. (4:5)

Of primary importance to this study is the process of information transmission. In this research, a human operator will attempt to manually track an image of a maneuvering aircraft displayed on a video monitor using a stick controller. The task is to reproduce the input stimulus, that is the image of the maneuvering aircraft, as accurately as possible but in a different form (stick movement).

Of equal importance to the study of human performance, but less relevant to this study, is the process of information reduction. This process involves processing the input stimulus, sorting out the superfluous information, and reassembling the information needed to produce a response. Elaboration is the process of generalization. That is, the

human processes the input stimulus and generates a response which contains a greater amount of information than that provided by the input. (10:25-26) As will be seen later, the choice of input stimulus (forcing functions), in part, minimizes this last process, although for a totally different reason.

2.3 Information Theory

The process of human information transmission is similar to that exhibited by a physical communication channel. Both the human and the physical channel accept inputs from outside sources, perform some internal process on the information, and produce specific responses. Therefore, in modelling the performance of a human operator while performing transmission tasks, it is possible to draw some analogies from the physical communication model. (10:26)

Using the analogies from the physical model and drawing from the theories developed by Shannon, one can attempt to answer questions as to the capacity of the human channel, the quantification of the noise introduced by the human operator, and its effects on the capacity of the human channel while performing specific tasks. (11:110-111)

In 1954 Dr. Fitts felt it was possible to use information theory to quantify human performance. He stated

that the information capacity of a human operator performing a tracking task was limited only by the amount of average noise measured over multiple experimental trials. (3:383) The next section addresses some of the more significant work done in trying to quantify human performance in terms of capacity and noise.

2.4 Previous Research

One of the most significant studies pertaining to the calculation of human capacity, in terms of Shannon's theories, was performed by E.R.F.W. Crossman in 1960. In his study, Crossman determined that a human operator performing a tracking task exhibits a capacity of 5 bits per second. (2:15)

However, the problem of determining the amount of noise the human operator introduces during the processing of information still remained unsolved. This was a considerable problem since, in general, noise decreases the capacity of a communication channel. Fitts recognized the significance of quantifying noise and observed that it was possible to experimentally determine the noise associated with different types of tasks. He predicted that the average information capacity per response and the maximum transinformation rate could be calculated from the ratio of the magnitude of the noise to that of the possible range of

responses. (3.382) He also observed that to estimate channel capacity in the case of a continuous signal it was necessary to determine the average power of the noise associated with the output signal. (3:383)

In a compensatory tracking task the human operator is asked to track a signal that is continuously and randomly moving on a display. The objective of the human operator is to track the signal as closely as possible. The difference between the operator's response and the input signal forms the basis for analysis of the noise. This difference is described as the portion of the human operator's output that is not correlated with the input. (6:172) This is essentially the noise or remnant that the human operator injects into the process.

Human operator noise is contributed primarily by the following sources: (3:6-8)

1. Observation noise. This results from the design and location of the display. The display may be difficult to read or poorly positioned. In this case, there is uncertainty in the input observed by the operator and therefore his response is less precise and more noisy.

2. Scanning noise. This type of noise is most prevalent when multiple displays are used. In this case the operator must scan several displays to select the necessary information before making the appropriate response. The

operator has more information available, however, he must sort through it to determine the appropriate response.

3. Equalization noise. This is the dominant noise source in tracking tasks since it is associated with the internal processing the human operator must provide. In tracking tasks, it is the noise generated as a result of the operator recognizing how far and how rapidly the signal is changing and then determining what the reaction should be.

4. Crosstalk noise. This type of noise is associated with tracking tasks where a response can be multi-dimensional. This is minimized in this study since the range of motions are restricted to only one axis.

5. Neuromuscular noise. This is usually a direct result of the physiological interactions between the nerves and muscles required to provide motion. The effect becomes more pronounced when the amplitude of the required motion is larger and when the changes in direction are more frequent.

Although the different noise sources are well defined, it is impossible to accurately predict their individual effects on capacity. Therefore, Levison and others have modelled human operator noise as a single, lumped noise process. This is based on the assumptions that the noise sources are independent from one another and are modelled as additive white Gaussian noise processes. (6:174)

Levison provided the model and theoretical foundation (using spectral analysis) for predicting human operator noise and verified experimentally that the model was valid for a one-dimensional tracking task.

Sheridan and Ferrell, using the model provided by Levison, performed an information theory analysis to quantify human performance. The results were consistent with those obtained by Crossman, Fitts, and Levison. (10:135-160)

III. Theory

3.1 Introduction

In this chapter, the theoretical analysis is developed for determining the capacity of the human operator while performing a compensatory tracking task. Classical control theory analysis and information theory techniques are applied to the model developed by Elkind and Sprague to determine the transinformation rate and capacity of the operator. (4:58-60)

3.2 Model of the Compensatory Tracking Task

The purpose of the study is to quantify, in terms of transinformation rate and capacity, the performance of a human operator performing a tracking task, under passive and active stick operation. Figure 3.1 shows a classical control theory block diagram for this type of task.

In a compensatory tracking task, the objective is to track the motion of the simulated target (forcing function) as accurately as possible. In this type of task the human operator does not observe the actual motion associated with the forcing function, but sees the difference, or error signal, between the input function and his response (system output). The forcing function is made up of a sum of sinusoids.

density (PSD) from that of the signal in the non-linear process depicted in Figure 2. However, by restricting the class of inputs to random sinusoids, it is possible to analyze the human operator as quasi-linear model and measure the signal and noise PSDs. (7:7)

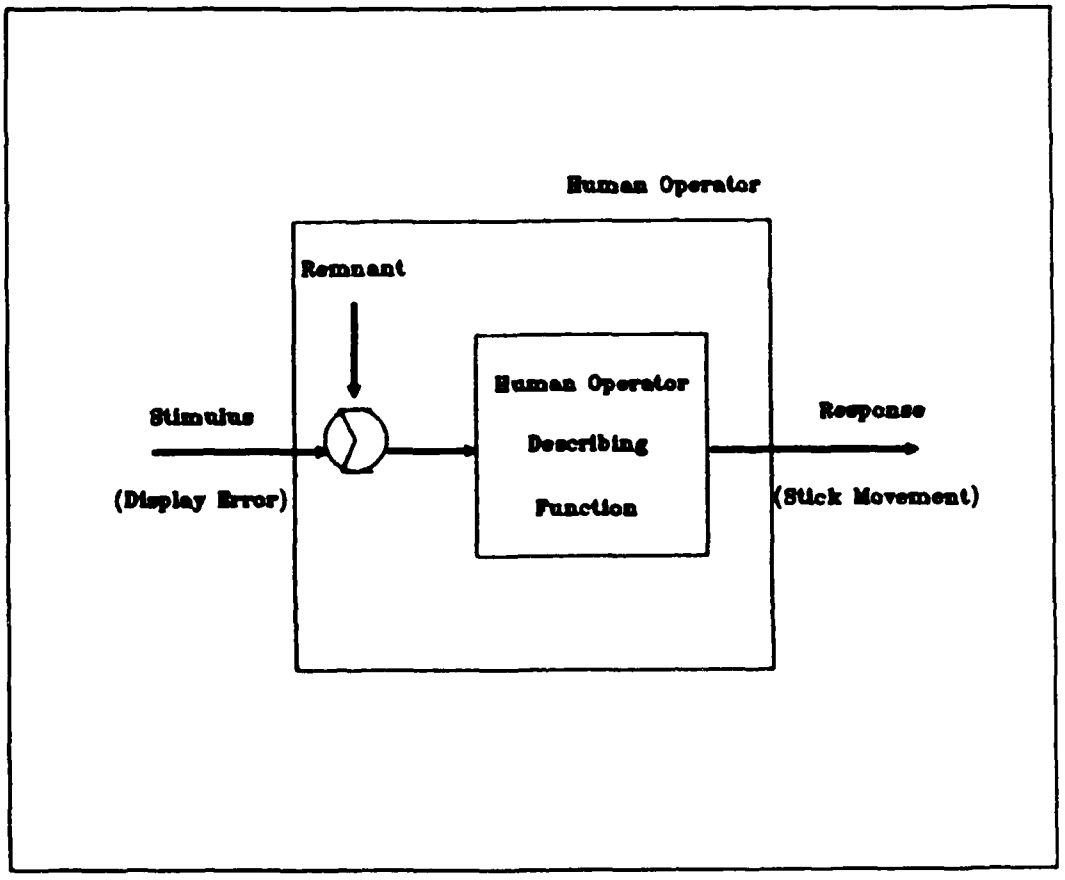

Figure 2. Model for Human Operator

Therefore, if the input forcing function r(t) is defined as

$$r(t) = \sum_n A_n \sin(n w_o + \phi_n) \qquad (1)$$

where

n is an integer from a set of relatively prime numbers

A_n = Amplitude of sinusoid associated with specific n

ϕ_n = Uniformly distributed (0-2π) random phase

w_o = Fundamental frequency (radian/second)

the frequency domain representation is a discrete sum of impulse functions.

$$R(w) = \sum_n \delta(w - n w_o) \exp(j\phi_n) \qquad (2)$$

In effect, the input power is concentrated at selected frequencies, and any power that is measured at any frequency other than the original input frequencies must be noise that the human operator injects into the task. (7:7)

As explained in the Chapter II, noise actually results from many different sources; however, it can adequately be modeled as additive white Gaussian. (6:102) Figure 3 shows a further refinement of the model used in this study.

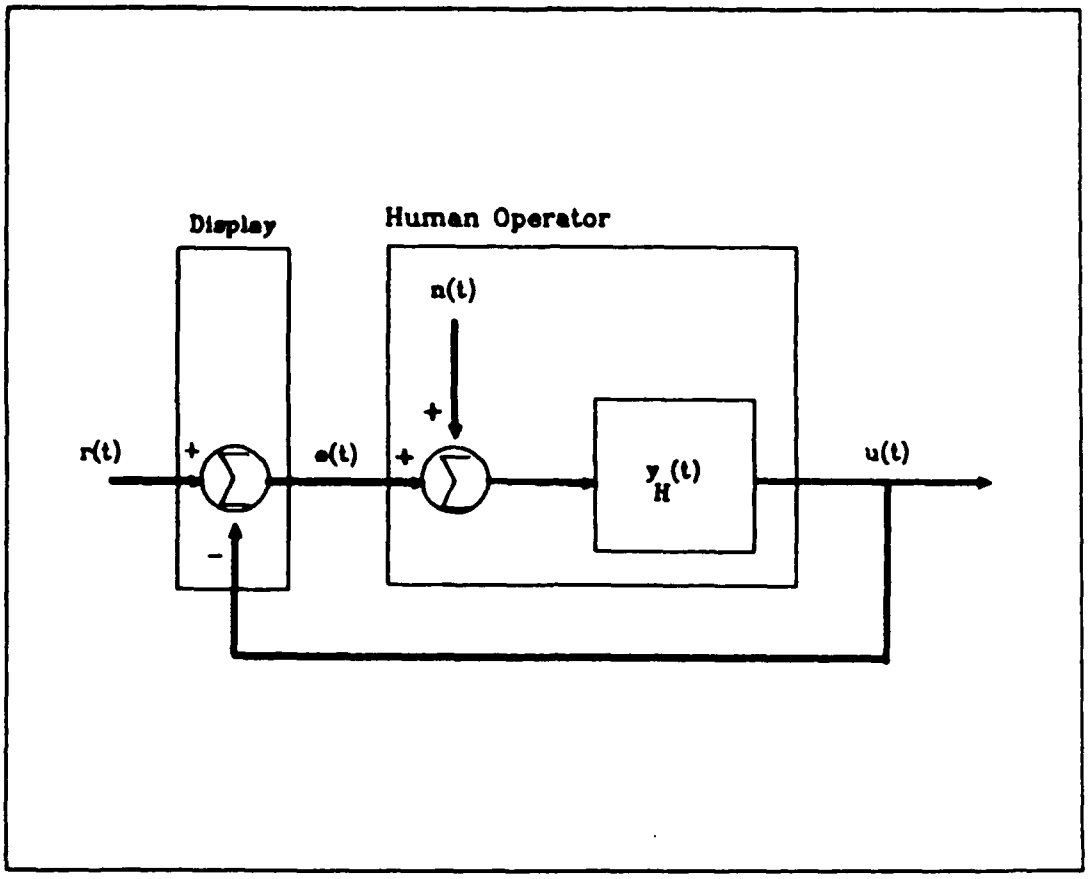

Figure 3. Revised Model for Compensatory Control System

where

r(t) = Forcing function

e(t) = Display error

n(t) = Noise or human operator remnant

$y_H(t)$ = Human operator describing function

u(t) = Human operator response (stick position)

3.3 Frequency Domain Analysis of the Compensatory Control System

In this study the analysis is performed in the frequency domain and is a combination of the techniques used by Sheridan and Ferrell (10:207-223) and Levison (6:102-104). The power spectral densities of the various signals shown in Figure 3 are determined. The power spectral density (PSD) of the forcing function, $\Phi_{rr}(w)$, is defined as the Fourier transform of the autocorrelation of the forcing function. Therefore, the PSD of the forcing function is

$$\Phi_{rr}(w) = \lim_{T\to\infty} \frac{1}{2T} \int_{-\infty}^{\infty} R(w) \cdot R(-w)\ dw \qquad (3)$$

However, if we restrict this integral to a small frequency band, dw, (an infinitesimally small bandwidth about each spectral line) then this expression becomes

$$\Phi_{rr}(w) = \lim_{T\to\infty} \frac{1}{2T} [R(w) \cdot R(-w)] \qquad (4)$$

Similarly, the PSD of the noise and the error signals are defined as

$$\Phi_{nn}(w) = \lim_{T\to\infty} \frac{1}{2T} [N(w) \cdot N(-w)] \qquad (5)$$

$$\Phi_{ee}(w) = \lim_{T\to\infty} \frac{1}{2T} [E(w)\cdot E(-w)] \qquad (6)$$

Note, however, that $E(w)$ can be written as

$$E(w) = R(w) - U(w) \qquad (7)$$

Also

$$U(w) = [E(w) + N(w)]\cdot Y_H(w) \qquad (8)$$

Therefore E(w) becomes

$$E(w) = \frac{1}{1 + Y_H(w)} [R(w) - Y_H(w)\cdot N(w)] \qquad (9)$$

Using Eq. 9 and the assumption that the noise is uncorrelated with the forcing function, the PSD for the display error can be rewritten as

$$\Phi_{ee}(w) = \left|\frac{1}{1 + Y_H(w)}\right|^2 \Phi_{rr}(w) + \left|\frac{Y_H(w)}{1+ Y_H(w)}\right|^2 \Phi_{nn}(w) \qquad (10)$$

Applying the same technique to U(w), the PSD of the human operator response becomes

$$\Phi_{uu}(w) = \left|\frac{Y_H(w)}{1 + Y_H(w)}\right|^2 \Phi_{rr}(w) + \left|\frac{Y_H(w)}{1 + Y_H(w)}\right|^2 \Phi_{nn}(w) \qquad (11)$$

The first term in both Eq. 10 and Eq. 11 represents the amount of power in the output that is correlated with the forcing function, while the second term represents the uncorrelated, or noise, power in the PSDs. Therefore, the PSD of the output can be written as

$$\Phi_{uu}(w) = \Phi_{uuc}(w) + \Phi_{uun}(w) \qquad (12)$$

where $\Phi_{uuc}(w)$ is the portion of the output correlated with the input and $\Phi_{uun}(w)$ uncorrelated portion.

$$\Phi_{uuc}(w) = \left|\frac{Y_H(w)}{1 + Y_H(w)}\right|^2 \cdot \Phi_{rr}(w) \qquad (13)$$

and

$$\Phi_{uun}(w) = \left|\frac{Y_H(w)}{1 + Y_H(w)}\right|^2 \cdot \Phi_{nn}(w) \qquad (14)$$

The PSD of the noise process can now be determined from Eq. 13 and Eq. 14 as

$$\Phi_{nn}(w) = \frac{\Phi_{uun}(w)}{\Phi_{uuc}(w)} \cdot \Phi_{rr}(w) \qquad (15)$$

The last component required to totally characterize the model is $Y_H(w)$. This can be expressed as the ratio of the correlated part of the human response to the correlated portion of the display error.

$$\left| Y_H(w) \right|^2 = \frac{\Phi_{uuc}(w)}{\Phi_{eec}(w)} \qquad (16)$$

3.4 Capacity of The Human Channel

The results derived this far will now be used to calculate the transinformation rate and the capacity of the human operator. As discussed in Chapter II, the analogy of the human operator and the information channel is appropriate since the human operator is continuously receiving and processing information in response to stimuli. The task is to quantify the relationship between the stimulus and response using information theory.

The most common representation of an information channel is illustrated in Figure 4 on the next page.

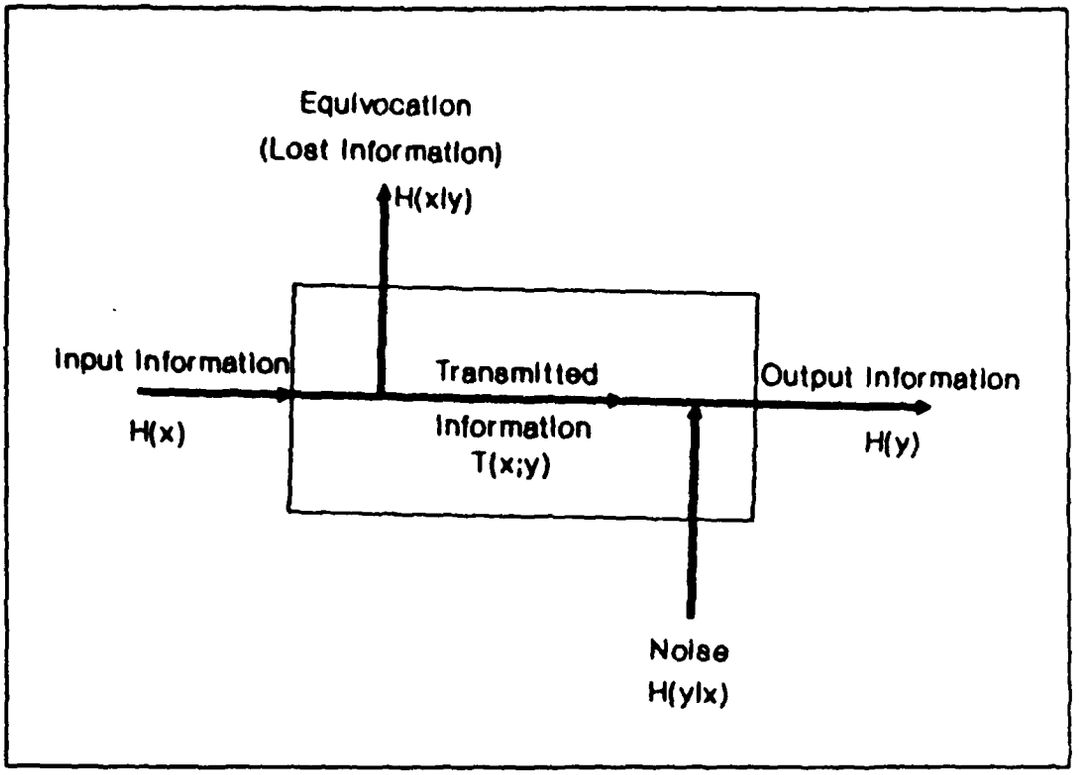

Figure 4. Diagram of an Information Channel (11:67)

The basic operation of the channel is to pass, as accurately as possible, information from the input to the output. If the received information is not an accurate representation of the transmitted signal, then either information was lost or noise was introduced in the process. Information theory measurements have their basis in entropy calculations. Entropy is defined as the amount of information (bits) contained in a signal. The signals under study are actually random waveforms. Therefore, the entropy, viewed as the

uncertainty of the waveform, is related to the probability density function of the random waveform. If the input signal is a random variable X, then the information contained in the input is the entropy of X.
For a continuous channel the entropy of the input, H(X), is defined as

$$H(X) = -\int f(x) \cdot \log_2 f(x) \quad dx \tag{17}$$

where f(x) is the probability density function of the input waveform. Similarly, the output information is defined as the entropy of the output waveform, Y, and can be determined by

$$H(Y) = -\int f(y) \cdot \log_2 f(y) \; dy \tag{18}$$

where f(y) is the probability density function of the random output waveform. If the human operator is considered as a perfect channel (no noise and no equivocation) then

$$H(X) = H(Y)$$

Noise, $H(Y|X)$, represents the entropy in the output from the perspective of the transmitter (channel input). It is defined as the uncertainty of what was actually received given that a specific stimulus was transmitted.

Noise can be determined as follows (1:58)

$$H(Y|X) = -\int f(y|x)\cdot\log_2 f(y|x)\ dy \qquad (19)$$

The transinformation, T(X;Y), represents the information actually received at the output. It is the difference between the information content of the input stimulus and the information lost in the channel and is represented as

$$T(X;Y) = H(X) - H(X|Y) \qquad (20)$$

Since the transinformation is symmetric (1:149-150), Eq. 18 can be rewritten as

$$T(Y;X) = H(Y) - H(Y|X) \qquad (21)$$

With these information theory terms defined, we now move to the specific analysis of the compensatory tracking task shown in Figure 3. Since the noise process, n(t), is assumed to be an additive white gaussian noise (AWGN) process and the forcing function, r(t), is the sum of 15 sinusoids with random phases, the analysis for the transinformation is greatly simplified. The random phases are selected prior to each tracking task and are not changed

during trial. Therefore, the forcing function is actually deterministic for each trial. Also, since the human operator describing function is linear, it does not add any noise to the process. As a result, not only is n(t) an AWGN process, but so is the operator response, u(t).

Using Eq. 19, the transinformation can be calculated as follows

$$T[u(t);e(t)] = H[u(t)] - H[u(t)|e(t)] \tag{22}$$

The second term in the expression is a property of the channel and is defined as the noise information rate. (10:140-141) Because n(t) is an AWGN process, it can be written as

$$H[u(t)|e(t)] = \log_2[2\pi\ N_u(w)] \tag{23}$$

where $N_u(w)$ is the total noise measured at the receiver and is defined as

$$N_u(w) = \left| Y_H(w) \right|^2 \Phi_{nn}(w) \tag{24}$$

To maximize the transmission rate requires maximizing the entropy which can be determined from its PSD (1:247), and can be written as

$$H[u(t)] = \log_2\{2\pi[S_u(w) + N_u(w)]\} \tag{25}$$

where

$S_u(w)$ = Portion of $\Phi_{uu}(w)$ correlated with the forcing function

Substituting Eqs. 21 and 23 into Eq. 20 yields

$$T[u(t);e(t)] = \log_2 \frac{S_u(w) + N_u(w)}{N_u(w)} \tag{26}$$

Since the human operator is considered a continuous channel, the capacity, C, can be calculated by integrating the transinformation rate over all usable frequencies.

$$C = \max \int_w \log_2 \frac{S_u(w) + N_u(w)}{N_u(w)} \, dw \tag{27}$$

However, due to the discrete nature of the PSDs, the integration can be replaced by a summation.

Therefore, the capacity of the human operator (in bits/sec) is given by

$$C = \frac{1}{2\pi} \sum_n T(w_n) \tag{28}$$

where 2π radians is constant of proportionality to convert from radian frequency and insure the capacity is given in bits/sec.

IV. Methods of Testing

4.1 Introduction

This chapter describes the experimental apparatus and data gathering techniques used throughout the experiment.

Experiments were conducted to determine the capacity of the human operator using the stick in both the passive and active modes. The subjects were provided with a single axis lateral (side to side) compensatory tracking task. The input forcing function minus the plant output was displayed on a video monitor. The plant was unity gain and its input was the subject's stick output.

4.2 Experimental Hardware

4.2.1 Computers. An Electronic Associate, Inc. 680 analog computer was used to drive the display units and compute the root mean squared system errors. An SEL 32/77 digital computer was used to generate the forcing functions and convert analog data to digital formats for storage on a 9-track, 800 bpi magnetic tape recorder. A DEC PDP-1134 computer generated the data projections that were displayed on the monitor.

4.2.2 Chair. The subject's chair was an F-4 fighter aircraft ejection seat located in room 104 of the Armstrong Aerospace Medical Research Laboratory, Wright- Patterson AFB, OH. The chair was equipped with an arm rest so as not

to put undue strain on the subject's arm. The stick could be accurately manipulated using only hand and wrist motion.

4.2.3 Display. The subject was provided with a Panasonic Model TR-930U video display placed approximately 50 inches away. Display brightness and contrast levels were adjusted for maximum viewing comfort, and a constant level of room lighting was maintained throughout the data collection period.

The image produced on the display unit, and illustrated in figure 4.1, was that of an aft view of a maneuvering aircraft. The aircraft only moved in the horizontal direction. The movement was controlled by the difference signal between the forcing function and the operator's output. The subject's task was to minimize the distance of the maneuvering aircraft from an image of a gun sight.

4.2.4 Control. The control stick was the primary device through which the subject interfaced with the information displayed on the video monitor. The stick was used in both the passive and the active mode. In the passive mode, the stick behaved as any other passive controller where the force was provided entirely by the operator. In this mode, the stick moves with negligible force and is called a displacement stick. In the active mode, the stick produced resistive forces on the subject's

hand which were a function of the operator output. In the active mode, the sick requires substantially more force and is referred to as a force stick. The stick was allowed to move freely in the horizontal axis for all the data runs.

A transducer provided electrical outputs proportional to the horizontal displacements as measured by the rotational potentiometer located in the base of the stick. The outputs were sampled and recorded on magnetic tape and were the basis for the calculations.

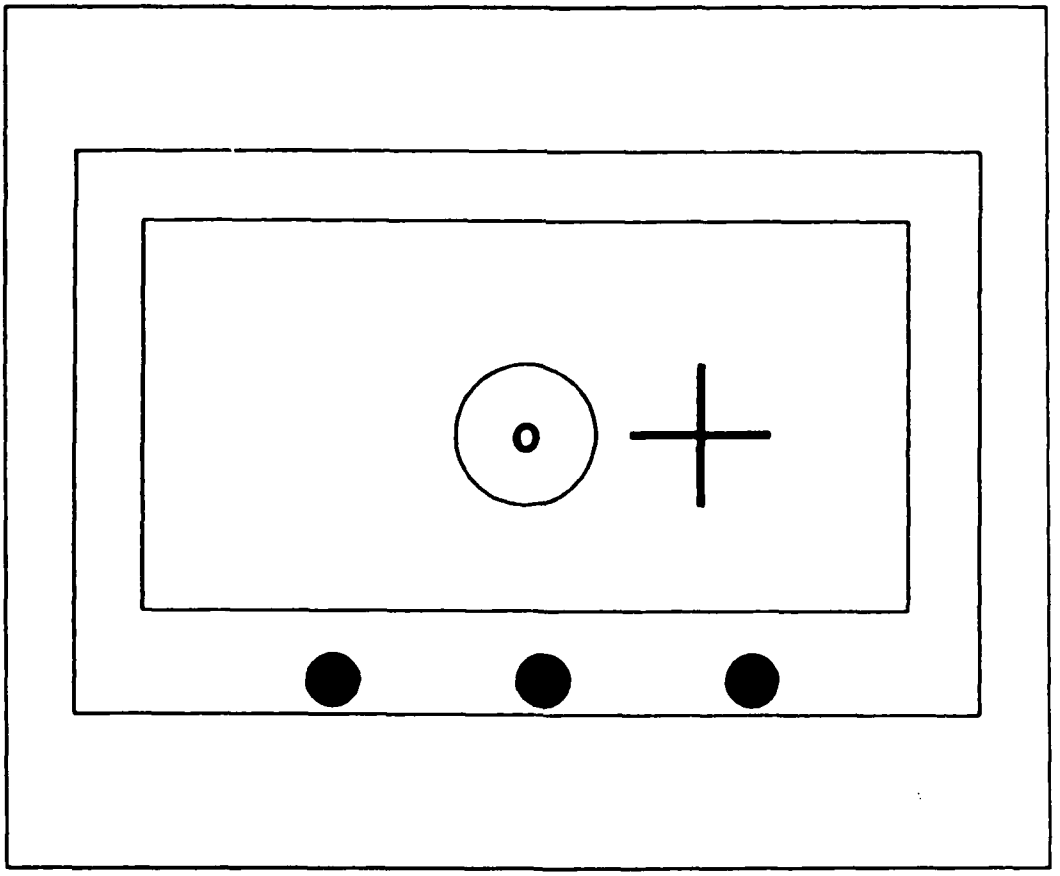

Figure 5. Video Display Unit

4.3 Forcing Functions

Three forcing functions were used during this experiment. To insure stationarity in the overall experiment, the class of forcing functions used was restricted to functions which exhibited stationary characteristics. (7:12) Moreover, the forcing functions had to appear to the subjects as random processes, otherwise the subjects could detect and learn to anticipate the deterministic nature of the input forcing function.

Both stationarity and randomness were satisfied by using forcing functions consisting of sums of sinusoids. It was determined that a forcing function of at least five sinusoids was sufficient to cause the subjects to view the forcing functions as random processes. (10:62)

In this experiment, each forcing function was a sum of fifteen sinusoids, each with a random initial phase which provided for random appearing signals. Forcing Function #1 (FF #1) was generated by processing this sum of sinusoids through a second-order Butterworth filter with a cutoff frequency of 1 Hz. Forcing Function #2 (FF #2) was generated by processing the same sinusoids through a second-order Butterworth filter with a cutoff frequency of 2 Hz. The third forcing function (FF #3) was generated by processing the sum of sinusoids through a Gaussian filter with a 1 Hz cutoff frequency. To insure orthogonality among

the fifteen component frequencies, the measurement time interval of 81.96 seconds contained an integral number of cycles of each component. Thus, each component was a harmonic of the fundamental frequency w_o

$$w_o = 2\pi/T = .07666 \qquad (29)$$

Therefore each forcing function was of the form

$$f(t) = \sum_n A_n \sin(w_n t + \phi_n) \qquad (30)$$

where

$w_n = k_n w_o$

k_n is an integer from a set of relatively prime numbers

A_n are the amplitudes for each component

ϕ_n are the initial phases

Figure 6 shows the frequency response of three forcing functions used for this experiment.

The initial phase shifts associated with each component were randomly selected from a uniform distribution between 0 and 2π to insure the subjects could not predict the tracking tasks. The randomness of the phases between each frequency also prevented large positive or negative swings. As previously stated, the individual frequencies of the forcing functions were made up of relatively prime numbers insuring

that there could never be any periodicity which the subjects could recognize and learn to anticipate.

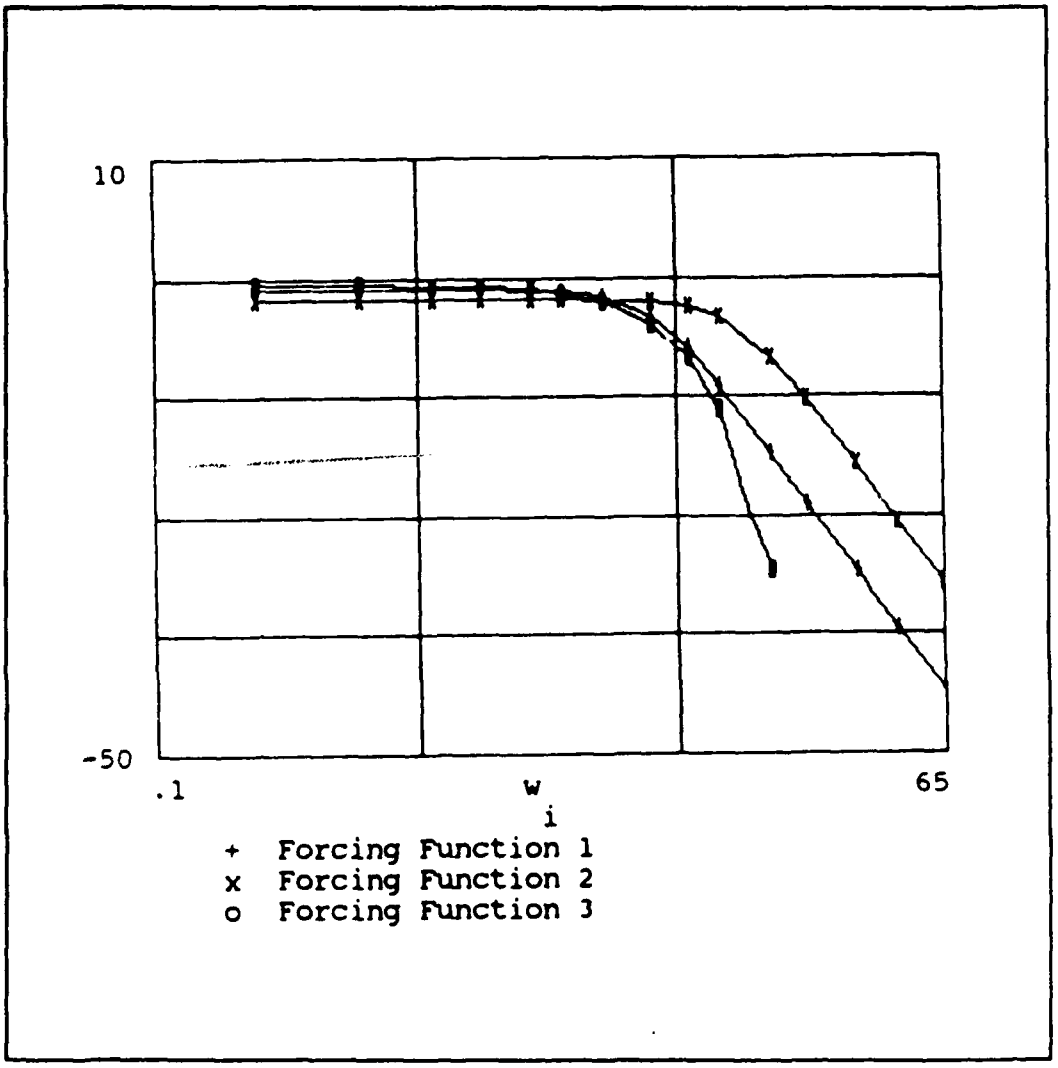

Figure 6. Forcing Functions Used in the Experiment

The amplitudes of each of the forcing functions were scaled so that all three forcing functions had equal power

and produced the same displacement on the display. The total input power for each forcing function was approximately 3.7 watts. Table 1 shows the approximate frequencies in radians/sec, the number of harmonics, and amplitudes for each forcing function number.

TABLE 1. FORCING FUNCTION DESIGN

Sinusoid Number	Harmonic $w_i = nw_o$	Frequency (rad/sec)	Amplitude (volts)		
			FF #1	FF #2	FF #3
1	3	0.230	0.979	0.867	1.035
2	7	0.537	0.979	0.867	1.032
3	13	0.997	0.979	0.867	1.022
4	19	1.457	0.978	0.867	1.008
5	29	2.224	0.971	0.867	0.973
6	37	2.838	0.959	0.866	0.935
7	53	4.065	0.903	0.863	0.840
8	79	6.059	0.717	0.845	0.650
9	107	8.207	0.495	0.798	0.441
10	139	10.661	0.321	0.704	0.245
11	211	16.184	0.146	0.448	0.038
12	283	21.706	0.082	0.276	0.003
13	419	32.137	0.037	0.131	0.001
14	58	45.022	0.019	0.067	0.001
15	839	64.351	0.009	0.033	0.001

4.4 Training and Experimental Procedures

4.4.1 Subjects. Six subjects participated in this study. All, by virtue of their profession, were assumed to possess good eyesight and a fairly reasonable ability for manual control. Three of the subjects had participated in similar experiments and had prior experience with the stick control characteristics. The remaining three subjects were novices with regard to the stick control. None of the subjects had prior experiences with the forcing functions used in this experiment.

4.4.2 Instructions. The subjects were instructed to minimize the distance of the maneuvering aircraft from the center of the gun sight displayed on the screen. This, in turn, minimized mean-squared errors. After each run their score was posted on the CRT display.

4.4.3 Run Length. All training and testing runs lasted 81.96 seconds with a 2 minute rest period between each run. Each session consisted of 9 runs (3 for each forcing function) and lasted approximately 40 minutes.

4.4.4 Training. To minimize variability due to practice effects, each subject was trained to a stable level of performance. This meant that each subject participated in at least four sessions. Two subjects required one additional session to insure that their scores had leveled off, indicating they were not still in the learning mode.

After each session the scores were analyzed to determine if the subjects had reached the trained level. If the subjects were not showing substantial changes in error scores over the last three days, they were considered trained. The data was recorded during every session. However, the subjects were unaware of which day's data was to be used for analysis. This prevented additional strain which might have affected their performance. Figure 7 shows a typical proficiency curve.

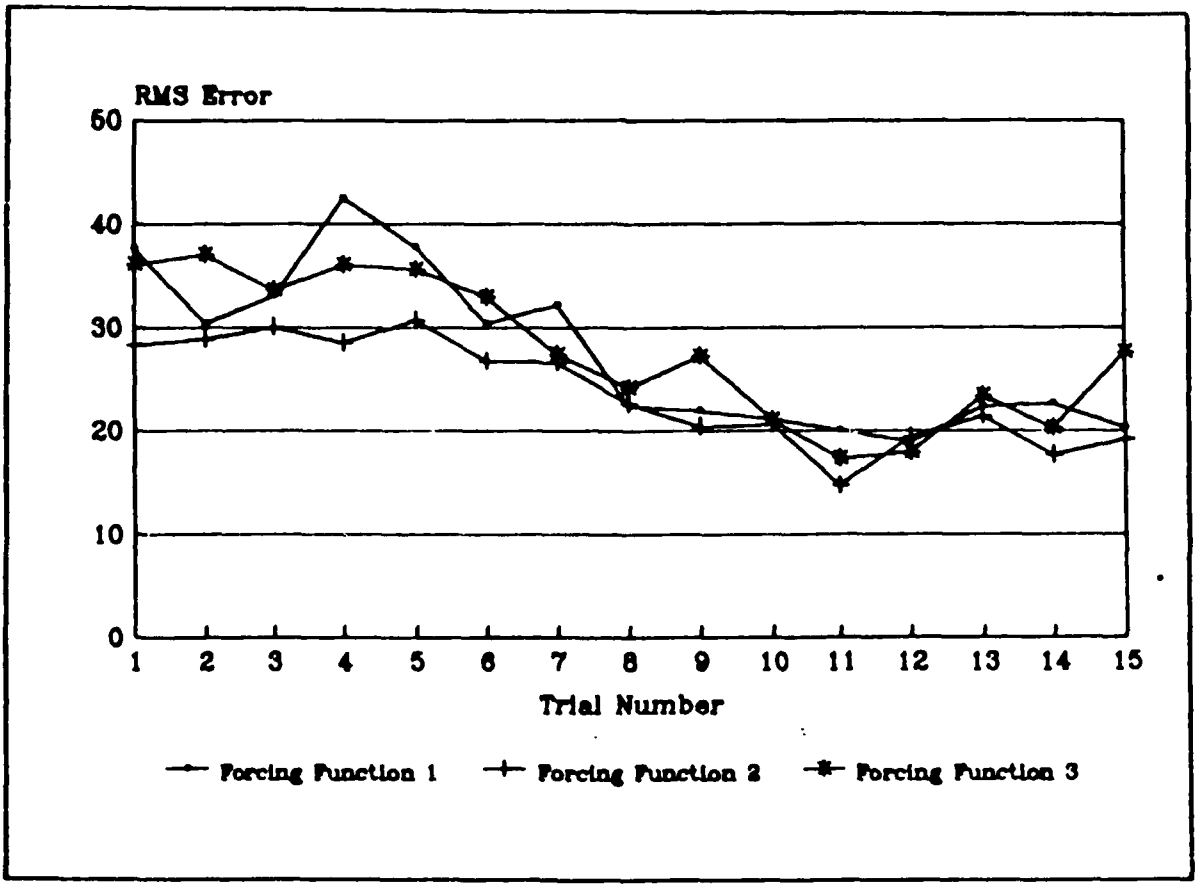

Figure 7. Typical Proficiency Curve

V. Experimental Results

5.1 Introduction

In this chapter typical data for one subject using the same forcing function is analyzed for both the passive and active setups to validate the calculation methods used in this study. Next, having justified these methods, the various performance measures (noise remnant and capacity) for the rest of the subjects are summarized to reveal key trends. Throughout the experiment, a program based on the Cooley-Tukey fast Fourier transform (FFT) algorithm was used to produce the power spectral densities of the various input/outputs sampled during each experimental run.

5.2 Method of Analysis

To insure that the FFT algorithm used was a good approximation to the continuous Fourier transform, on which the theory is based, three parameters, controllable by the experimenter, had to be determined. These were the sampling rate which had to satisfy the Nyquist criteria (at least twice the highest frequency present in the waveform), the length of time record which determined the lowest recoverable frequency, and the total number of points which determine the frequency resolution. The maximum frequency containing any appreciable power was 10.242 Hz. The length

of the time record was set to 81.96 seconds, and the number of samples set at 2048. These values then establish the minimum sampling frequency at 25 Hz, a maximum frequency of 12.5 Hz, and a frequency resolution of .012201 Hz.

5.3 Key Parameters

One of the key parameters needed to calculate the human capacity was the noise remnant introduced by the subject. As reported in chapter IV, a shaped sum of sinusoids was used as a forcing function. This class of forcing functions was used to simplify the calculation of signal and noise power. As reported by Levison, the noise cannot be easily separated from the signal power at the input frequencies. However, by concentrating the input power at selected frequencies through the use of sinusoidal forcing functions, the separation of noise power from the linear response to the forcing function is facilitated. Power measured at any frequency other than the original input frequencies must be remnant injected by the operator. (7:7) This does not take into account system noise and "noisy" generation of the forcing function. In this experiment, the largest noise source not accounted for was that of the forcing functions. However, these were generated with a minimum of 30 dB signal to noise ratio at each of the fifteen frequencies.

The other measurements necessary to compute the transinformation rate were the spectrum of the stick roll ($\Phi_{uu}(w)$) and the spectrum of the display error ($\Phi_{ee}(w)$). From these two measurements the subject's transfer function was determined. The correlated and uncorrelated portions of the stick roll power spectral density (PSD) and the display error PSD were determined as outlined in Chapter III.

Table 2 tabulates data for one run for subject #3 with the stick in the passive mode and FF #2 as the input. Table 3 shows similar data with the stick operated in the active mode.

5.4 Analysis

The noise PSD injected by the subject was calculated using equation 15. Also, the human transfer function, defined as the ratio of the correlated portion of the stick roll (output) PSD and the correlated portion of the display error (input), was calculated using equation 16. Equation 26 was used to calculate the transinformation rate.

TABLE 2. Output Data For Subject #3

(Passive Mode)

w	$\Phi_{rr}(w)$	$\Phi_{uuc}(w)$	$\Phi_{uun}(w)$	$\Phi_{eec}(w)$	$\Phi_{een}(w)$
0.230	-3.2	-6.5	-32.6	-12.4	-29.5
0.537	-3.5	-8.2	-23.7	-9.7	-25.1
0.997	-2.9	-7.2	-27.6	-8.6	-25.9
1.457	-3.5	-9.3	-24.1	-7.3	-26.0
2.224	-3.3	-9.0	-27.0	-7.0	-26.2
2.838	-3.5	-10.2	-28.2	-4.6	-27.3
4.065	-4.0	-9.4	-29.9	-3.5	-28.3
6.059	-6.1	-10.3	-26.9	-3.0	-26.5
8.207	-9.3	-11.8	-26.6	-4.5	-26.2
10.661	-13.2	-14.4	-28.1	-8.4	-28.0
16.184	-19.9	-35.5	-38.8	-22.8	-38.7
21.706	-24.9	-44.9	-43.4	-26.0	-42.4
32.137	-31.8	-60.9	-57.3	-36.0	-48.8
45.022	-37.6	-99.0	-68.2	-39.8	-49.9
64.351	-44.2	-99.0	-68.5	-51.9	-50.6

Frequency values in Rad/sec
All other values in decibels

TABLE 3. Output Data For Subject #3
(Active Mode)

w (rad/sec)	Φrr(w) (dB)	Φuuc(w) (dB)	Φuun(w) (dB)	Φeec(w) (dB)	Φeen(w) (dB)
0.230	-4.4	-10.1	-29.0	-10.7	-26.9
0.537	-4.6	-10.0	-29.5	-10.6	-33.2
0.997	-4.5	-12.2	-31.3	-7.4	-34.1
1.457	-4.1	-10.9	-34.4	-7.6	-31.3
2.224	-4.2	-12.2	-35.8	-5.8	-34.8
2.838	-4.4	-12.2	-33.1	-5.1	-30.7
4.065	-4.6	-12.2	-30.9	-3.4	-28.2
6.059	-4.7	-13.7	-35.7	-2.4	-30.7
8.207	-5.1	-17.2	-34.4	-3.5	-32.0
10.661	-6.2	-17.1	-36.1	-4.9	-31.2
16.184	-10.2	-29.5	-40.5	-11.7	-37.4
21.706	-14.4	-37.2	-46.4	-14.9	-39.3
32.137	-20.8	-51.9	-56.0	-22.4	-43.2
45.022	-26.7	-99.0	-66.4	-28.8	-45.9
64.351	-32.7	-99.0	-67.5	-41.1	-46.2

Table 4 and 5 tabulate results for subject #3 using the stick in the passive and active mode respectively. It is necessary to note that not all values of the stick roll PSD were used. If the ratio of correlated to uncorrelated power at each input frequency was not greater than, or equal to unity, the estimate was deemed unreliable and not used in the calculations. The human capacity was next calculated using equation 28.

The following figures visually summarize the results for one run for subject #3 using forcing function #2. Figure 8 and figure 9 depict the operator's transfer function and noise remnant that he introduced into the task for both the passive and active modes, while figure 10 and 11 show the transinformation rates for both modes respectively.

TABLE 4. Results For Subject #3

(Passive Mode)

w(rad)	$\|Y_H\|^2$ (dB)	Φnn(dB)	T(bits-rad/sec)
0.230	5.9	-29.3	5.6176
0.537	1.5	-19.0	3.1295
0.997	1.4	-23.3	4.8963
1.457	-1.8	-18.3	3.6347
2.224	-2.0	-21.3	4.7730
2.838	-5.5	-21.5	5.6035
4.065	-5.8	-24.5	6.9556
6.059	-7.2	-22.7	6.5422
8.207	-7.2	-24.1	6.5248
10.661	-5.9	-26.9	6.1726
16.184	-11.2	-23.2	0.1882
21.706	---	---	---
32.137	---	---	---
45.022	---	---	---
64.351	---	---	---

TABLE 5. Results For Subject #3
(Active Stick)

w(rad/sec)	$\|Y_H\|^2$ (dB)	Φnn (dB)	T (bits-rad/sec)
0.230	0.5	-23.3	4.2373
0.537	0.6	-24.1	4.5007
0.997	-4.7	-23.6	5.3659
1.457	-3.3	-27.6	6.6503
2.224	-6.3	-27.8	7.2813
2.838	-7.0	-25.3	6.6888
4.065	-8.8	-23.3	6.6300
6.059	-11.2	-26.7	8.0481
8.207	-13.7	-22.3	6.2725
10.661	-12.2	-25.2	6.7616
16.184	-17.5	-21.2	3.1664
21.706	-21.8	-23.6	2.8878
32.137	-28.2	-24.9	0.8727
45.022	---	---	---
64.351	---	---	---

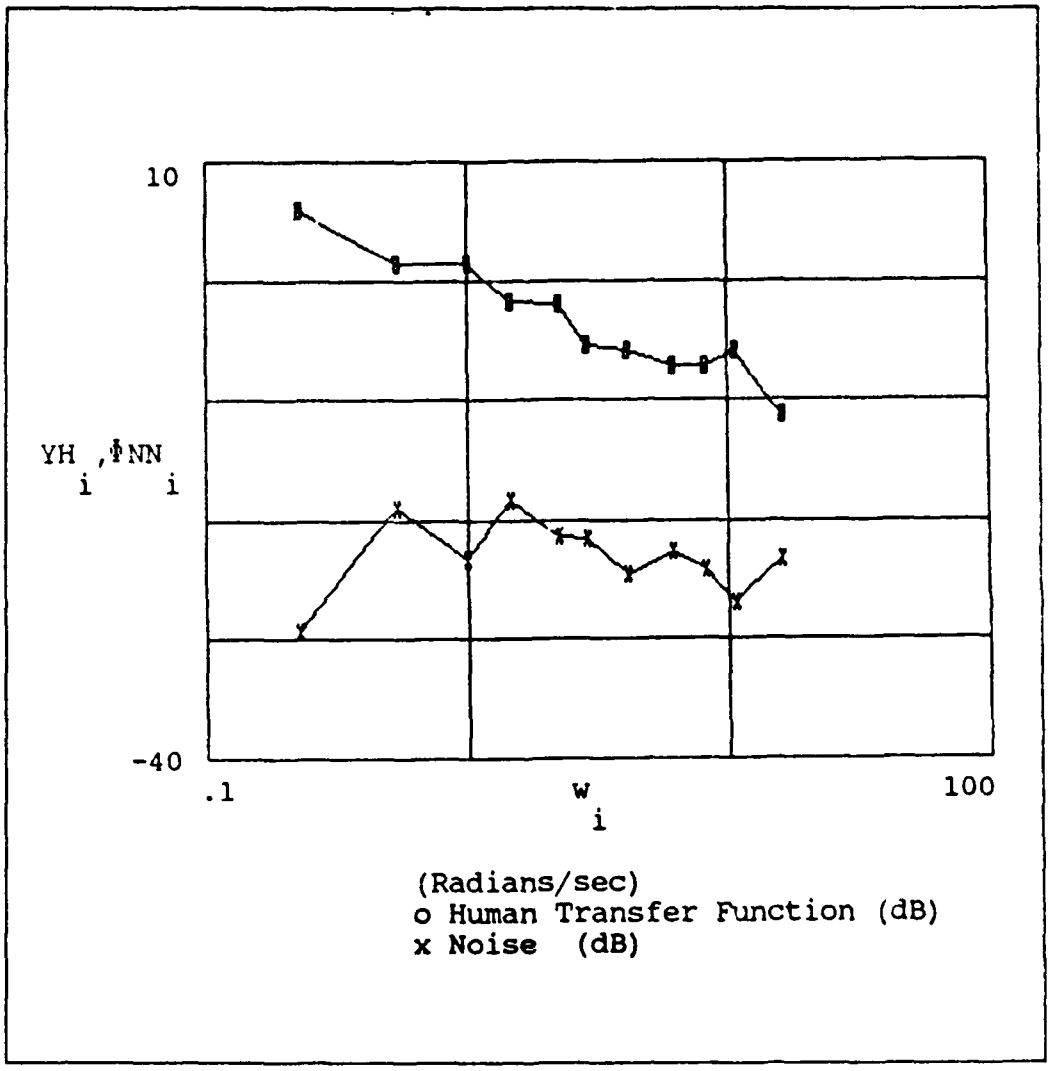

Figure 8. Human Transfer Function and Noise (Passive)

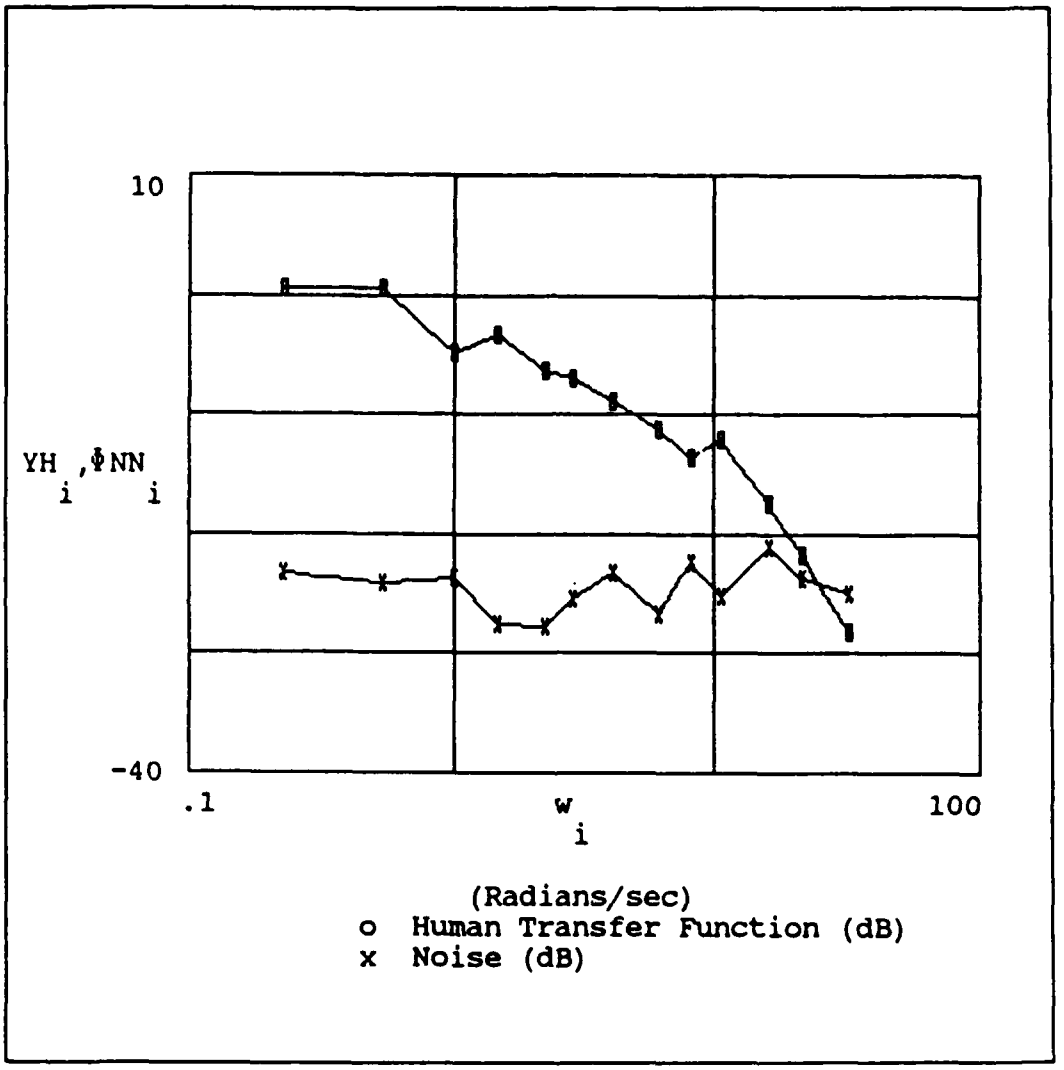

Figure 9. Human Transfer Function and Noise (Active)

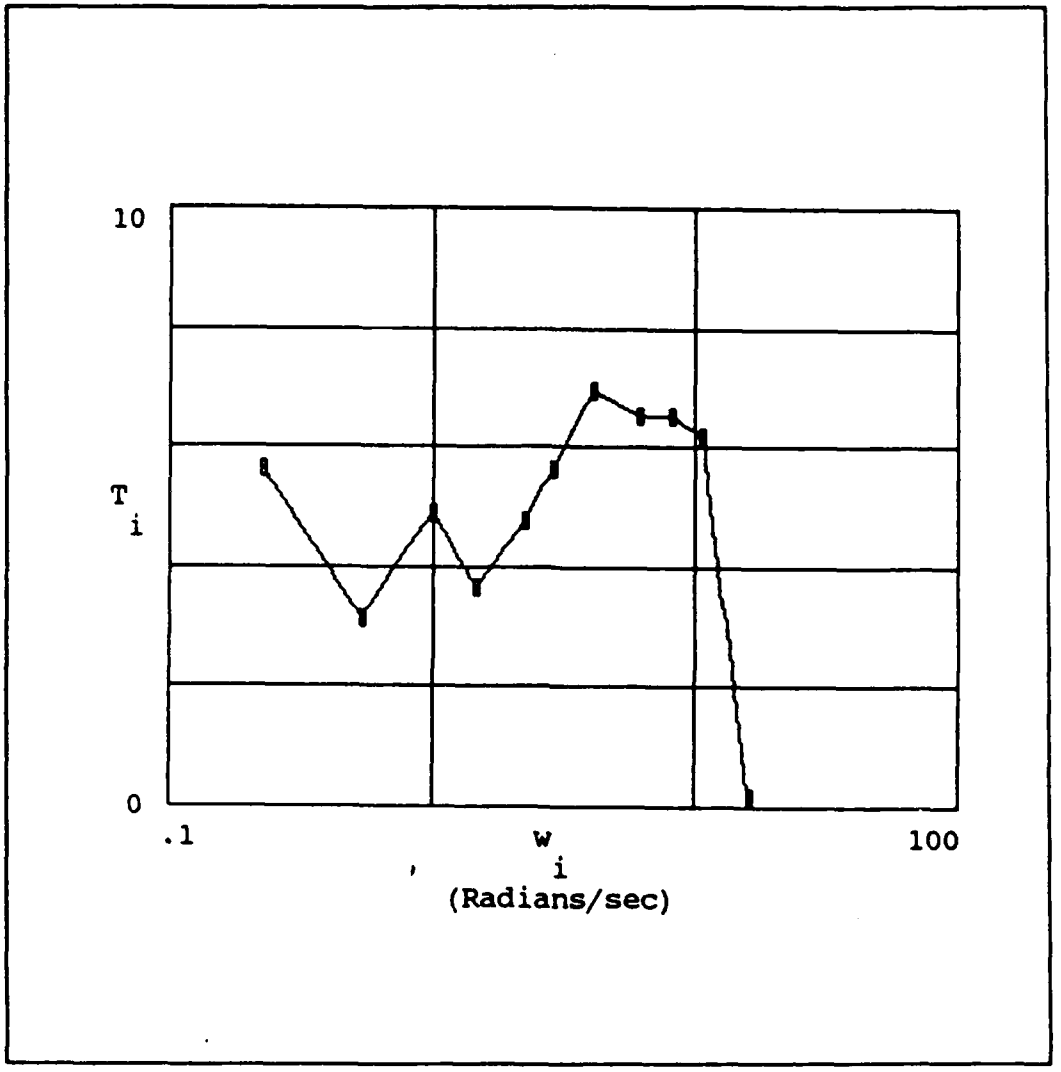

Figure 10. Transinformation Rate (Passive)

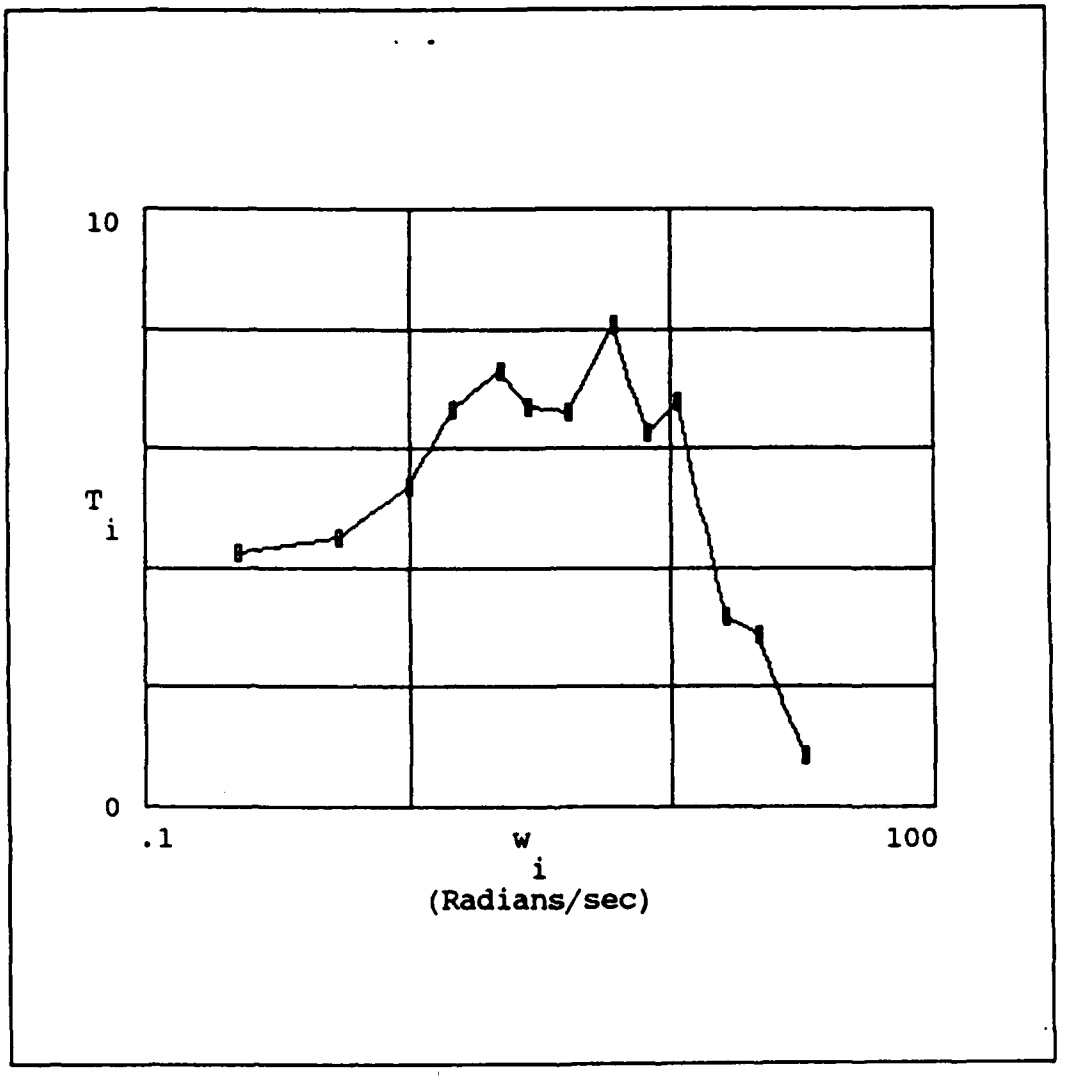

Figure 11. Transinformation Rate (Active)

From Tables 4 and 5 it is obvious that the shape of the noise spectra in the active and passive modes is similar and a slight decrease in the noise PSD for the active mode is observed. The transinformation rates also show similarities with a slight increase in the active mode.

To obtain a reliable measure of both the noise power and capacity for the operators while performing the tasks in this experiment, we averaged across trials for each forcing function and for each subject. As outlined in chapter IV, each subject was tested twice. First using the stick in the passive mode and subsequently using the stick in the active mode. Therefore, two data sessions were recorded, each consisting of 9 runs (3 for each forcing function). In the next few pages averages for each of the three forcing functions are shown. Because of the differences in the forcing functions, an average across the three inputs was not performed since we wanted to show human noise and capacity as a function of task difficulty. Similarly, as Levison reported, averaging across subjects using the same forcing function would not give an accurate measure of the noise injected. Each subject internally develops an individual tracking strategy and hence has a different transfer function. (7:5) Averaging only across the same forcing function and the same experimental setup for each subject allows us to interpret noise and capacity for

individual subjects as a function of task difficulty and stick mode.

5.4 Average Results

The following tables show the average results for subject #3 using the three forcing functions for both the passive and active modes. Table 6 shows averaged describing functions for the three forcing functions for both passive and active modes. Table 7 shows noise for both active and passive cases for the three forcing function and Table 8 shows the transinformation rate for the same conditions. Next, for quick visual comparison, the averaged results are depicted in Figure 12 through Figure 14 which show the key performance measures (transfer function, noise psd, and transinformation rates) for both the active and passive modes using forcing function #1. Similarly, Figures 15 through 17 and Figures 18 through 20 show the same performance measures for forcing function 2 and forcing function 3 respectively.

Table 6. Human Operator Describing Function (Subject #3)

	FF #1		FF #2		FF #3	
Freq	Passive	Active	Passive	Active	Passive	Active
0.230	3.16	1.01	3.71	1.28	3.73	0.60
0.537	0.86	0.34	0.16	-1.72	1.81	-1.28
0.997	-0.74	-1.97	-0.71	-2.34	-0.06	-2.26
1.457	-2.89	-4.23	-3.40	-3.62	-1.47	-4.24
2.224	-3.05	-4.78	-5.35	-5.56	-2.71	-4.68
2.838	-6.08	-6.22	-5.44	-5.47	-3.89	-5.54
4.065	-6.36	-7.35	-6.67	-7.23	-4.28	-7.63
6.057	-7.99	-8.55	-8.21	-8.76	-6.69	-8.60
8.207	-7.71	-8.94	-9.55	-10.46	-6.50	-9.74
10.661	-7.58	-9.26	-8.59	-10.28	-6.39	-9.91
16.184	-3.74	-5.72	-7.74	-8.03	---	---
21.706	---	-12.61	-14.00	-18.23	---	---
32.137	---	---	---	---	---	---
45.022	---	---	---	---	---	---
64.351	---	---	---	---	---	---

Note 1: Frequency values are in radians.
Note 2: All other values are in units of decibels.

Table 7. Human Operator Noise (Subject #3)

	FF #1		FF #2		FF #3	
Freq	Passive	Active	Passive	Active	Passive	Active
0.230	-23.14	-23.40	-18.42	-27.53	-22.22	-25.28
0.537	-23.31	-22.95	-24.40	-23.50	-23.22	-21.85
0.997	-22.32	-26.58	-23.31	-25.53	-23.80	-28.75
1.457	-20.64	-25.96	-22.95	-25.80	-20.09	-22.98
2.224	-21.61	-22.84	-17.46	-22.08	-21.57	-22.49
2.838	-22.24	-24.80	-20.97	-25.63	-24.40	-23.84
4.065	-22.81	-25.04	-21.29	-23.01	-24.36	-23.70
6.057	-22.24	-24.14	-21.14	-24.56	-22.57	-24.60
8.207	-24.90	-27.00	-20.77	-24.14	-27.37	-26.38
10.661	-24.95	-28.75	-24.16	-25.63	-26.64	-29.09
16.184	-27.00	-29.86	-23.12	-26.64	---	---
21.706	---	-32.73	-23.22	-23.34	---	---
32.137	---	---	---	---	---	---
45.022	---	---	---	---	---	---
64.351	---	---	---	---	---	---

Note 1: Frequency values are in radians.
Note 2: All other values are in units of decibels.

Table 8. Transinformation (Subject #3)

	FF #1		FF #2		FF #3	
Freq	Passive	Active	Passive	Active	Passive	Active
0.230	4.66	4.59	3.07	5.85	4.25	5.61
0.537	6.20	4.79	4.98	5.00	5.36	4.80
0.997	4.98	6.36	5.28	5.81	5.73	7.84
1.457	4.91	6.60	5.21	6.13	4.47	5.52
2.224	5.05	5.70	4.30	5.30	5.21	5.59
2.838	5.98	6.65	5.35	6.90	6.49	6.44
4.065	6.36	7.07	5.72	6.45	6.53	6.55
6.057	6.39	6.96	6.53	7.56	5.91	6.89
8.207	6.64	7.16	6.55	7.35	7.40	6.45
10.661	5.62	6.06	6.96	7.07	5.70	5.20
16.184	1.94	2.65	3.54	4.57	---	---
21.706	---	2.43	3.25	3.10	---	---
32.137	---	---	---	---	---	---
45.022	---	---	---	---	---	---
64.351	---	---	---	---	---	---

Note 1: Frequency values are in radians.
Note 2: All other values are in bits-rad/sec.

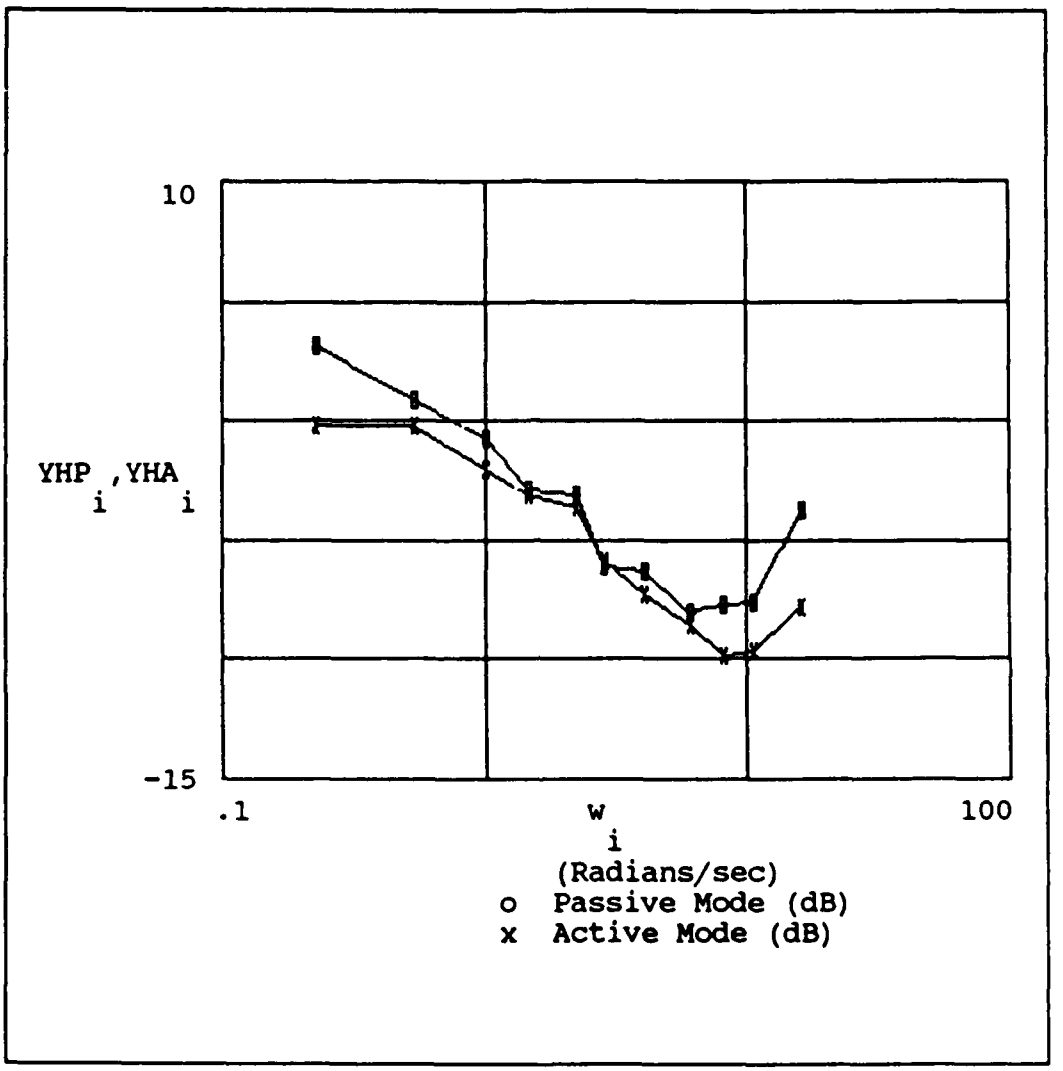

Figure 12. Human Transfer Function (FF #1)

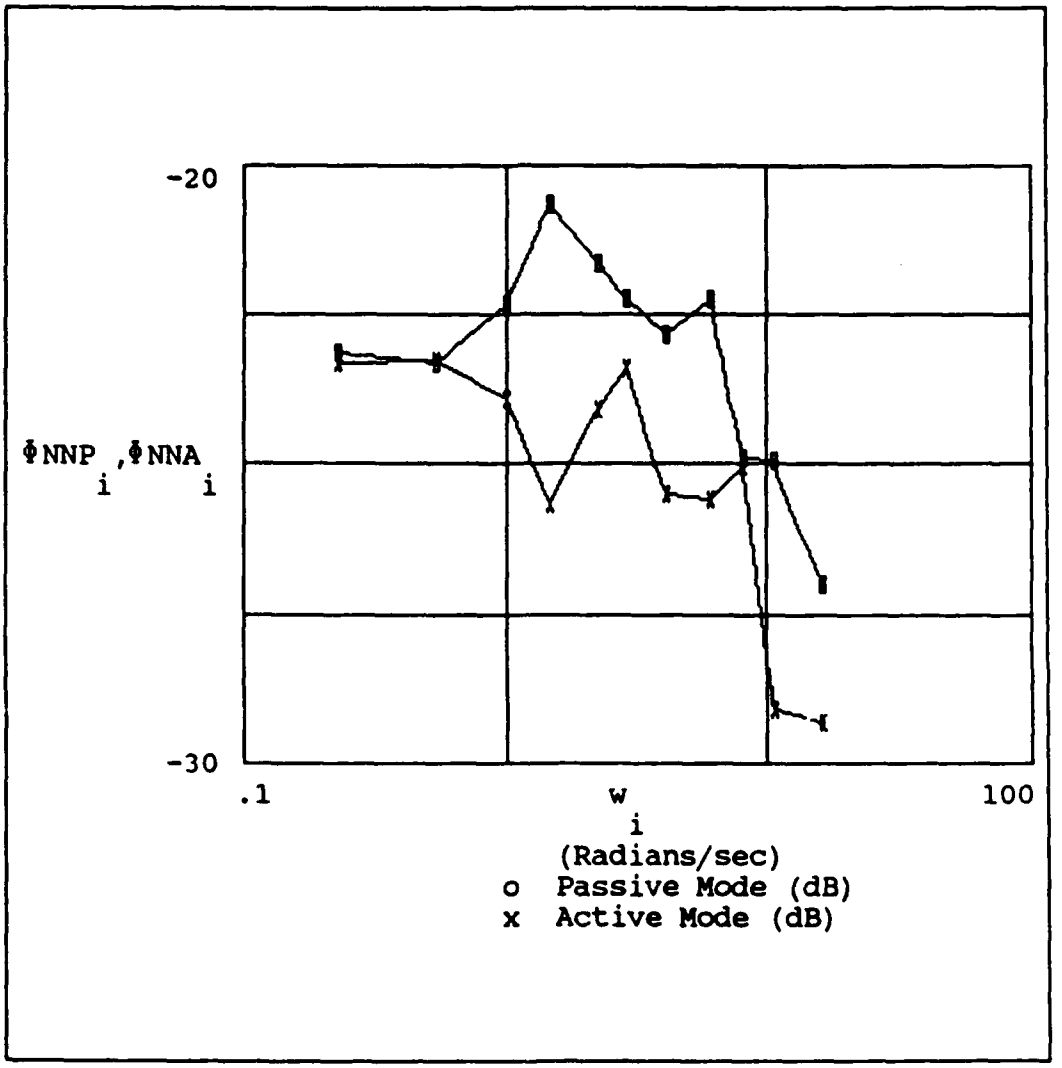

Figure 13. Human Noise Remnant (FF #1)

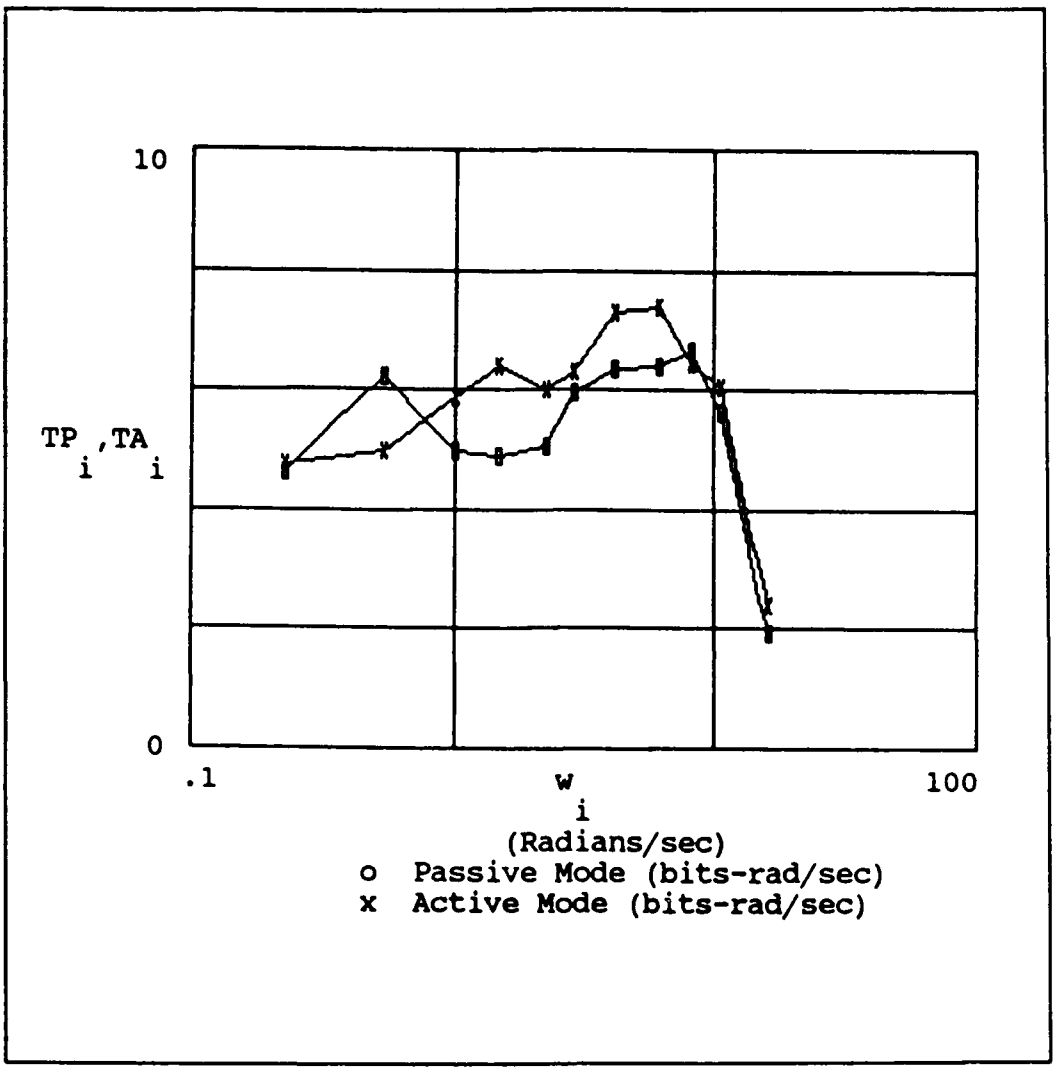

Figure 14. Transinformation Rate (FF# 1)

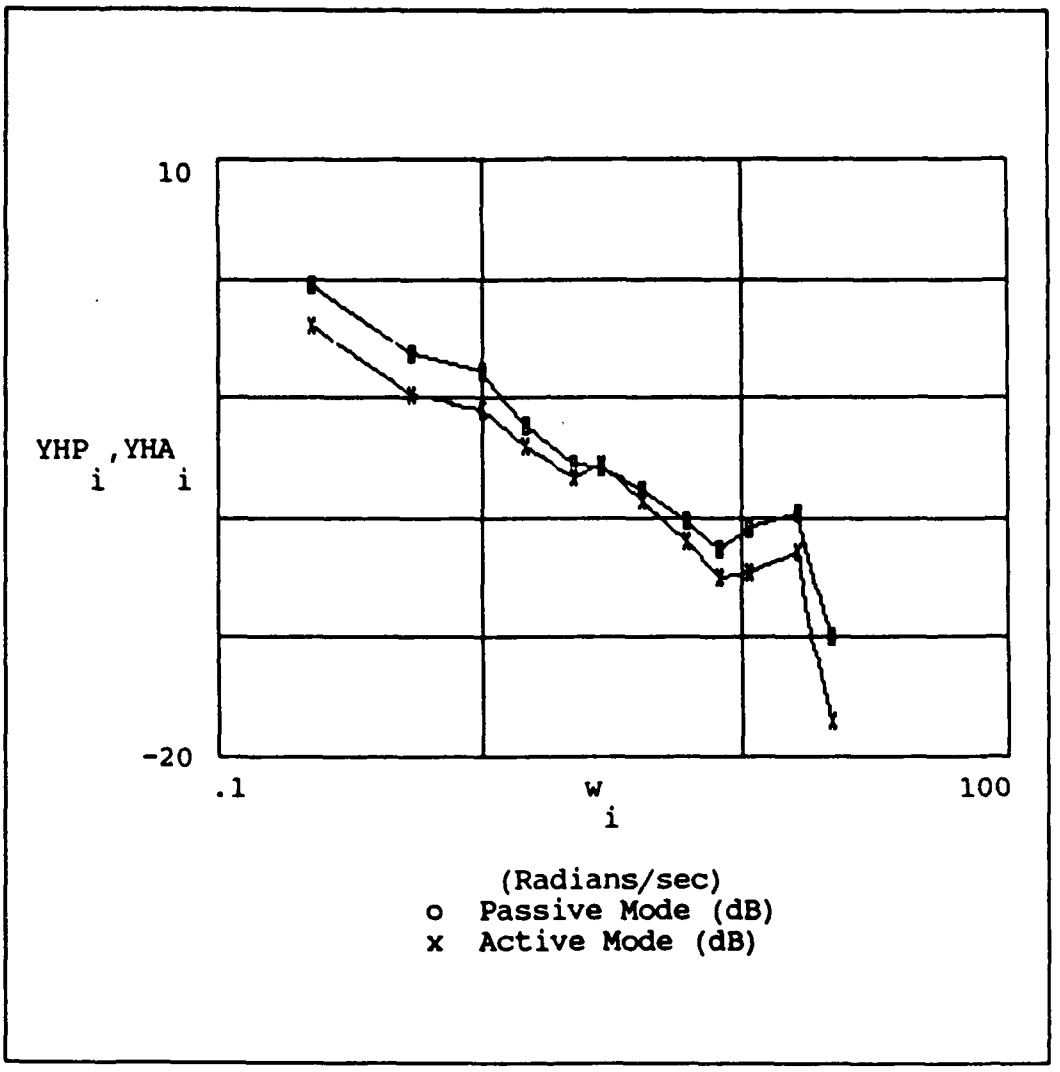

Figure 15. Human Transfer Function (FF #2)

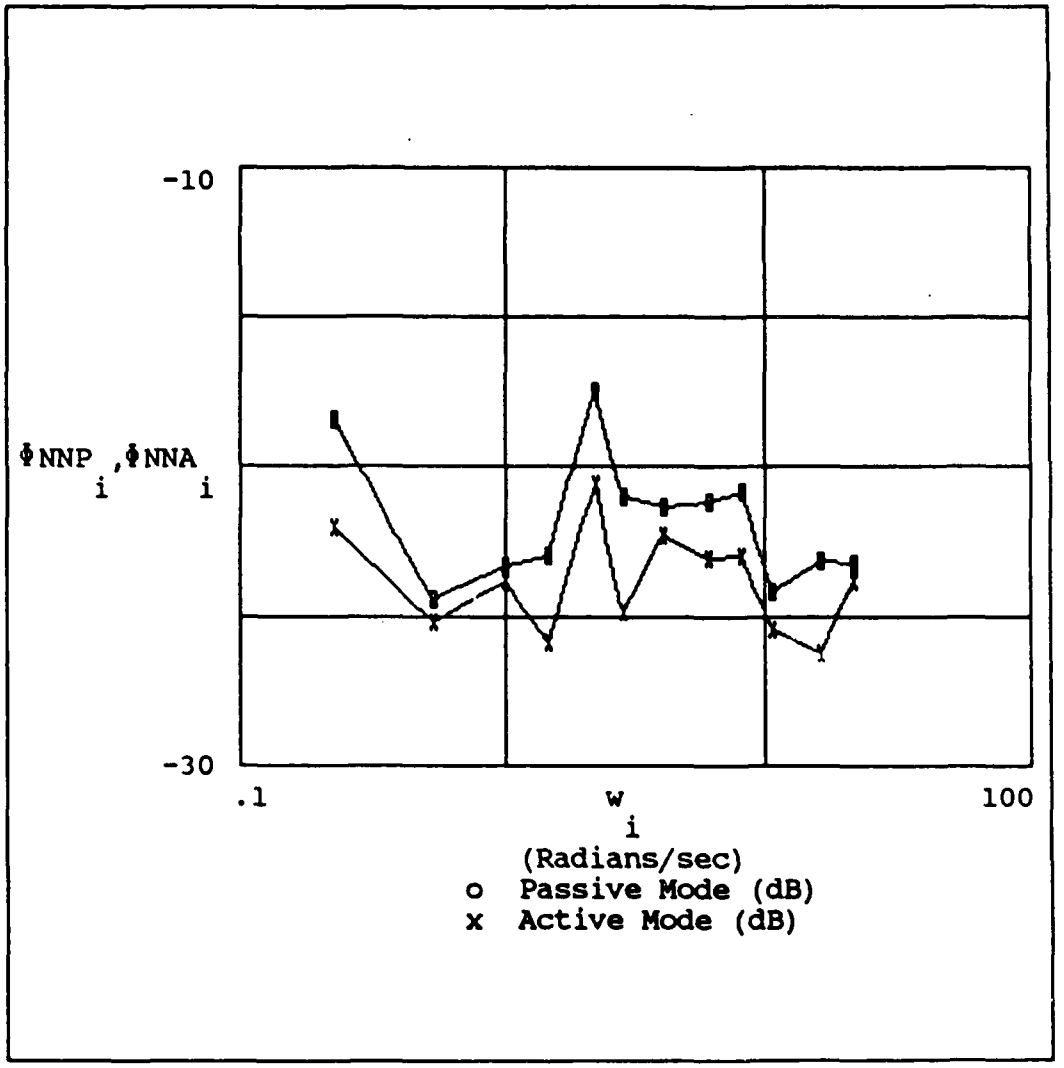

Figure 16. Human Noise Remnant (FF #2)

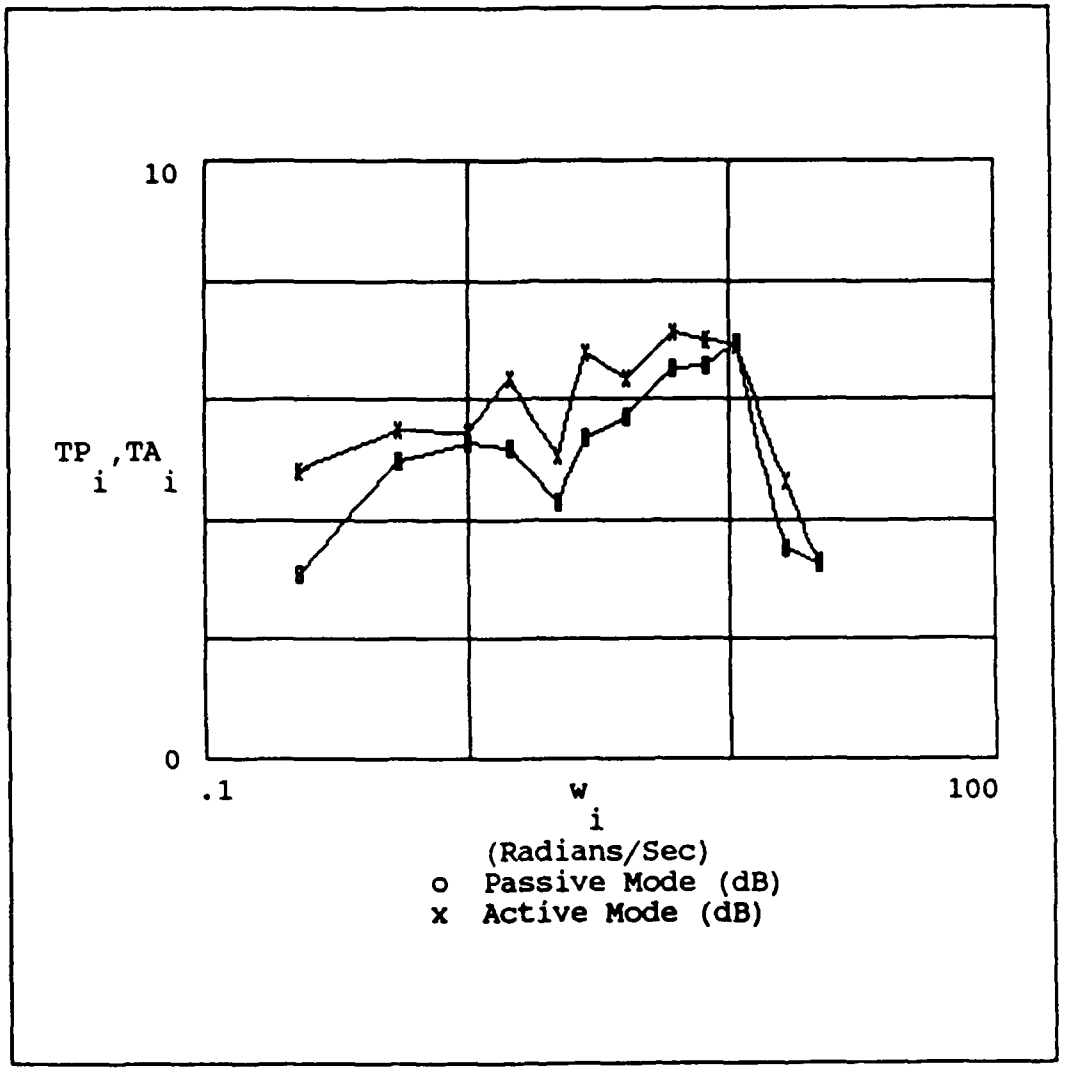

Figure 17. Transinformation Rate (FF #2)

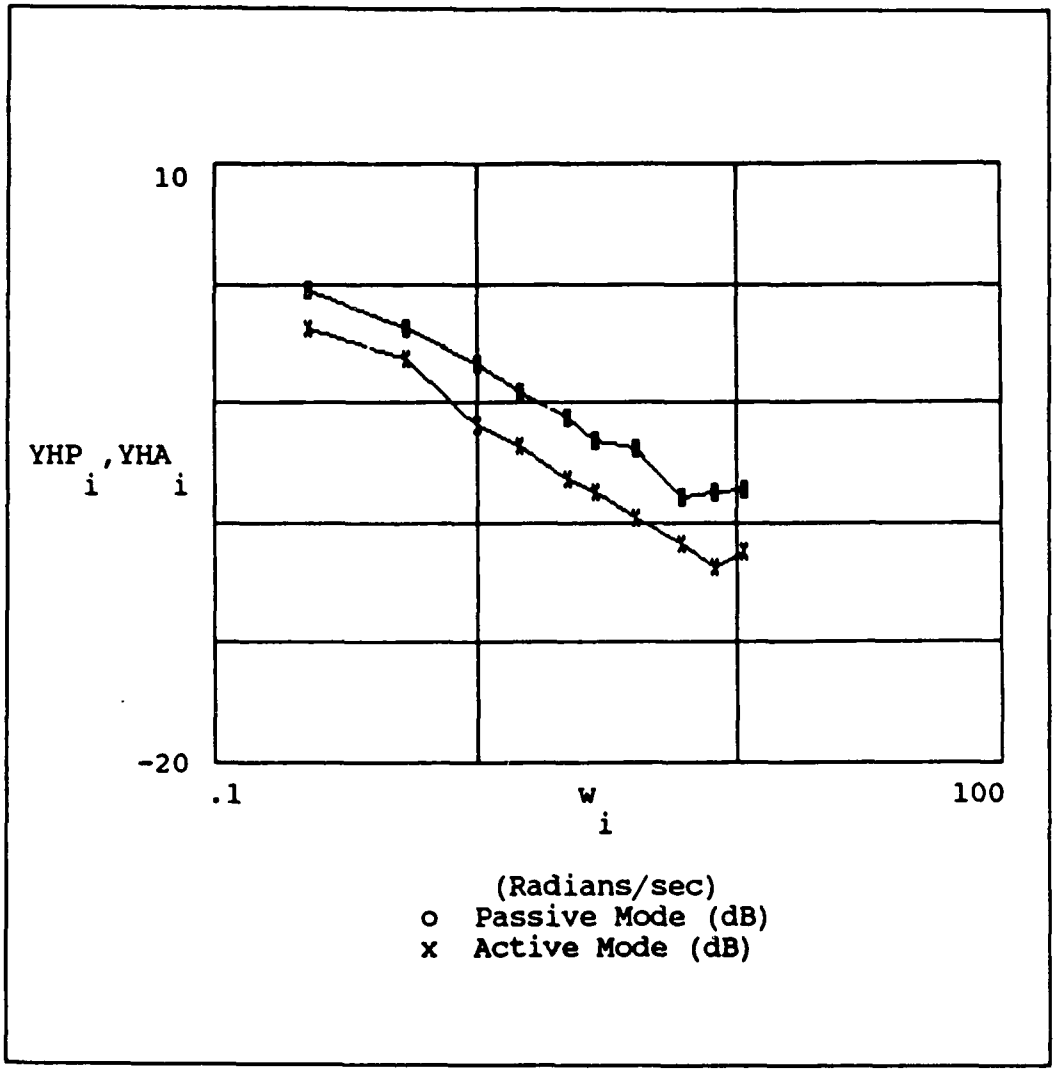

Figure 18. Human Transfer Function (FF #3)

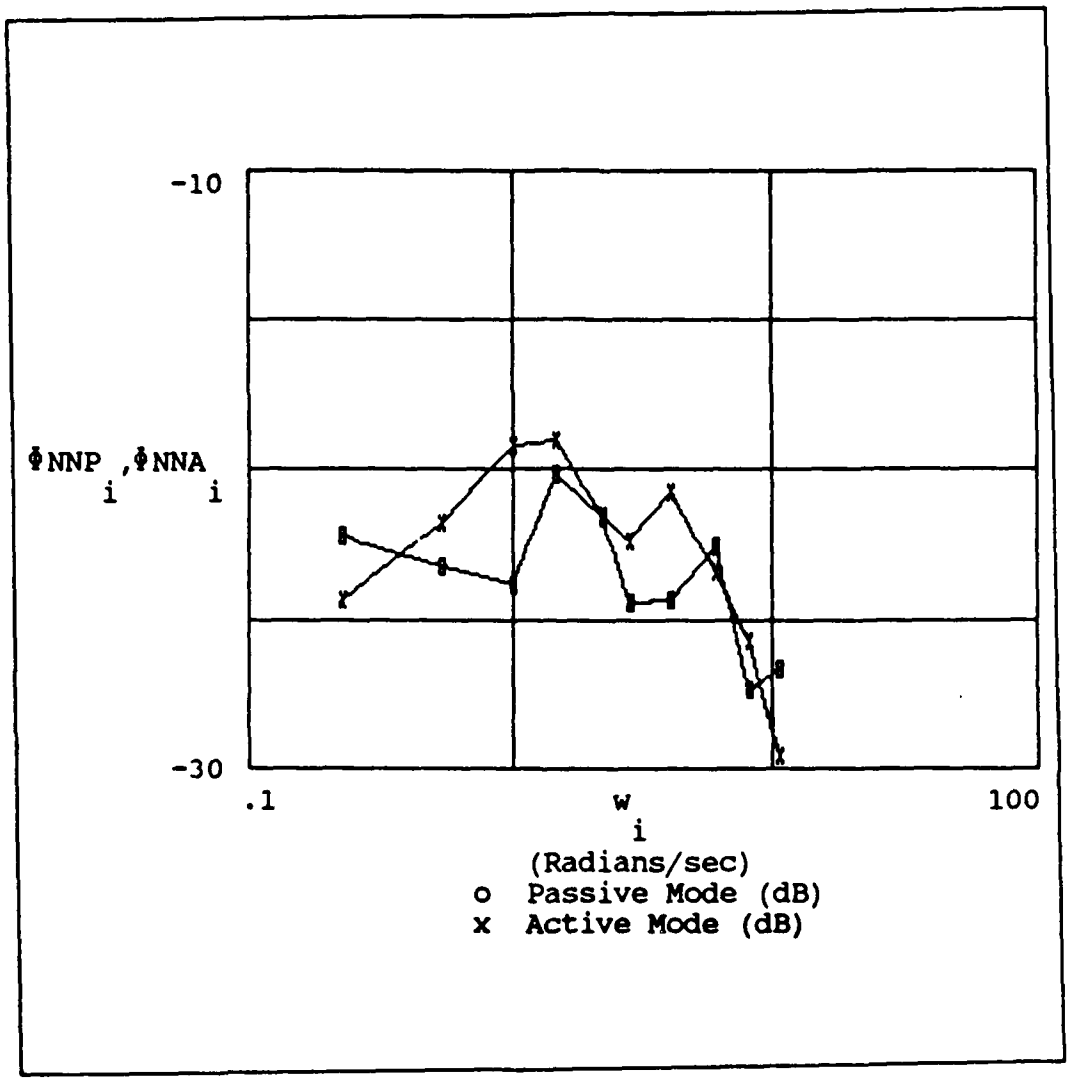

Figure 19. Human Noise Remnant (FF #3)

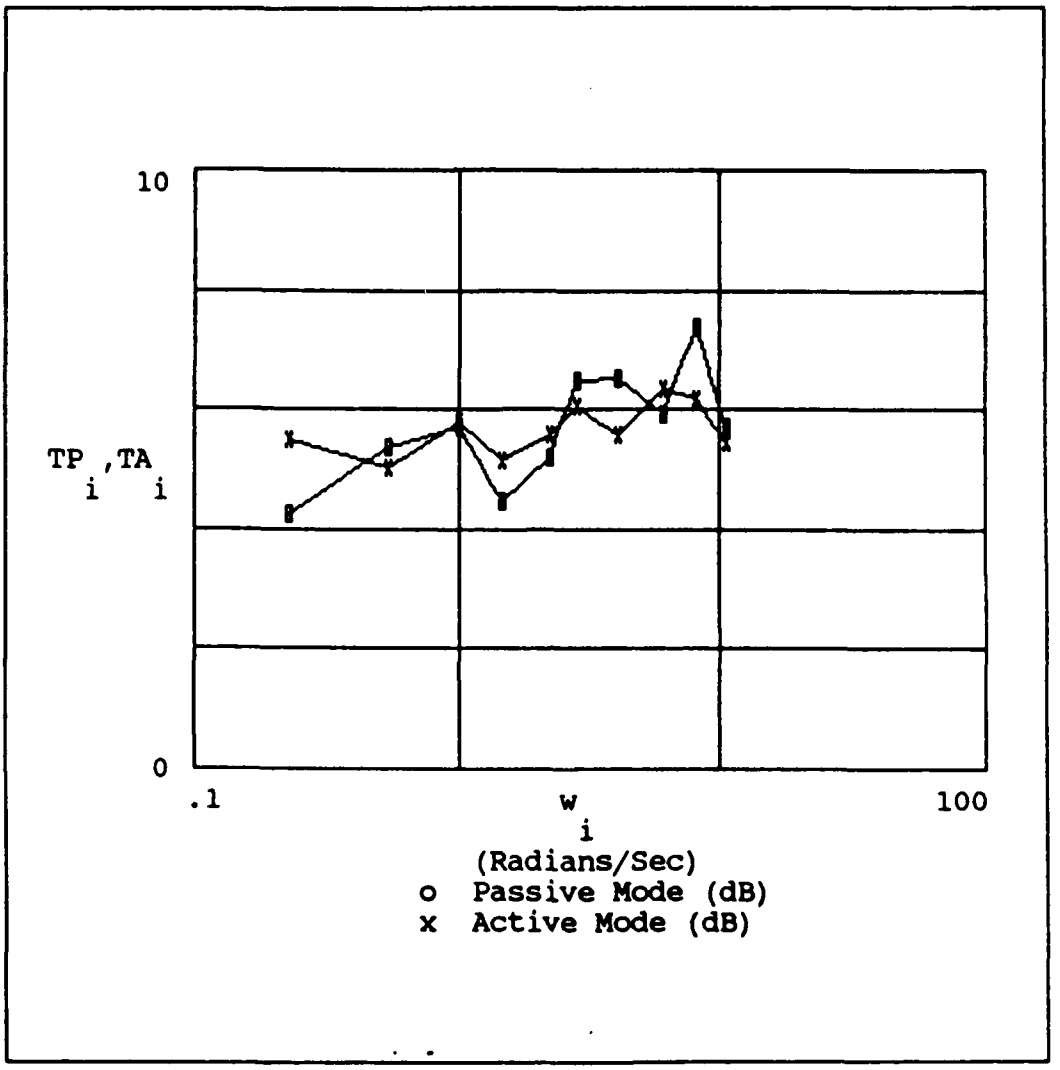

Figure 20. Transinformation Rate (FF #3)

As a final measure of comparison, the individual capacities as a function of forcing function and mode of operation are tabulated in table 9 and depicted in figures 21 through 23. As it can be observed, in 82 percent of the cases there is an improvement in capacity when the stick is operated in the active mode. The major exception is for subject #6, FF #1 which shows a decrease of 1.65 bits/sec. Subject #4 also shows a slight decrease (.51 bit/sec) for both FF #1 and FF #2. The best average capacity is achieved by using the second forcing function while the stick is operated in the active mode. The highest capacity observed in the experiment was 11.34 bits/sec and was achieved by subject #2 tracking FF #2 while the stick was operated in the active mode.

Table 9. Average Capacities (bits/sec)

	Capacity					
	FF #1		FF #2		FF #3	
Subject	Passive	Active	Passive	Active	Passive	Active
1	7.40	7.59	5.77	7.65	6.84	7.65
2	9.94	10.86	8.21	11.34	9.75	10.25
3	9.35	10.66	9.66	11.31	9.08	9.69
4	8.93	8.42	8.02	7.58	7.39	9.86
5	9.86	10.85	9.20	10.91	9.46	9.81
6	10.24	8.59	7.08	8.22	8.71	9.30

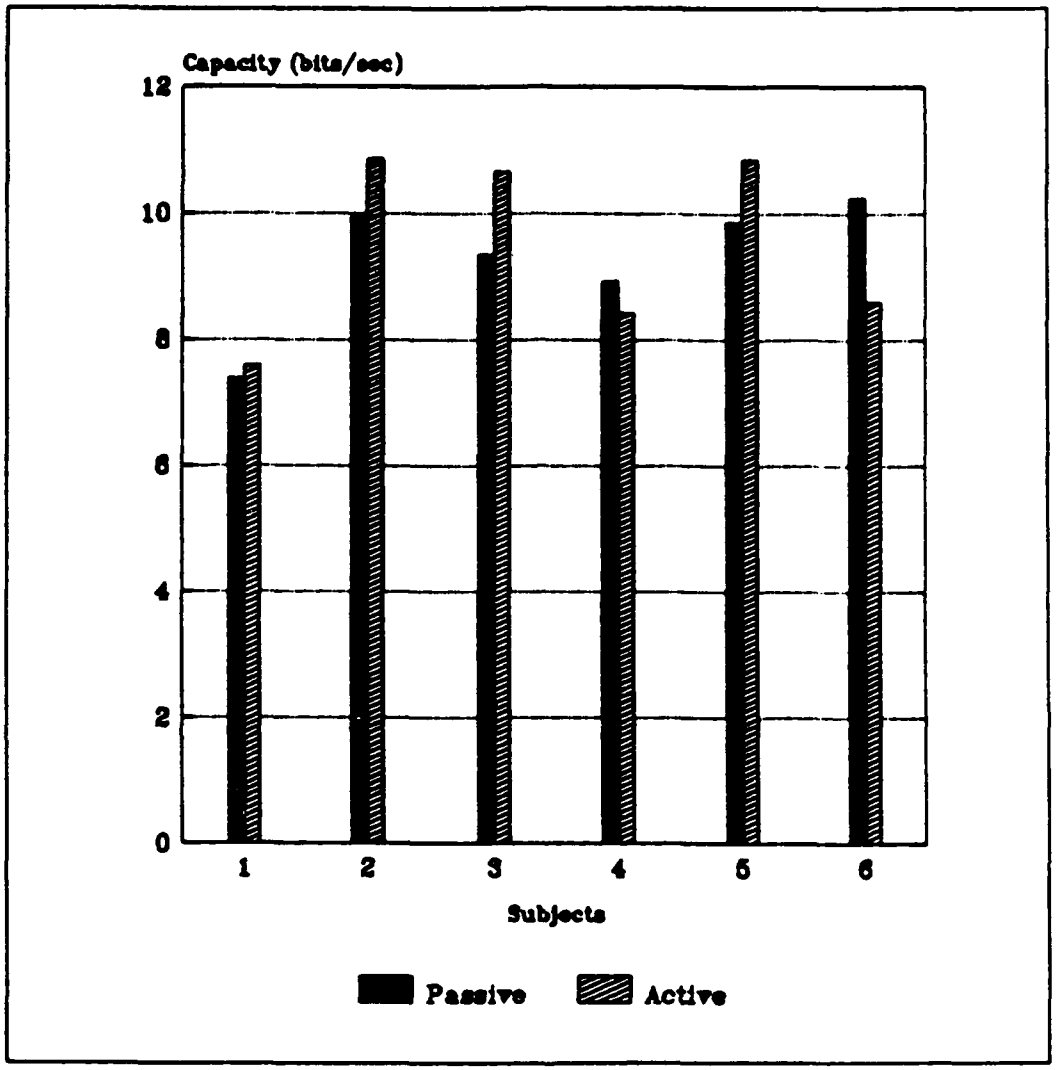

Figure 21. Comparison of Capacity for Active and Passive Modes (FF #1)

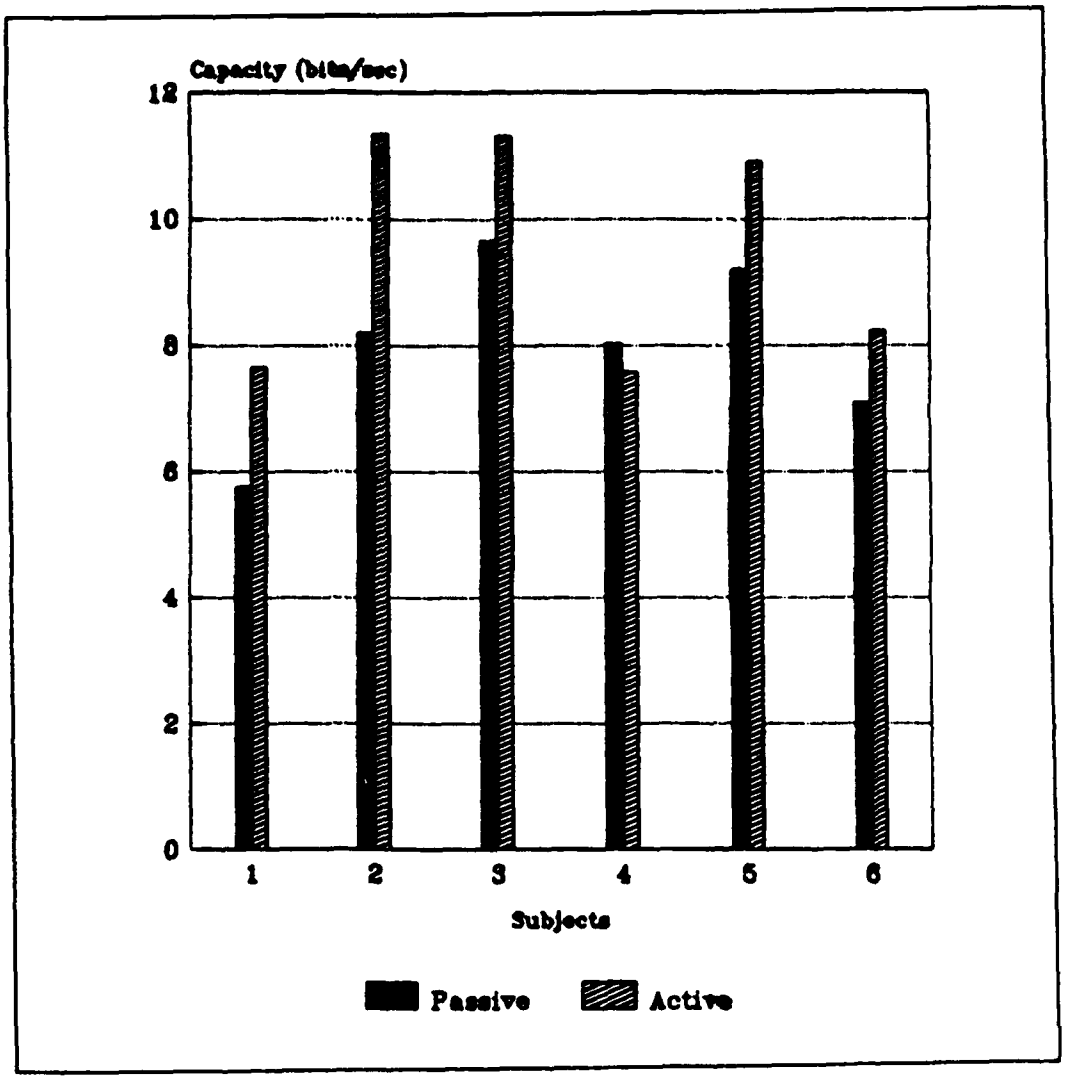

Figure 22. Comparison of Capacity for Active and Passive Modes (FF #2)

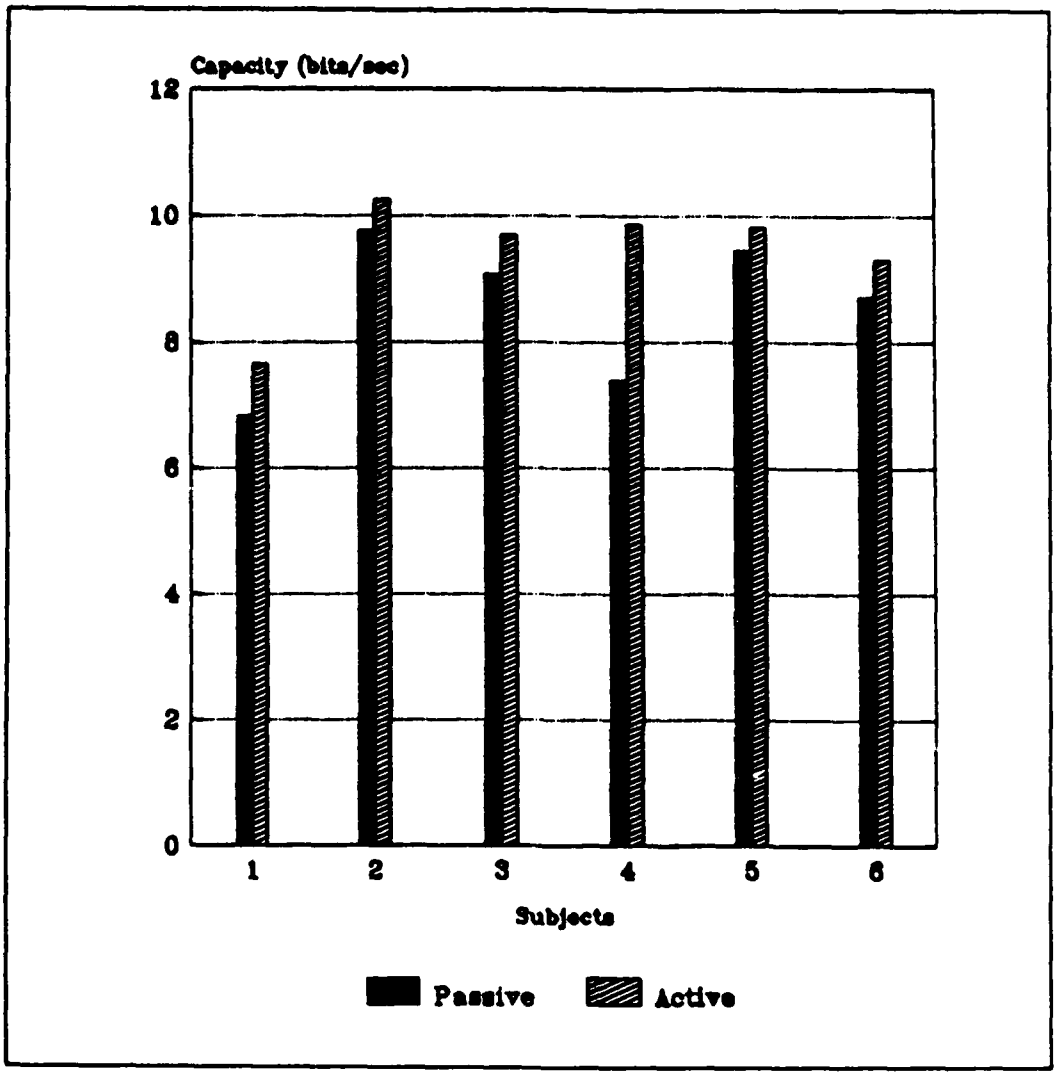

Figure 23. Comparison of Capacity for Active and Passive Modes (FF #3)

To analyze the reasons for the decrease in capacities for subject #4 and subject #6, it is necessary to examine the display error PSD, equation 10, the amount of information contained in the display error signal, and equation 26, the transinformation rate. The display error PSD, written as

$$\Phi_{ee}(w) = \left|\frac{1}{1 + Y_H(w)}\right|^2 \Phi_{rr}(w) + \left|\frac{Y_H(w)}{1 + Y_H(w)}\right|^2 \Phi_{nn}(w)$$

can be rewritten as

$$\Phi_{ee}(w) = \Phi_{eec}(w) + \Phi_{een}(w) \tag{31}$$

where $\Phi_{eec}(w)$ is the signal portion of the display error and $\Phi_{een}(w)$ is the noise component.

The input information to the human channel is the information contained in this signal which is given by the entropy and can be expressed as

$$H[e(t)] = \log_2 \frac{\Phi_{eec}(w) + \Phi_{een}(w)}{\Phi_{een}(w)} \tag{32}$$

or, in terms of the human transfer function, input forcing function PSD, and noise remnant PSD as

$$H[e(t)] = \log_2 \left[1 + \frac{\Phi_{rr}(w)}{|Y_H(w)|^2 \Phi_{nn}(w)} \right] \qquad (33)$$

The transinformation rate, expressed in chapter III as

$$T[e(t);u(t)] = \text{Log}_2 \frac{S_u(w) + N_u(w)}{N_u(w)}$$

can be rewritten in terms of the human transfer function, input forcing function PSD, and noise remnant PSD as

$$T[e;u] = \log_2 \left[1 + \frac{\Phi_{rr}(w)}{|1 + Y_H(w)|^2 \Phi_{nn}(w) + |Y_H(w)|^2 \Phi_{nn}(w)} \right] \qquad (34)$$

By allowing the human transfer function or the noise PSD to vary, four possible cases can occur. Note that the PSD of the input forcing function does not change from active to passive and cannot affect the outcomes of the four cases. In cases I and II, $\Phi_{nn}(w)$ is kept constant and $Y_H(w)$ is allowed to change, while in cases III and IV $Y_H(w)$ is kept constant and $\Phi_{nn}(w)$ is allowed to change. When $Y_H(w)$ increases, the display error PSD decreases and, as a consequence, the amount of information in the signal also

decreases. Since the amount of input information decreases, so does the transinformation rate, and hence the capacity. When $Y_H(w)$ decreases, the display error PSD, the input information, and the transinformation rate increase. A similar analysis shows that when $\Phi_{nn}(w)$ increases and $Y_H(w)$ is kept constant, the display error PSD increases and the transinformation rate decreases. The opposite occurs when $\Phi_{nn}(w)$ decreases $Y_H(w)$ remains constant.

These four cases are summarized in figure 24.

Data analysis shows that there was a slight increase in the noise PSD for subject #4 tracking FF #1 and FF #2. This slight increase in noise PSD, seen in figures C-2 and C-5, account for the slight decrease in capacity. Since the magnitudes of the human transfer functions are approximately constant (figures C-1 and C-4), then subject #4 can be classified as case III. Subject # 6 is more difficult to classify in terms of the four cases outlined above since data analysis shows both a considerable increase in noise PSD and a decrease in the magnitude of his transfer function when tracking FF #1 in the active mode (see figures E-1 and E-2).

Case	$\Phi_{eec}(w)$	$\Phi_{een}(w)$	$\Phi_{ee}(w)$	H[e(t)]	T[e(t);u(t)]
I. $Y_H(w)$ ← , $\Phi_{nn}(w)$ →	→	←	→	→	←
II. $Y_H(w)$ ← , $\Phi_{nn}(w)$ →	←	→	←	←	→
III. $Y_H(w)$ → , $\Phi_{nn}(w)$ ←	↑	←	←	→	→
IV. $Y_H(w)$ → , $\Phi_{nn}(w)$ →	↑	→	→	←	←

Figure 24. Trend Analysis

A more accurate determination of the effects of both the noise PSD and the magnitude of the transfer function on the transinformation rate should be determines by performing a sensitivity analysis on Eq. 34.

Additional experimental results for the remaining subjects are provided in Appendices A through E.

VI. Conclusions and Recommendations

In this chapter the principal conclusions of the experimental program and recommended areas for future study are discussed.

6.1 Conclusions

The purpose of this study was to calculate and compare the capacity of a human operator performing a compensatory tracking task with the smart stick controller in both the passive and active mode. Six subjects participated in the study and over 100 individual data sessions were analyzed. In calculating the capacity, a detailed examination of human noise remnant and operator transfer functions was also performed. Definite changes in performance occurred when operating the stick in the active mode. These changes are manifested in terms of reduced injected noise and increased capacity. The following observations are made:

a. The capacity of the operator increased in 83 % of the cases when tracking with the stick operating in the active mode.

b. A maximum capacity of 11.34 bits/sec was exhibited by subject #2 tracking FF #2 with the stick in the active mode. A 27.6 % increase in capacity

from passive to active occurred for this case.

c. The capacity of two subjects decreased when tracking with the stick operating in the active mode. Subject #4 exhibited a decrease of approximately 0.5 bits/sec for both FF #1 and FF #2. This decrease is attributed to a slight increase in injected noise remnant. The capacity of subject #6 decreased by 1.65 bits/sec while tracking FF #1. The causes for this increase are more difficult to characterize since, as explained in Chapter V, both the noise and the transfer function changed.

d. Table 9 and Figures 21, 22, and 23 show that the capacity increased most notably when subjects were tracking a forcing function whose spectra had been shaped by a second order Butterworth filter with a 2 Hz cutoff frequency. In some cases the capacity improved by as much as 27.6 percent.

e. The magnitude of the noise remnant decreased in 89 % of the cases examined. Only Subject # 4 showed a slight increase in noise power.

f. No obvious conclusion can be made about the human transfer function. Each subject had a different tracking strategy. During the course of the experiment it was observed that individuals appeared to develop different tracking strategies when the stick was operated in the active mode. In general their stick movement was smoother, the magnitude of the transfer function decreased slightly and their tracking ability improved.

6.2 Recommendations

The above conclusions were based on sinusoidal forcing functions shaped by second order Butterworth and Gaussian filters. In addition, the model was tested with a unity gain control element and tracking was allowed only in one axis.

Since the largest capacities were measured with forcing functions whose spectra was shaped by the second order Butterworth filter with 2 Hz cutoff frequency, it is recommended that sinusoidal forcing functions shaped by higher order Butterworth filters with higher cutoff frequencies be tested to see if in an upper bound of human capacity, while performing compensatory tracking tasks, can be reached.

Since the purpose of the smart stick is to improve pilot performance in controlling an aircraft, plant dynamics of different aircraft should be examined to determine whether comparable performance improvements are also achieved. The possibility of tracking in both azimuth and elevation should be explored.

Finally, a sensitivity analysis of Eq. 34 should be performed to determine which parameter has the greatest influence on capacity.

Appendix A. Graphical Representation of Experimental Results (Subject #1)

This appendix contains the experimental results obtained by testing subject #1. Each graph consists of a visual comparison of the active and passive modes of operation for the human transfer function, the noise remnant, and the transinformation rate for the three forcing functions.

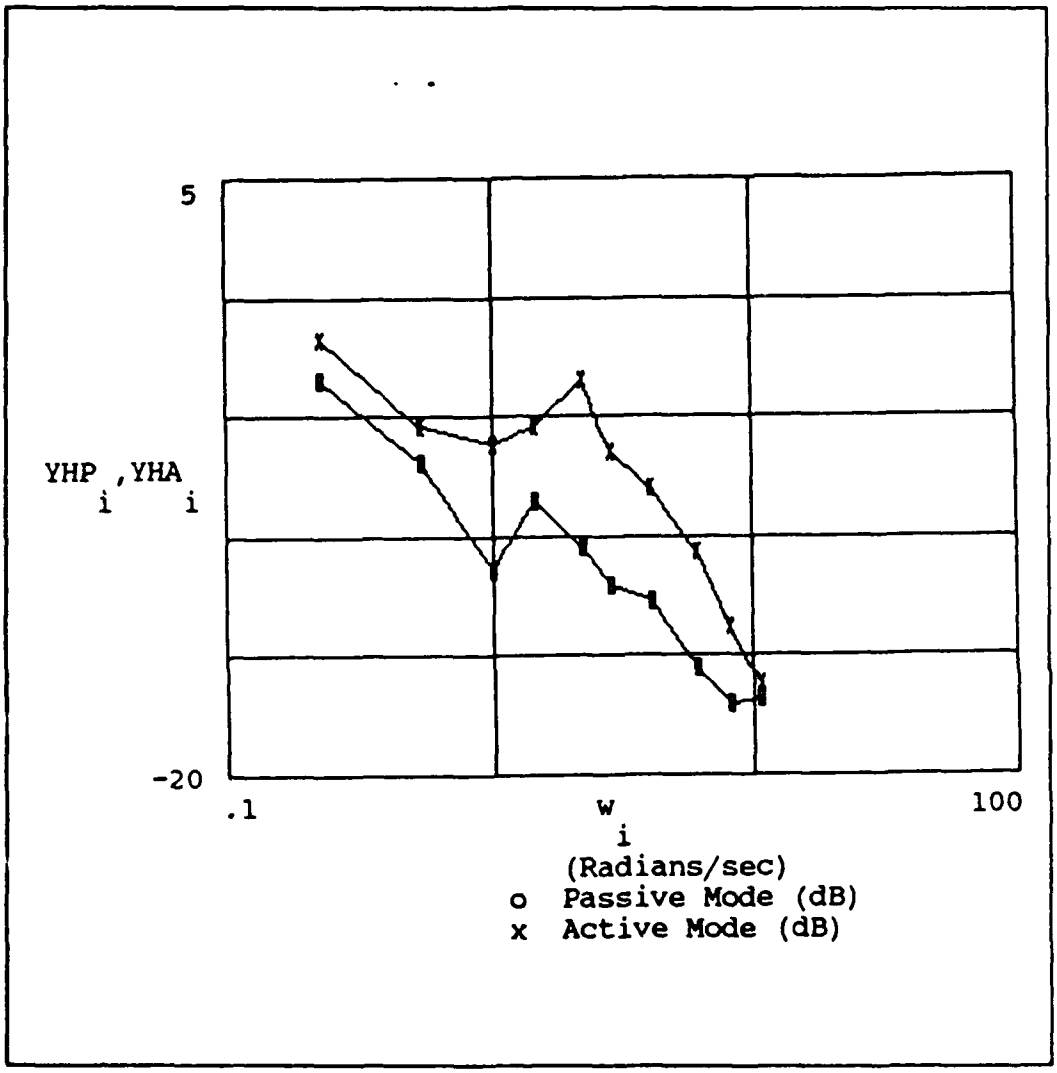

Figure A-1. Human Transfer Function (FF #1)

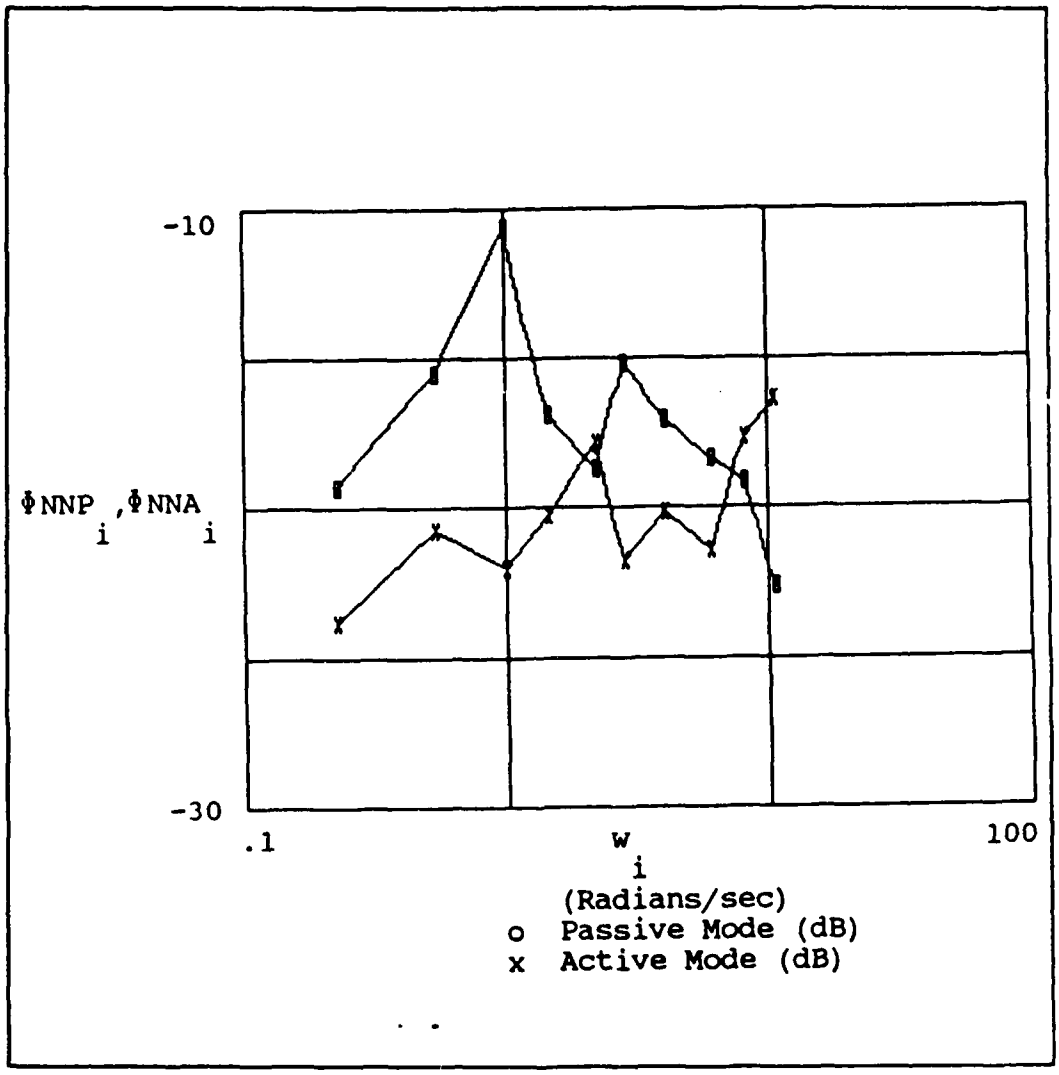

Figure A-2. Operator Noise (FF #1)

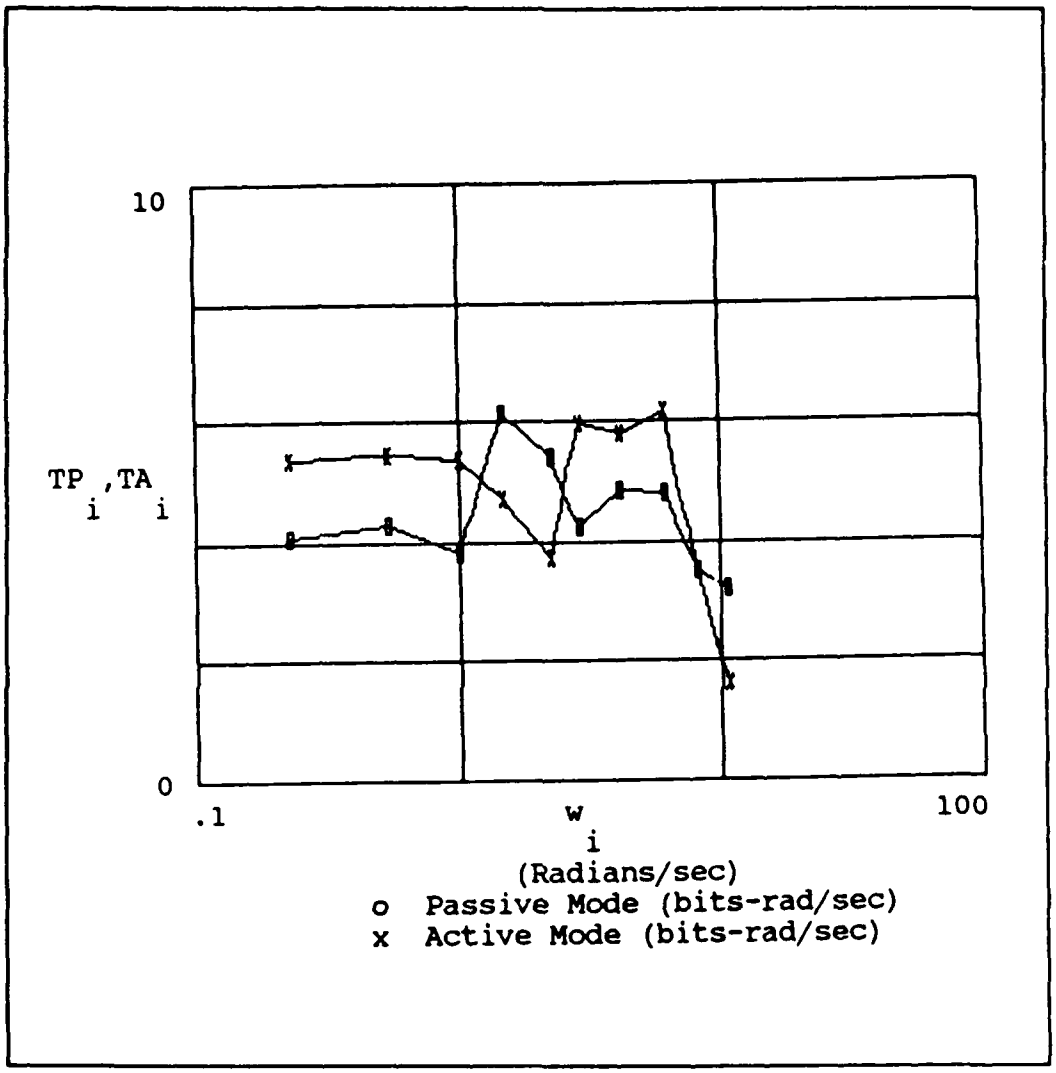

Figure A-3. Transinformation Rate (FF #1)

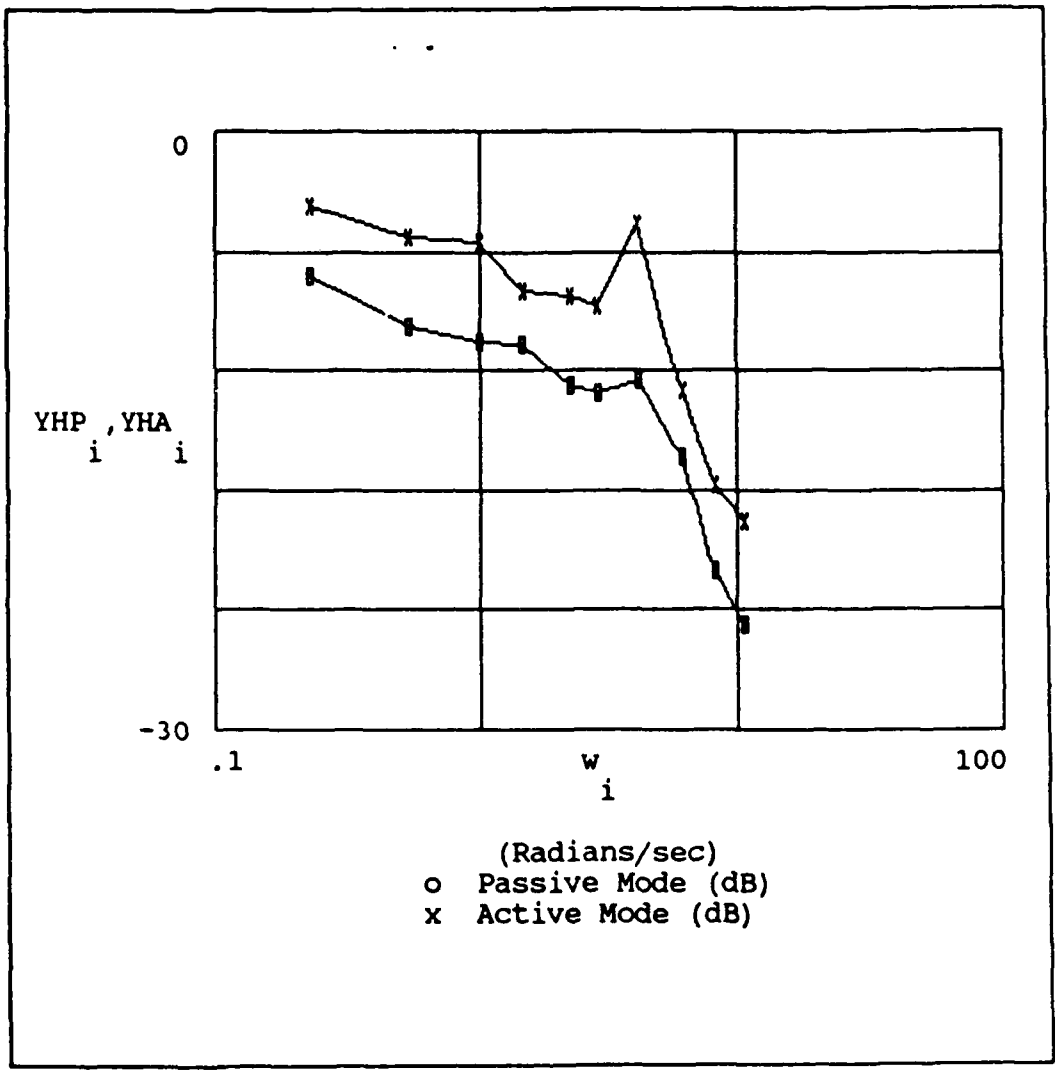

Figure A-4. Human Transfer Function (FF #2)

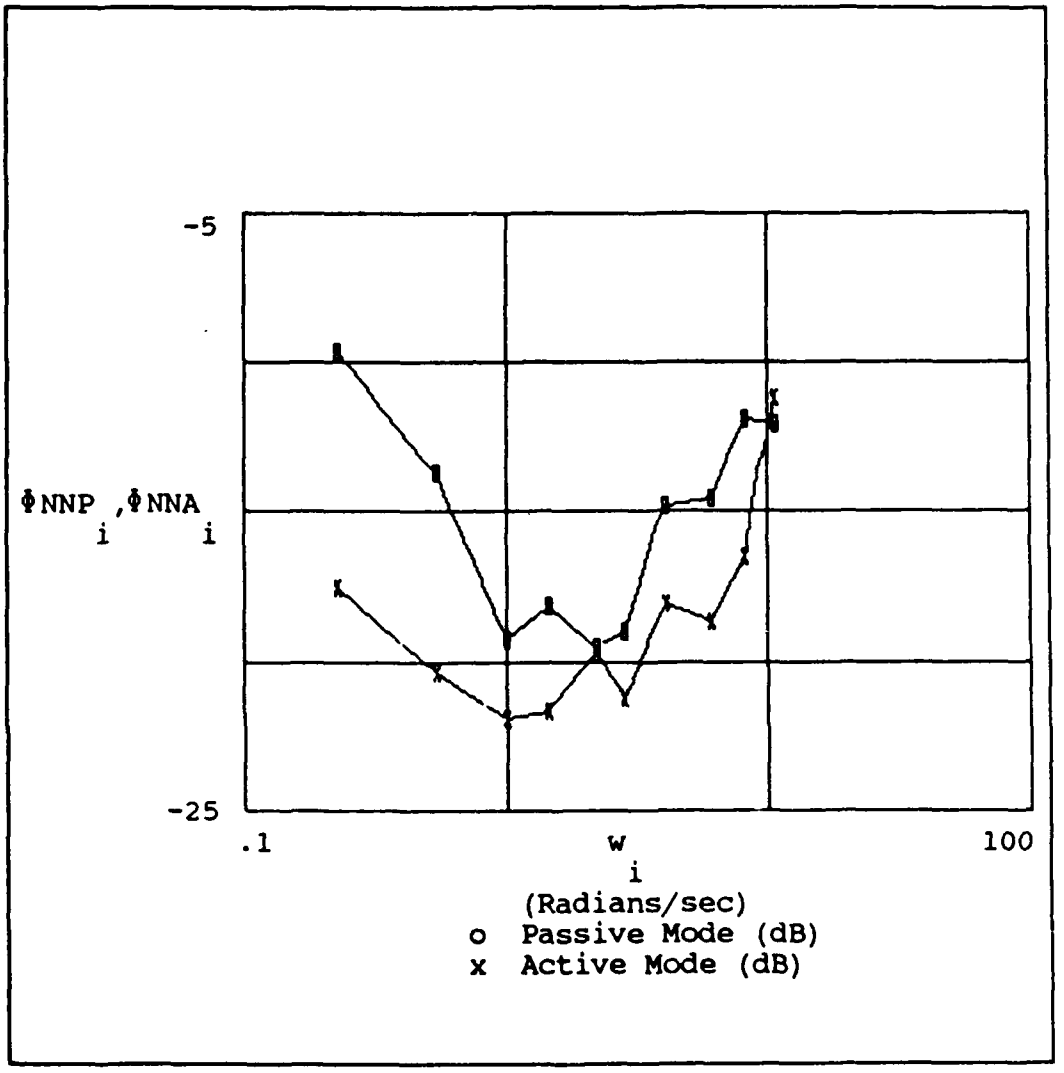

Figure A-5. Operator Noise (FF #2)

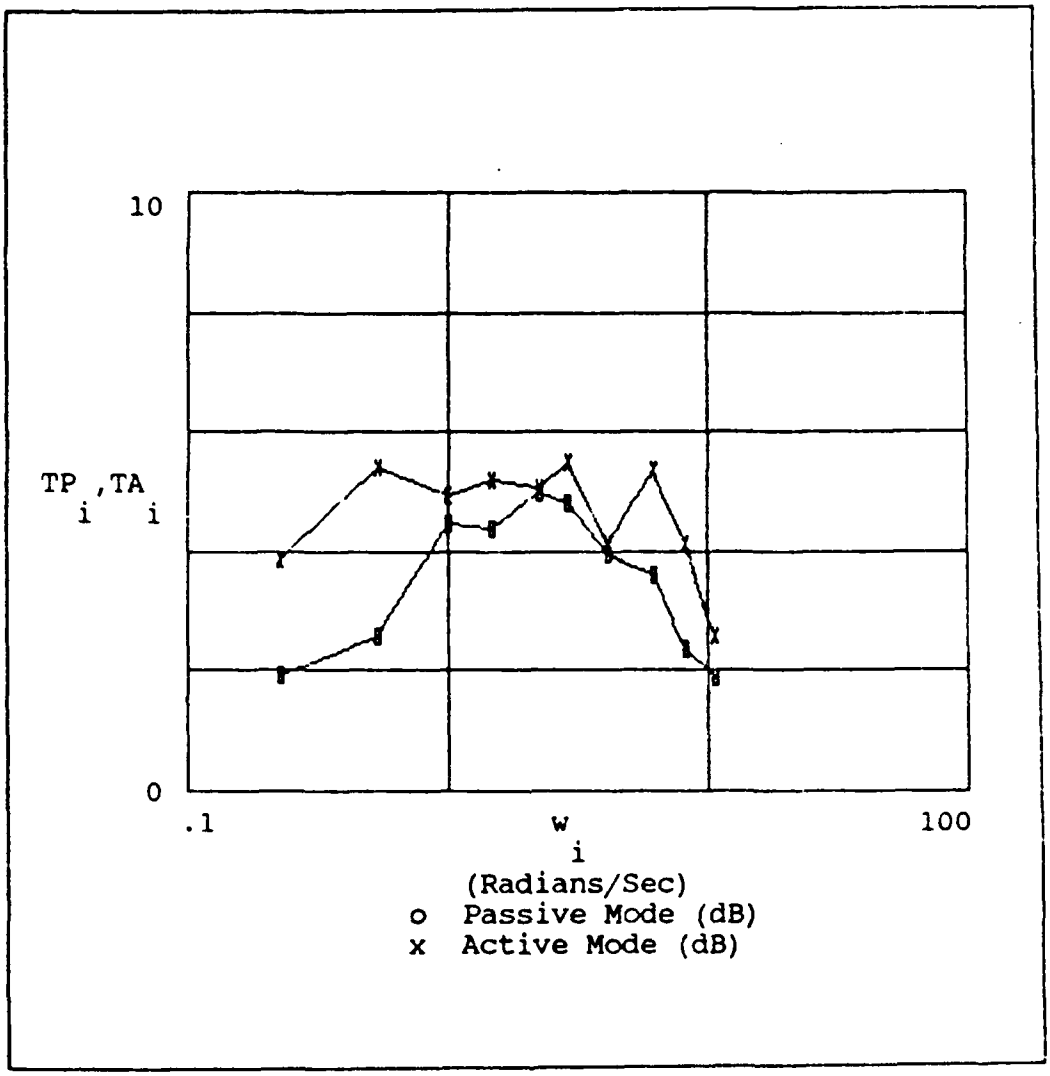

Figure A-6. Transinformation Rate (FF #2)

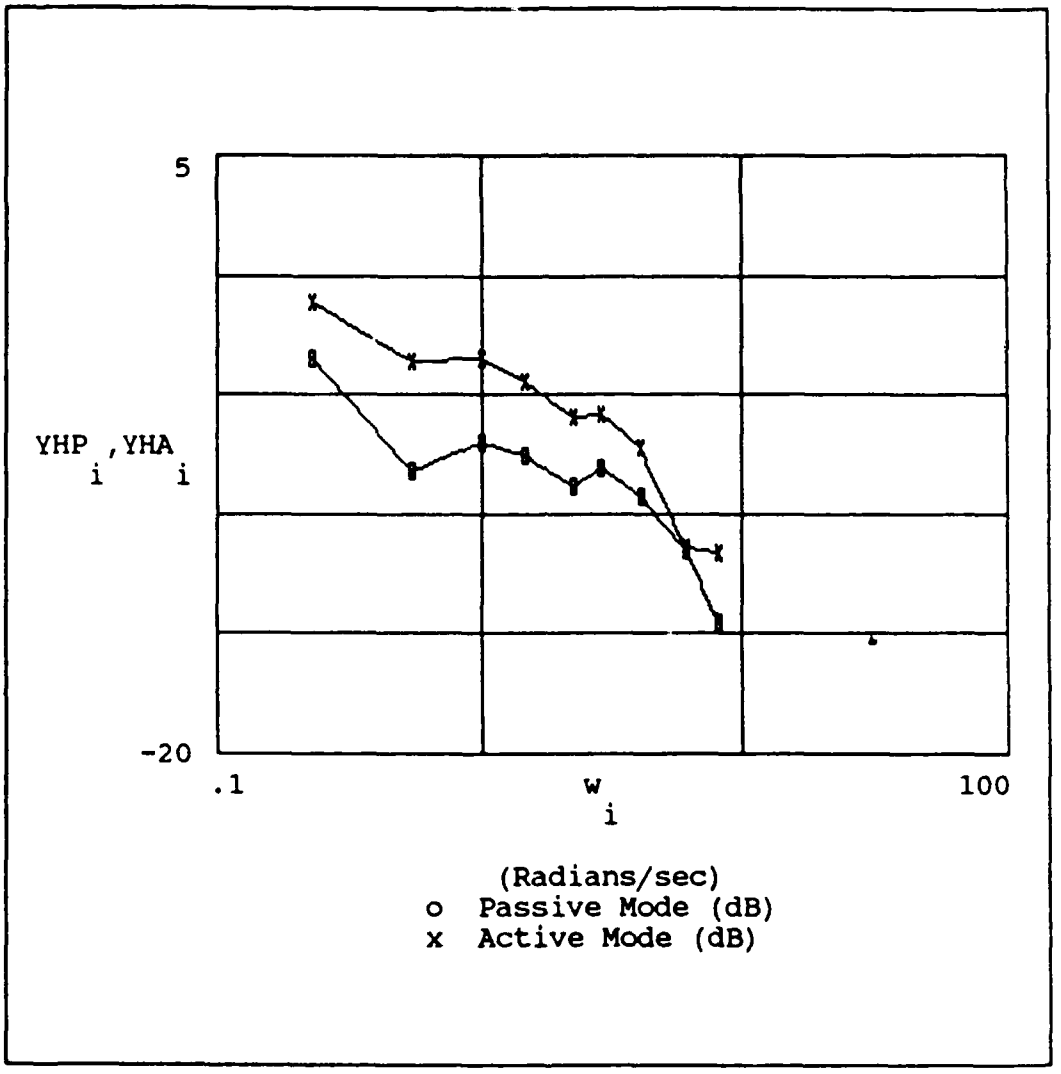

Figure A-7. Human Transfer Function (FF #3)

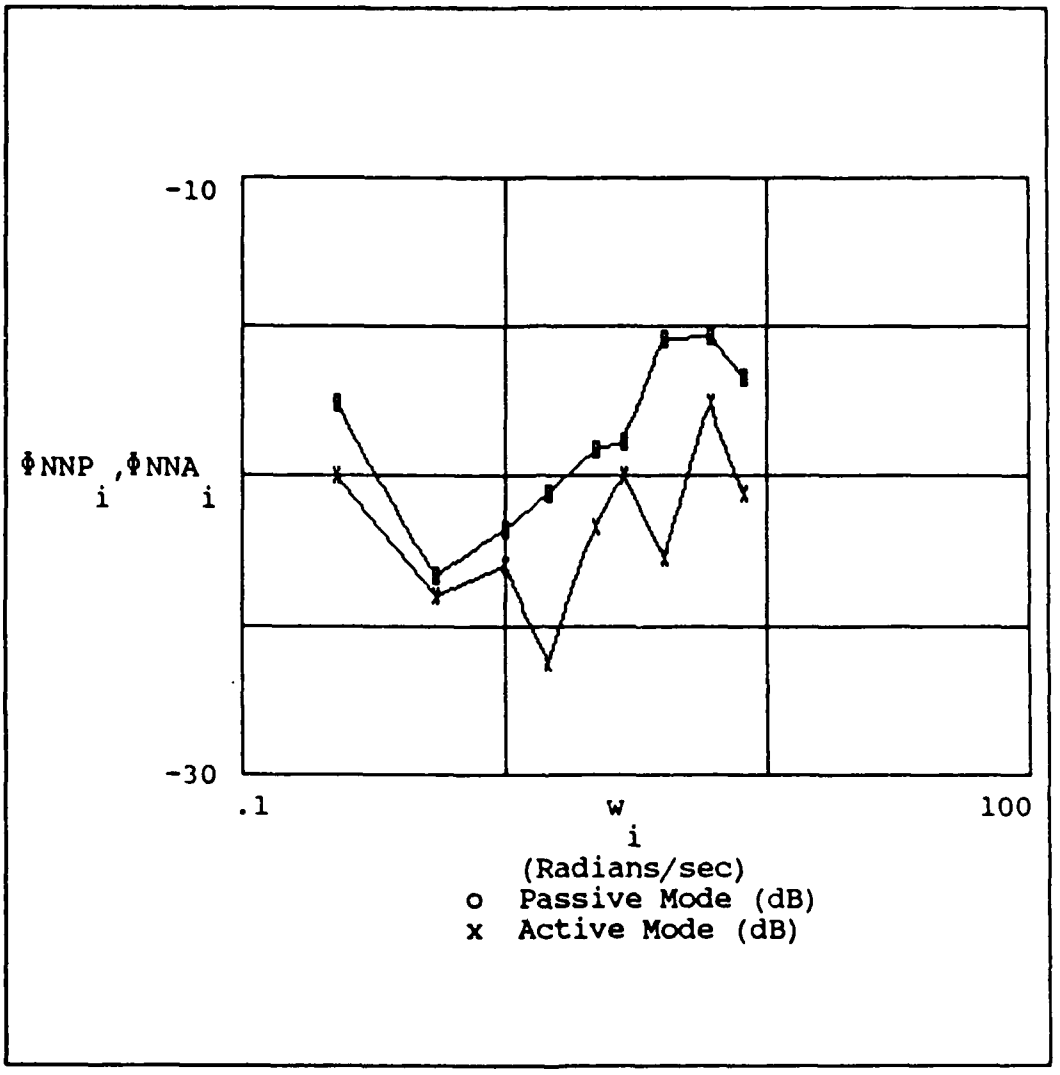

Figure A-8. Operator Noise (FF #3)

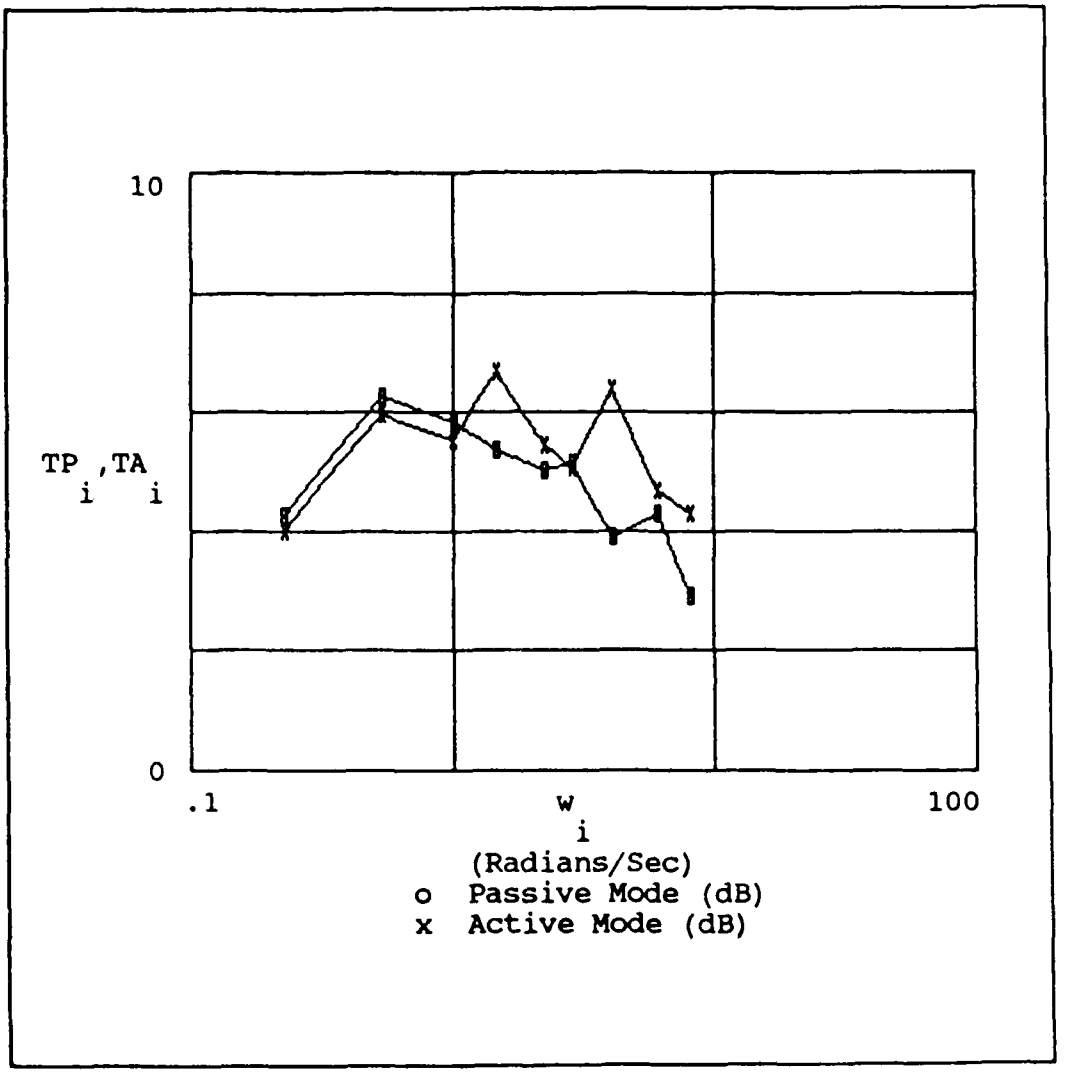

Figure A-9. Transinformation Rate (FF #3)

Appendix B. Graphical Representation of Experimental Results (Subject #2)

This appendix contains the experimental results obtained by testing subject #2. Each graph consists of a visual comparison of the active and passive modes of operation for the human transfer function, the noise remnant, and the transinformation rate for the three forcing functions.

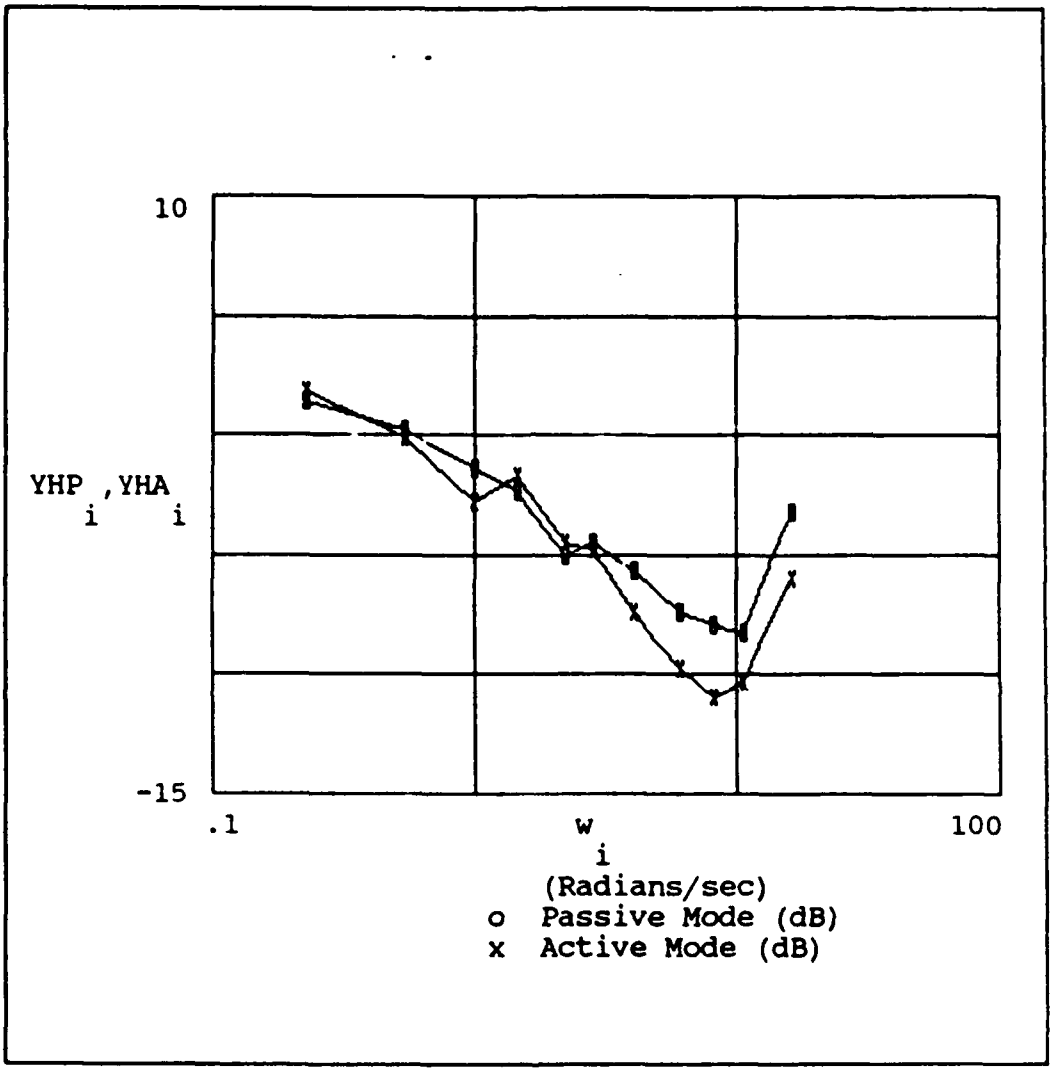

Figure B-1. Human Transfer Function (FF #1)

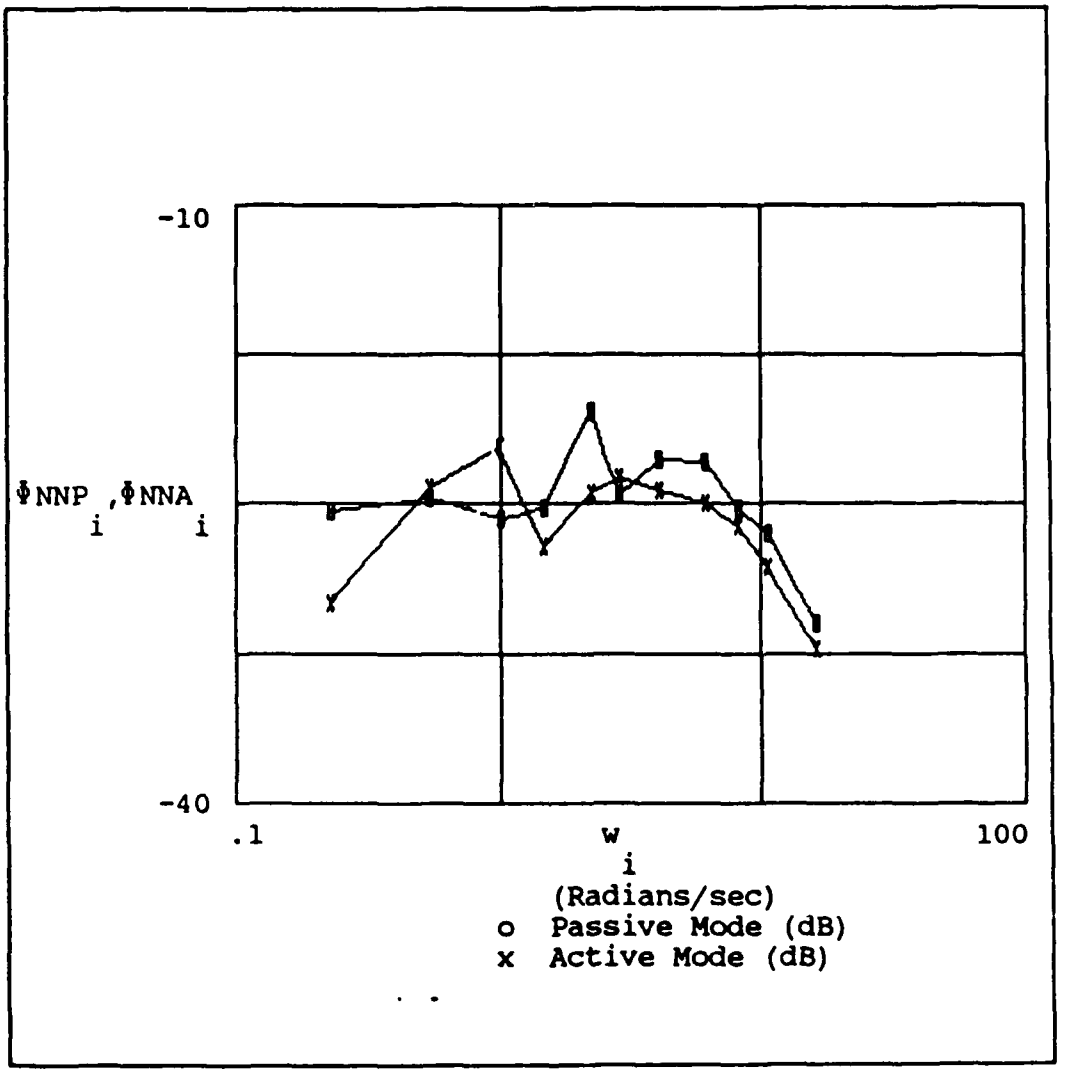

Figure B-2. Operator Noise (FF #1)

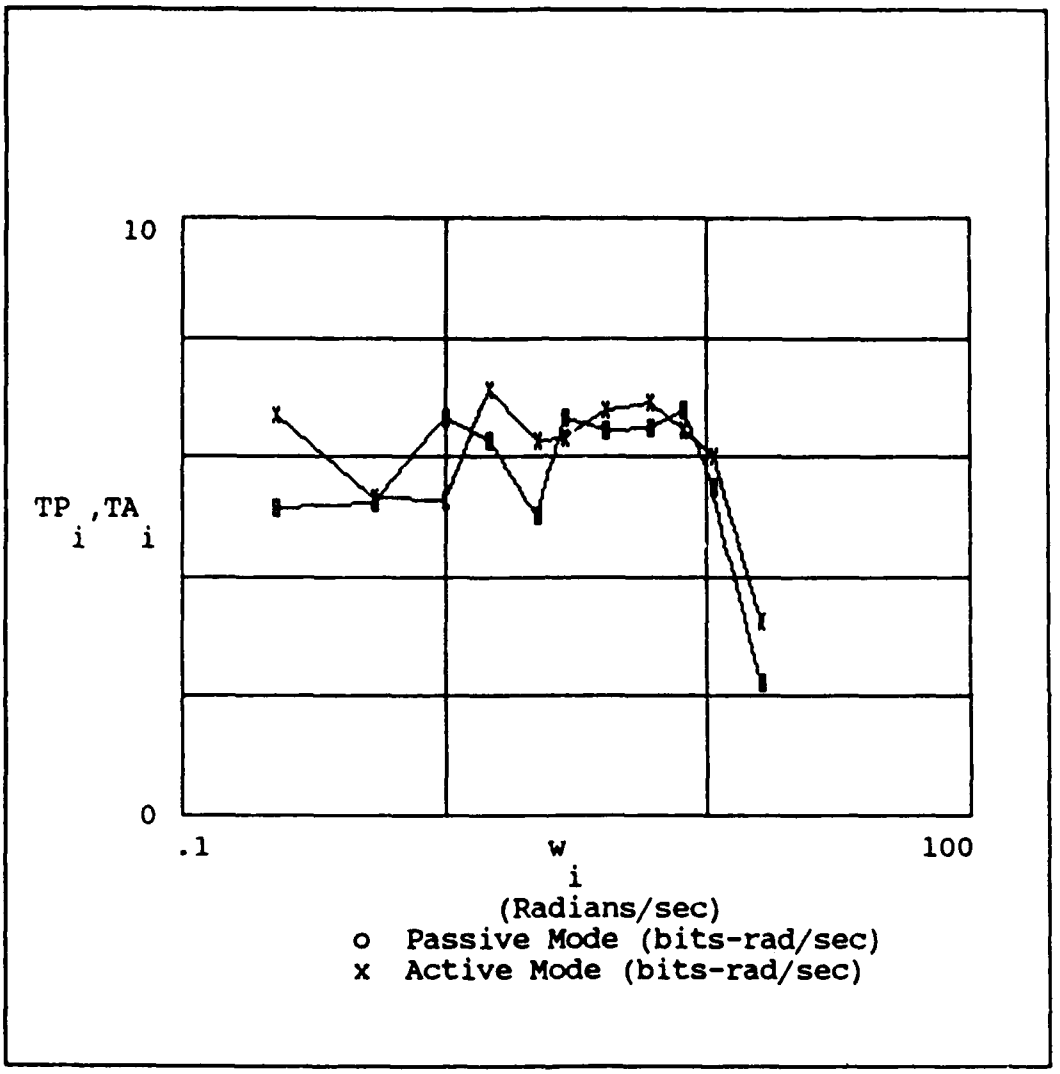

Figure B-3. Transinformation Rate (FF #1)

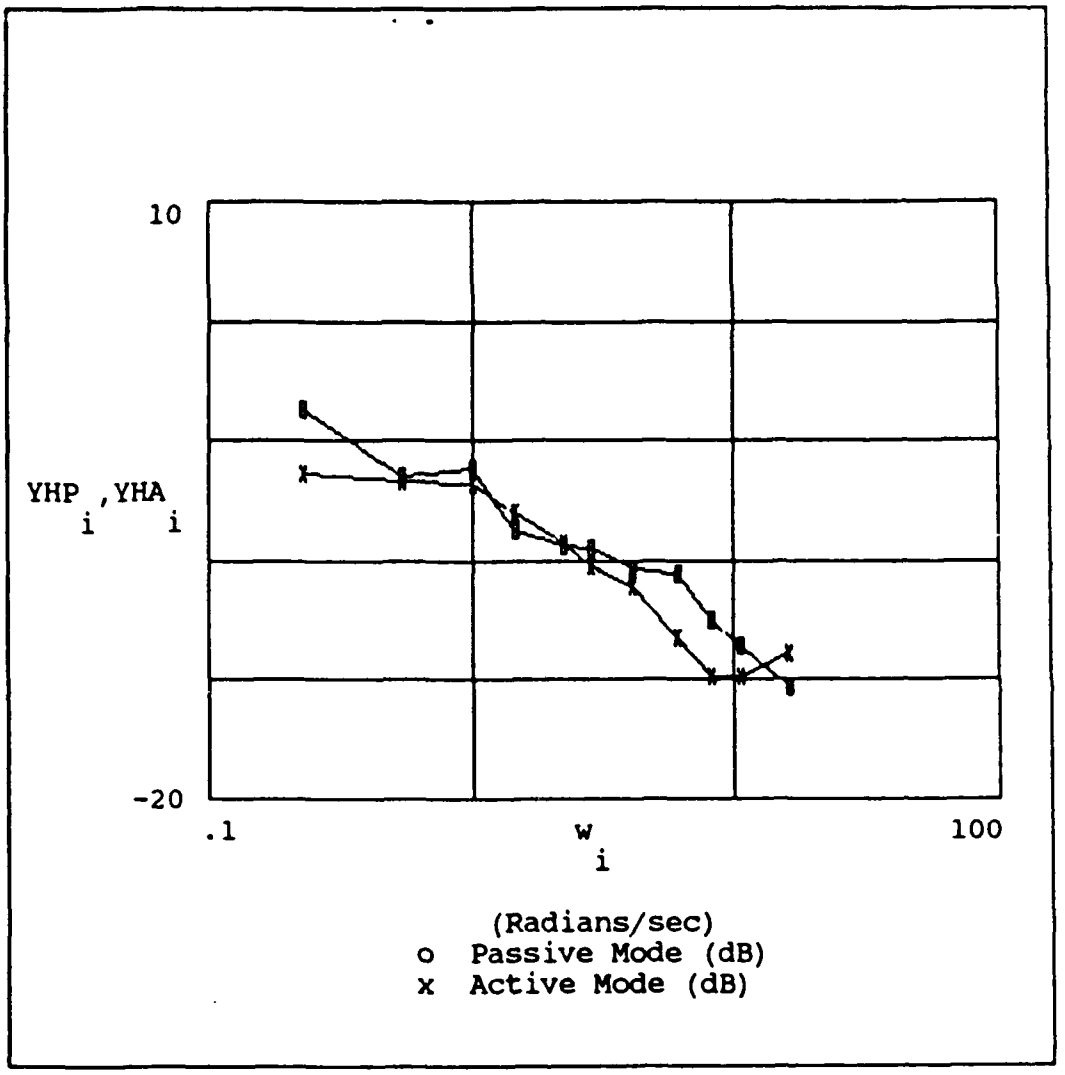

Figure B-4. Human Transfer Function (FF #2)

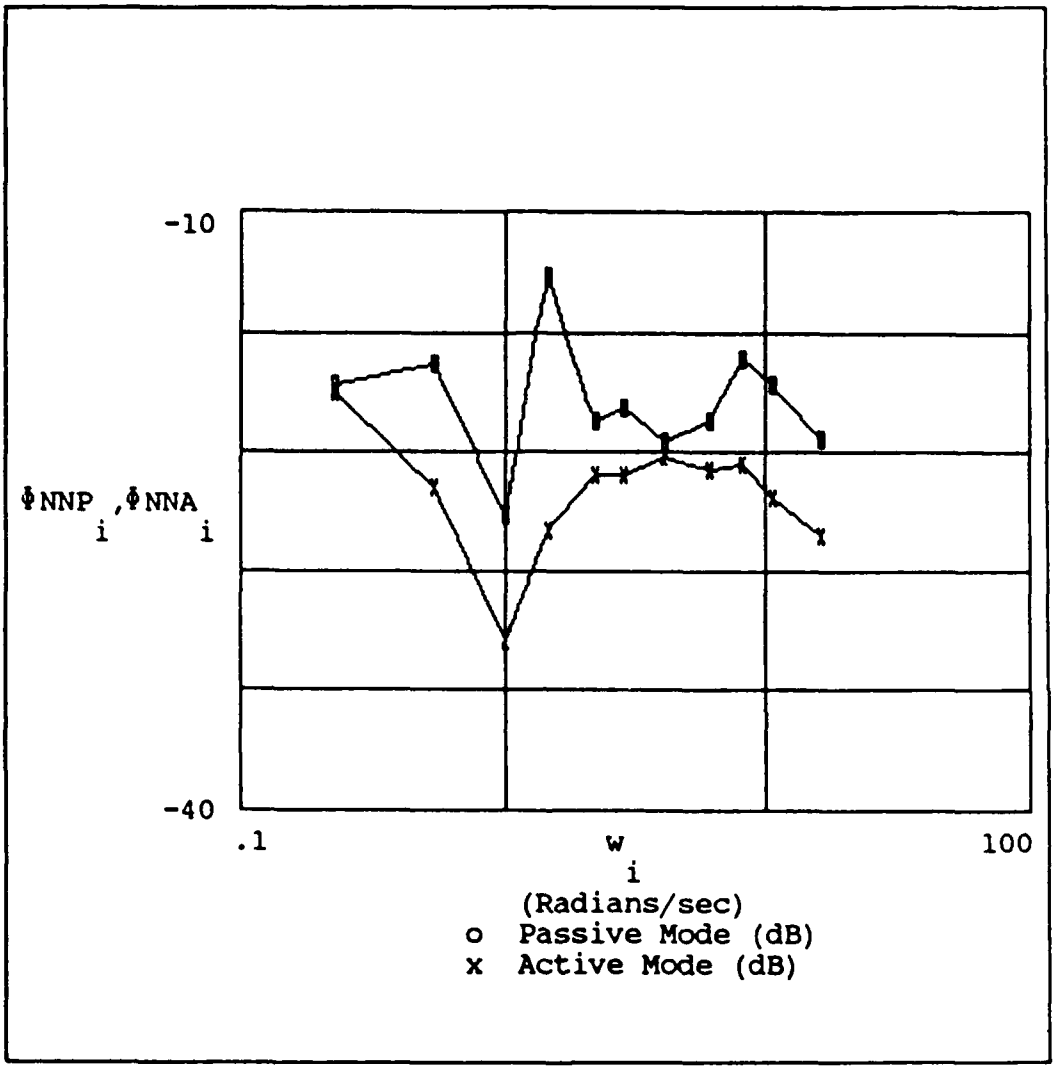

Figure B-5. Operator Noise (FF #2)

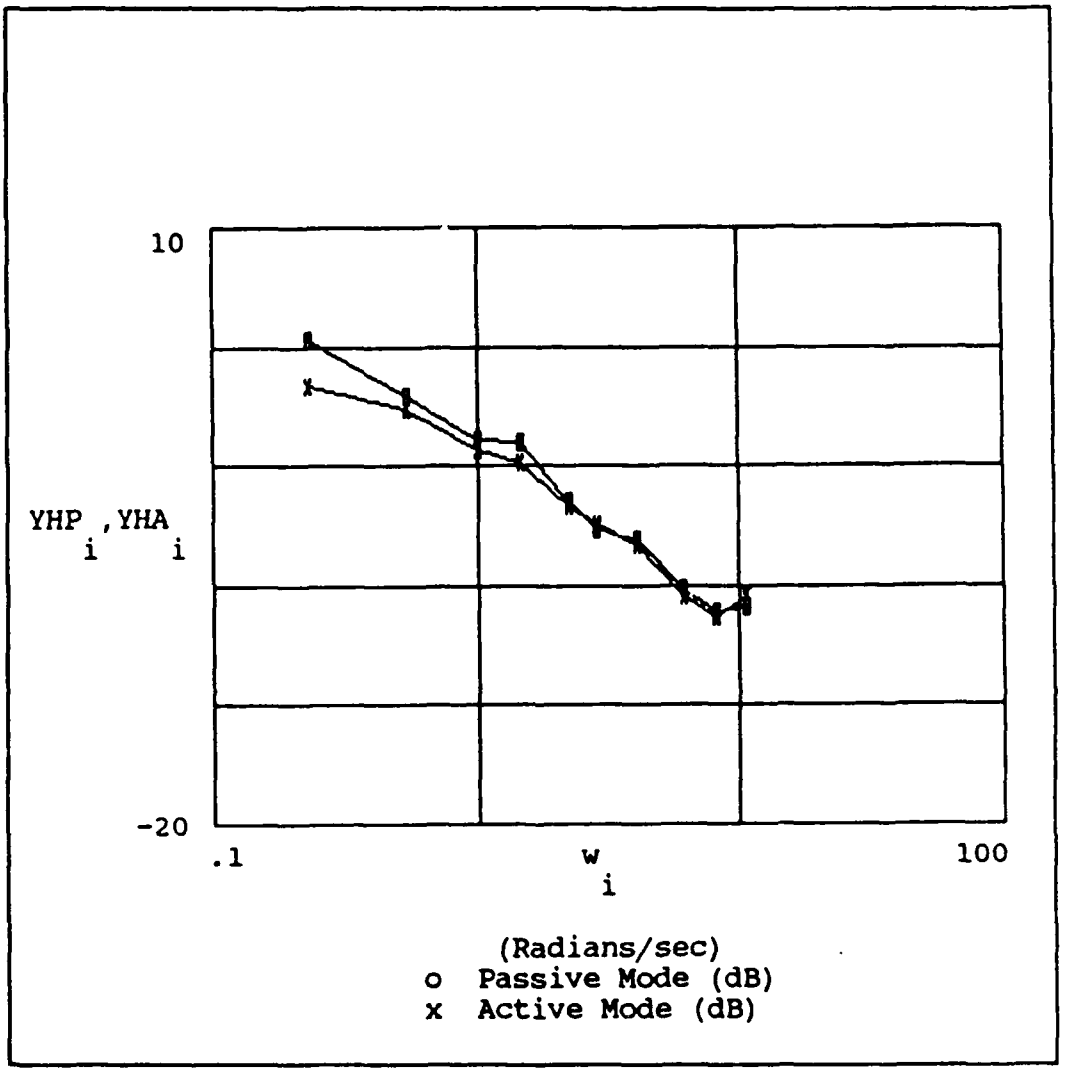

Figure B-6. Transinformation Rate (FF #2)

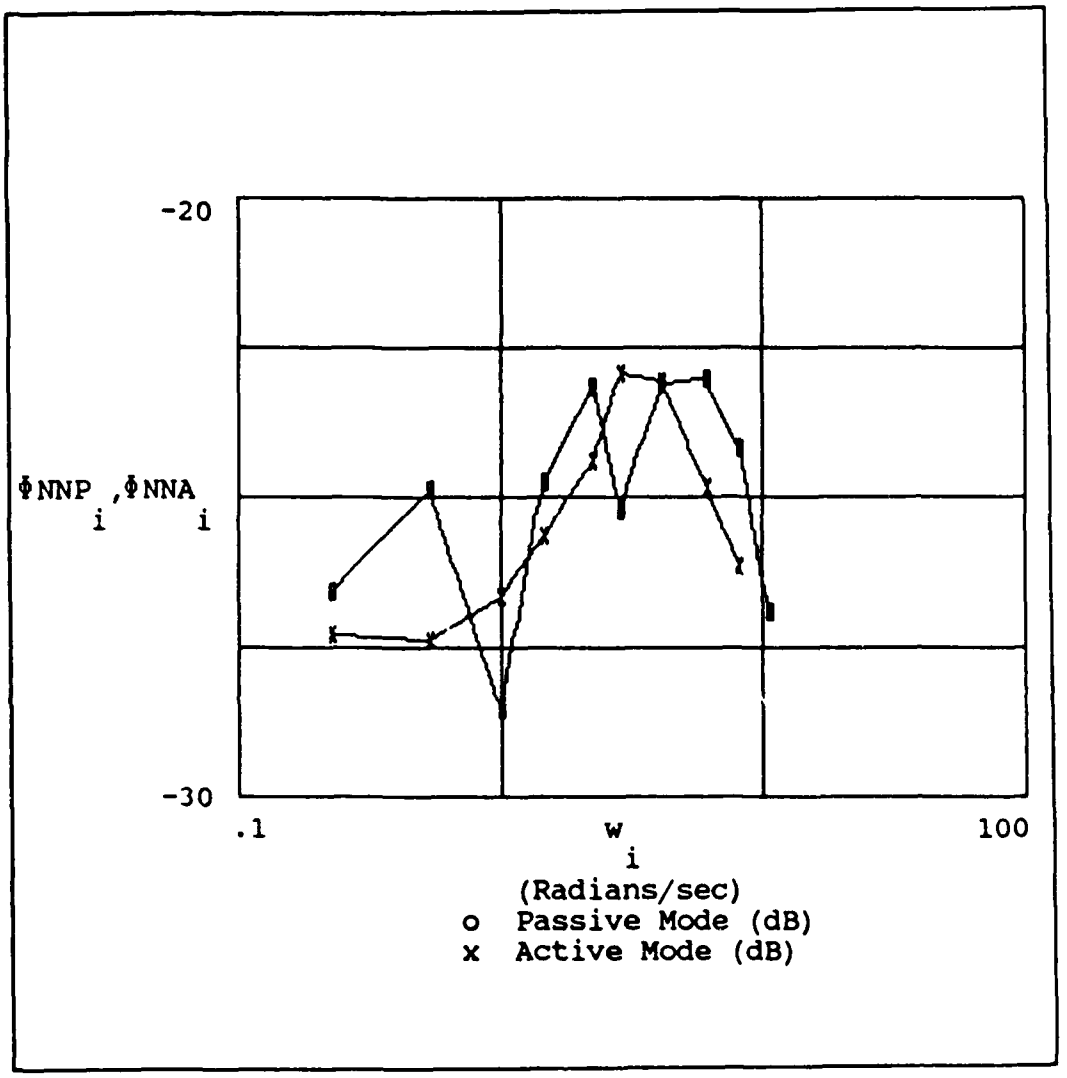

Figure B-7. Human Transfer Function (FF #3)

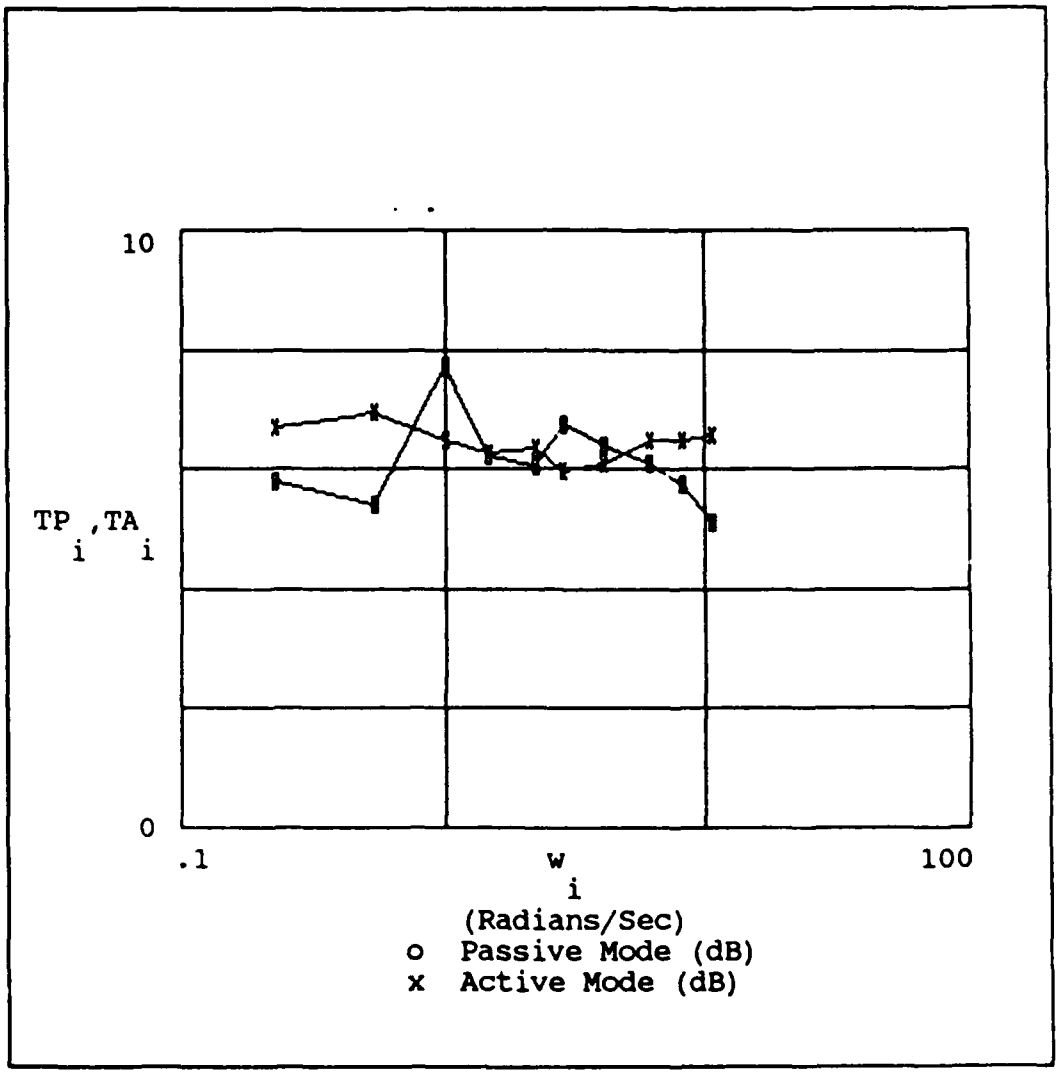

Figure B-8. Operator Noise (FF #3)

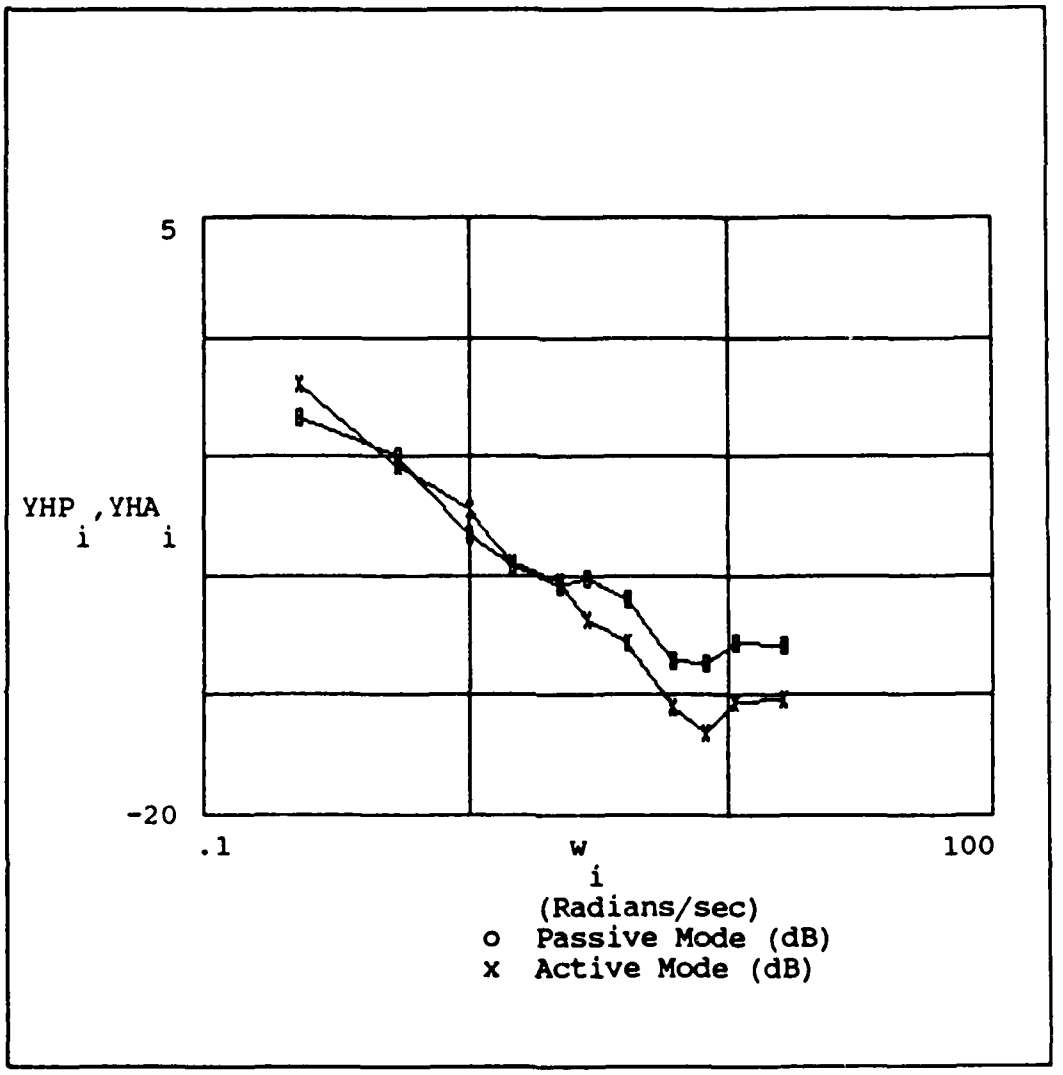

Figure B-9. Transinformation Rate (FF #3)

Appendix C. Graphical Representation of Experimental Results (Subject #4)

This appendix contains the experimental results obtained by testing subject #4. Each graph consists of a visual comparison of the active and passive modes of operation for the human transfer function, the noise remnant, and the transinformation rate for the three forcing functions.

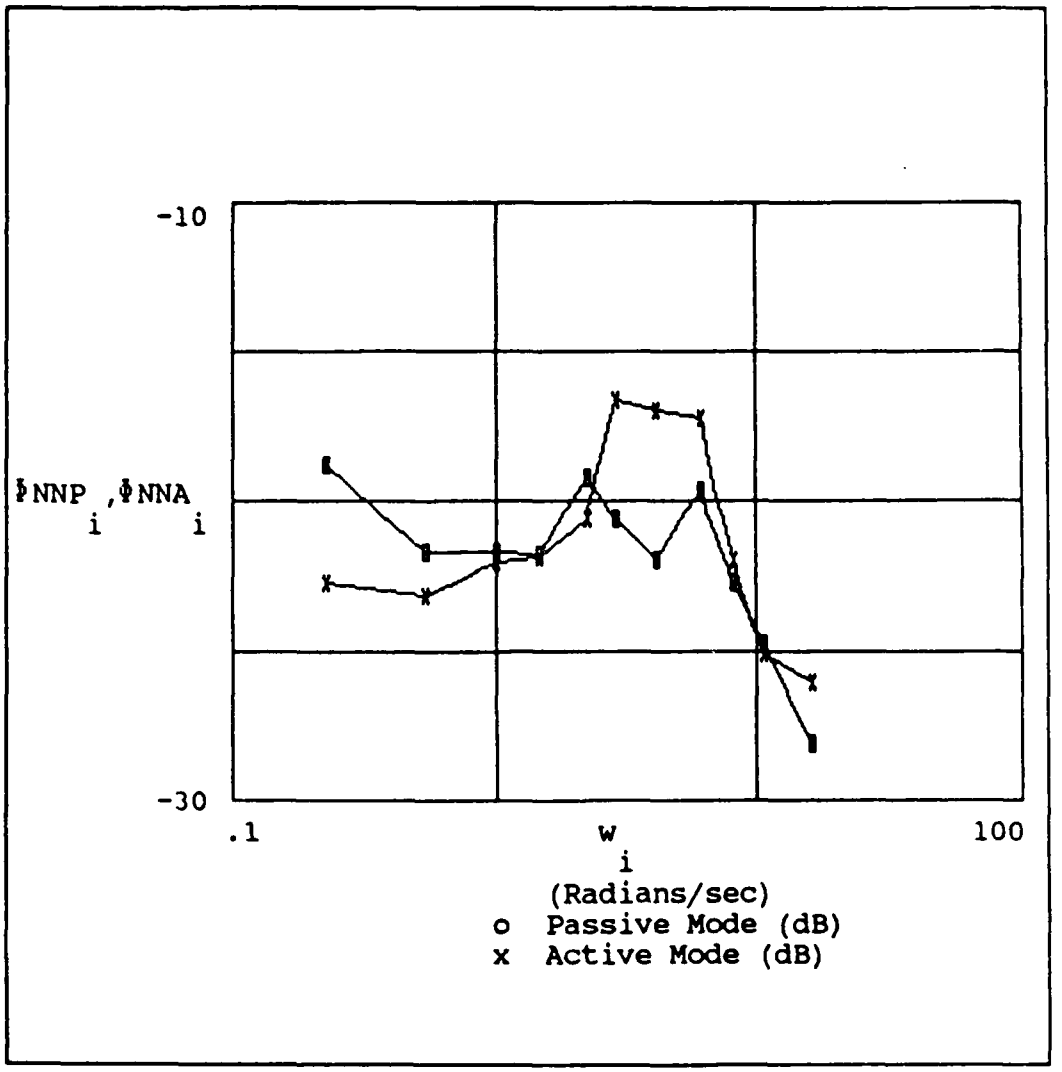

Figure C-1. Human Transfer Function (FF #1)

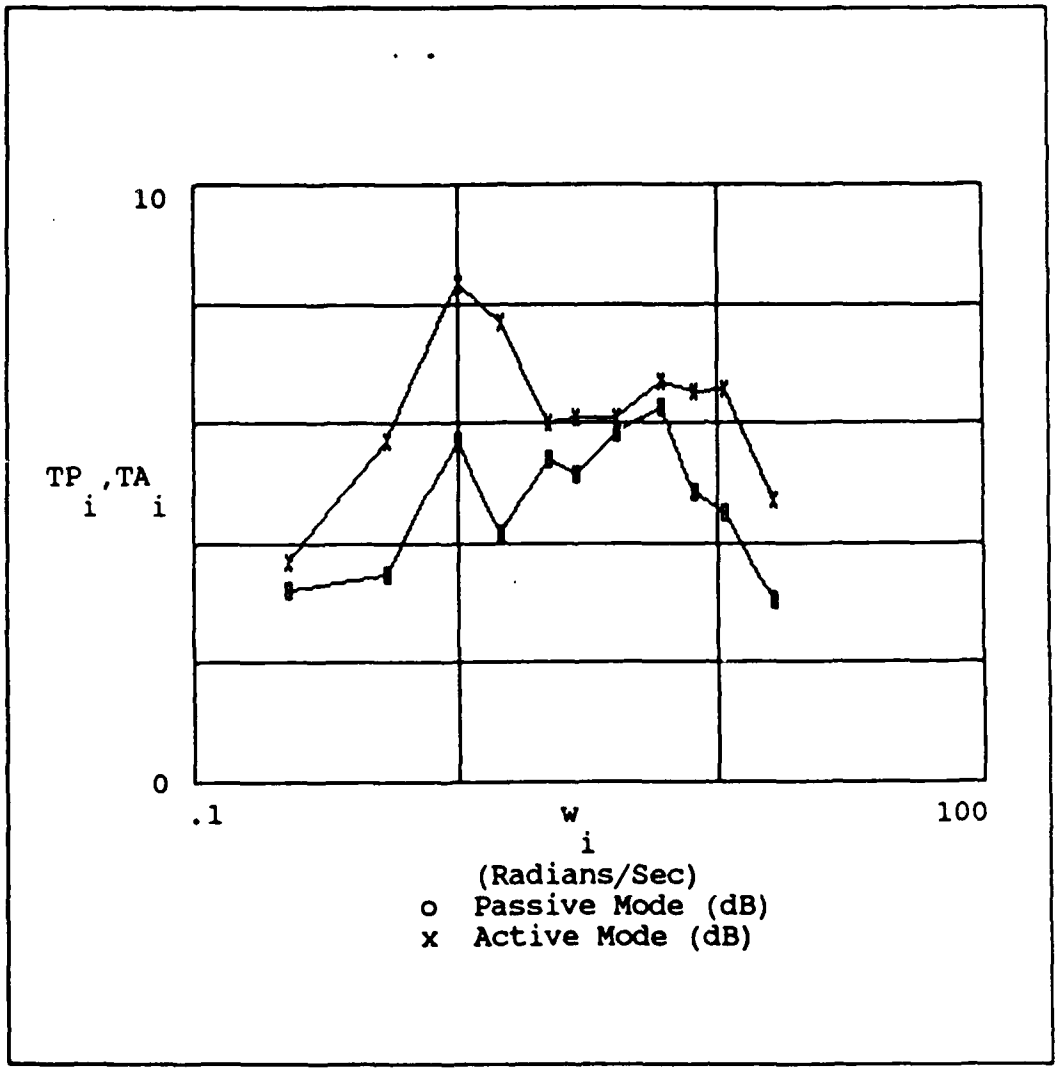

Figure C-2. Operator Noise (FF #1)

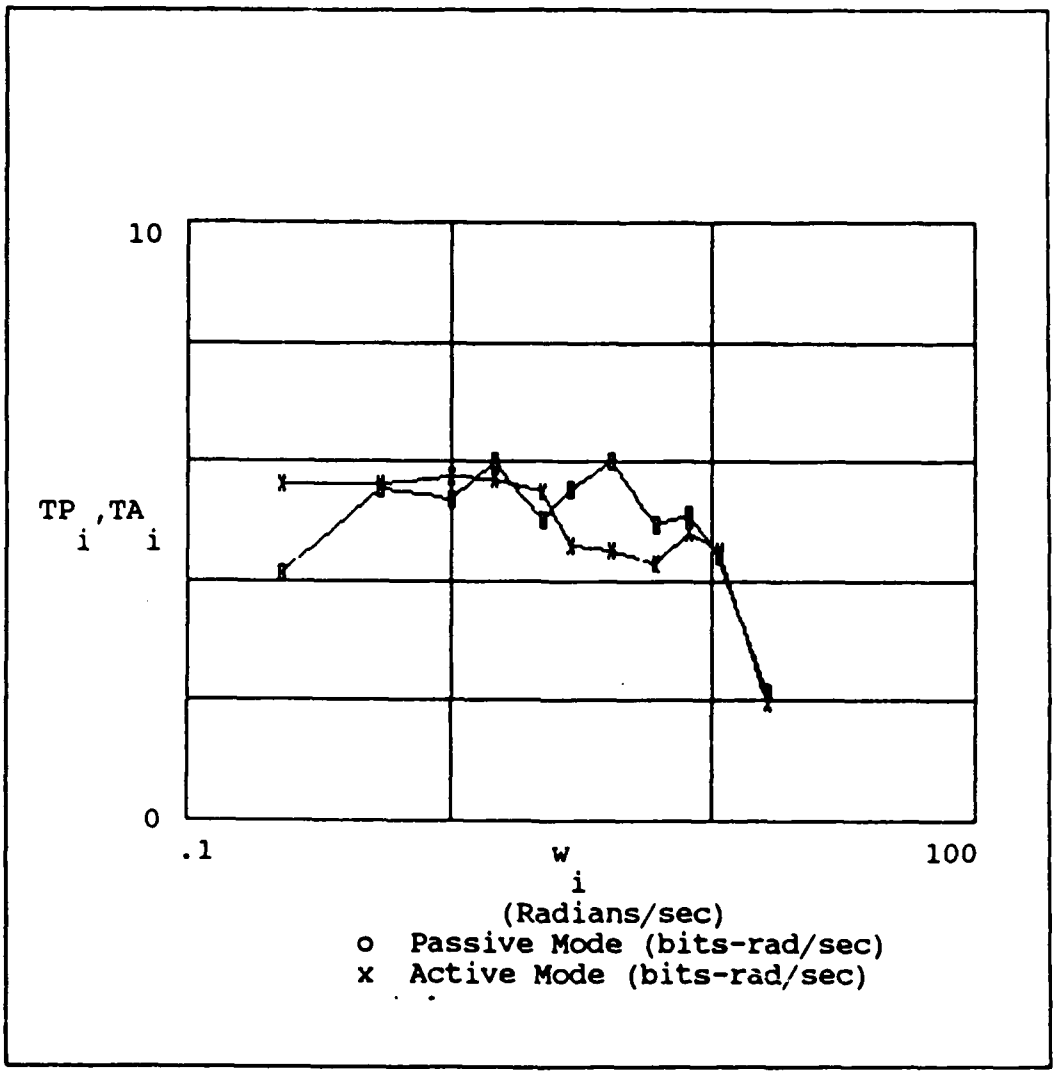

Figure C-3. Transinformation Rate (FF #1)

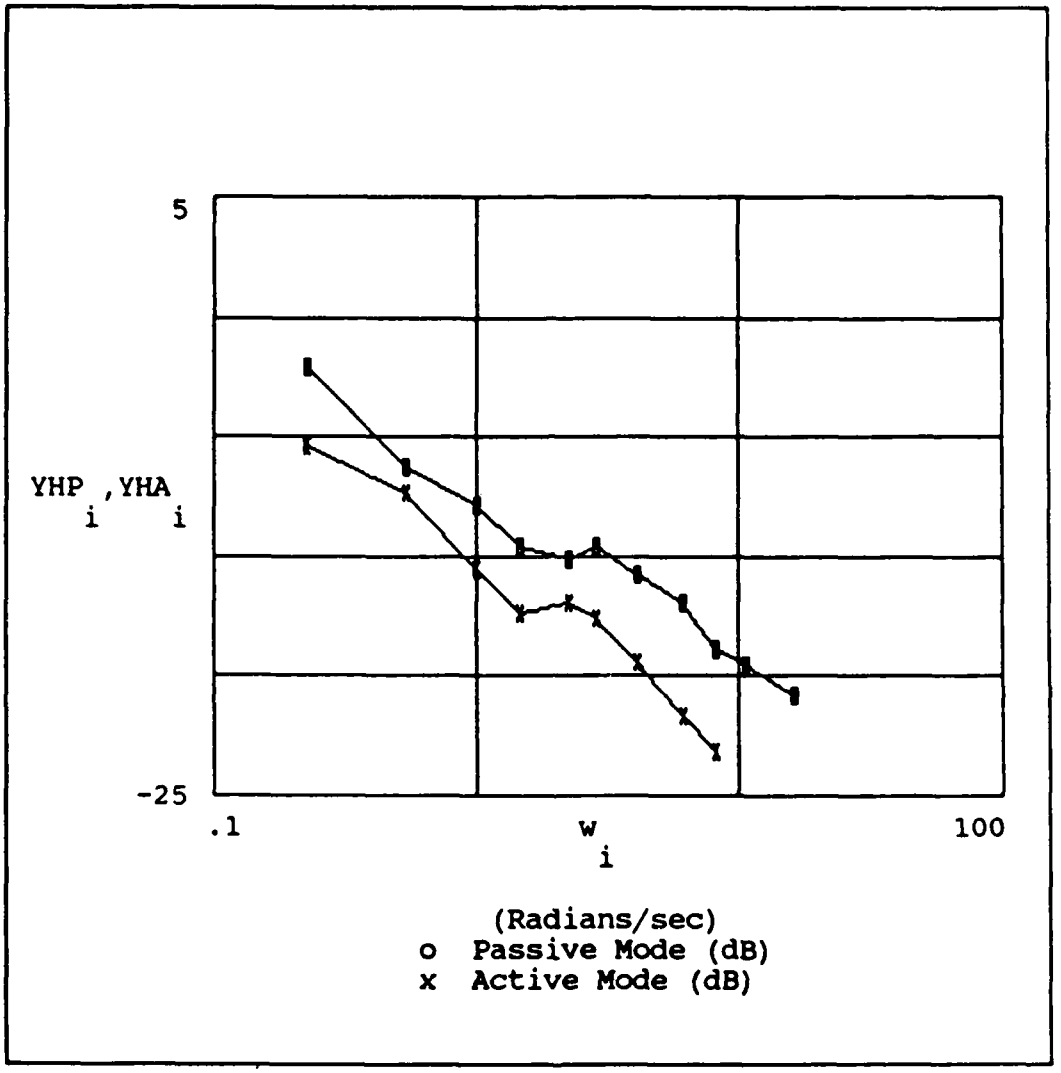

Figure C-4. Human Transfer Function (FF #2)

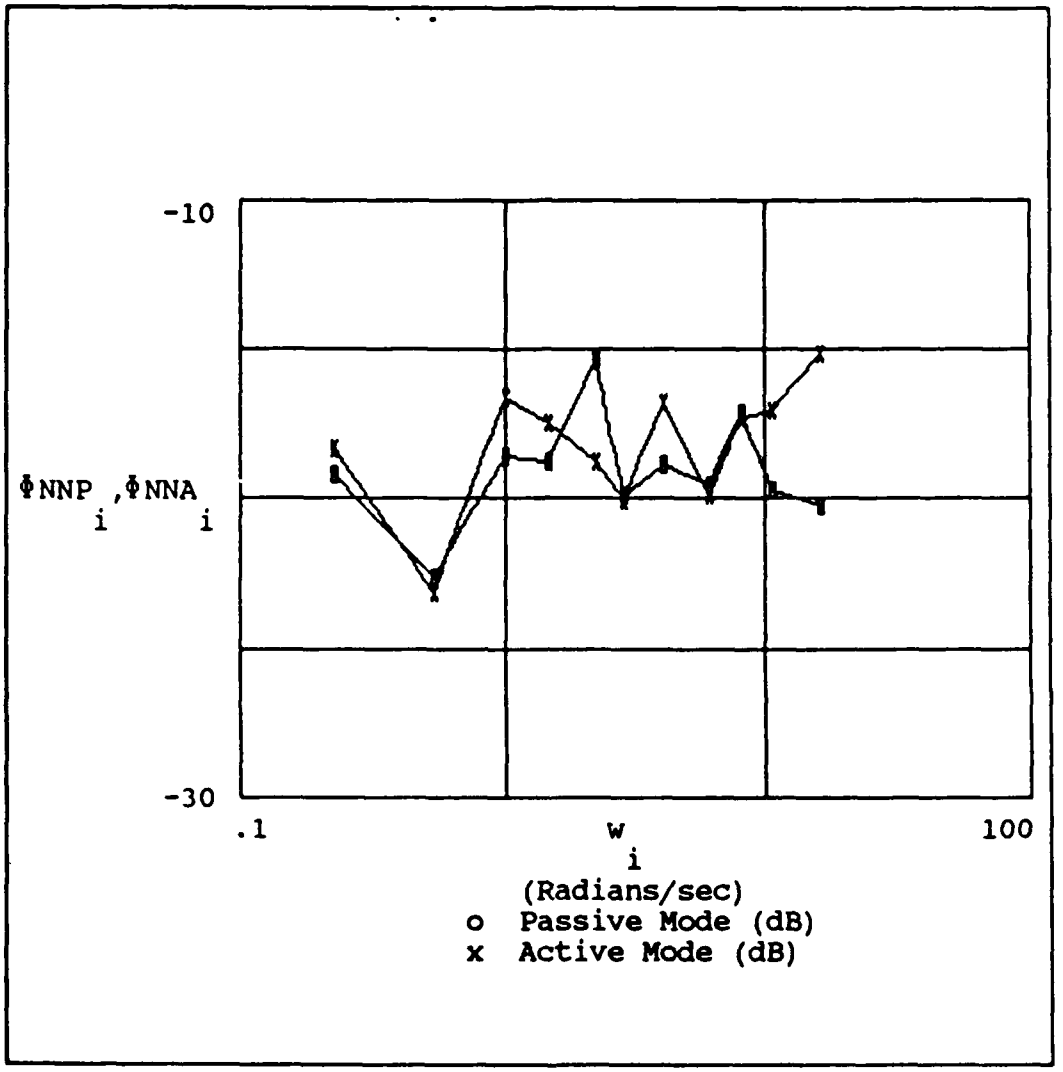

Figure C-5. Operator Noise (FF #2)

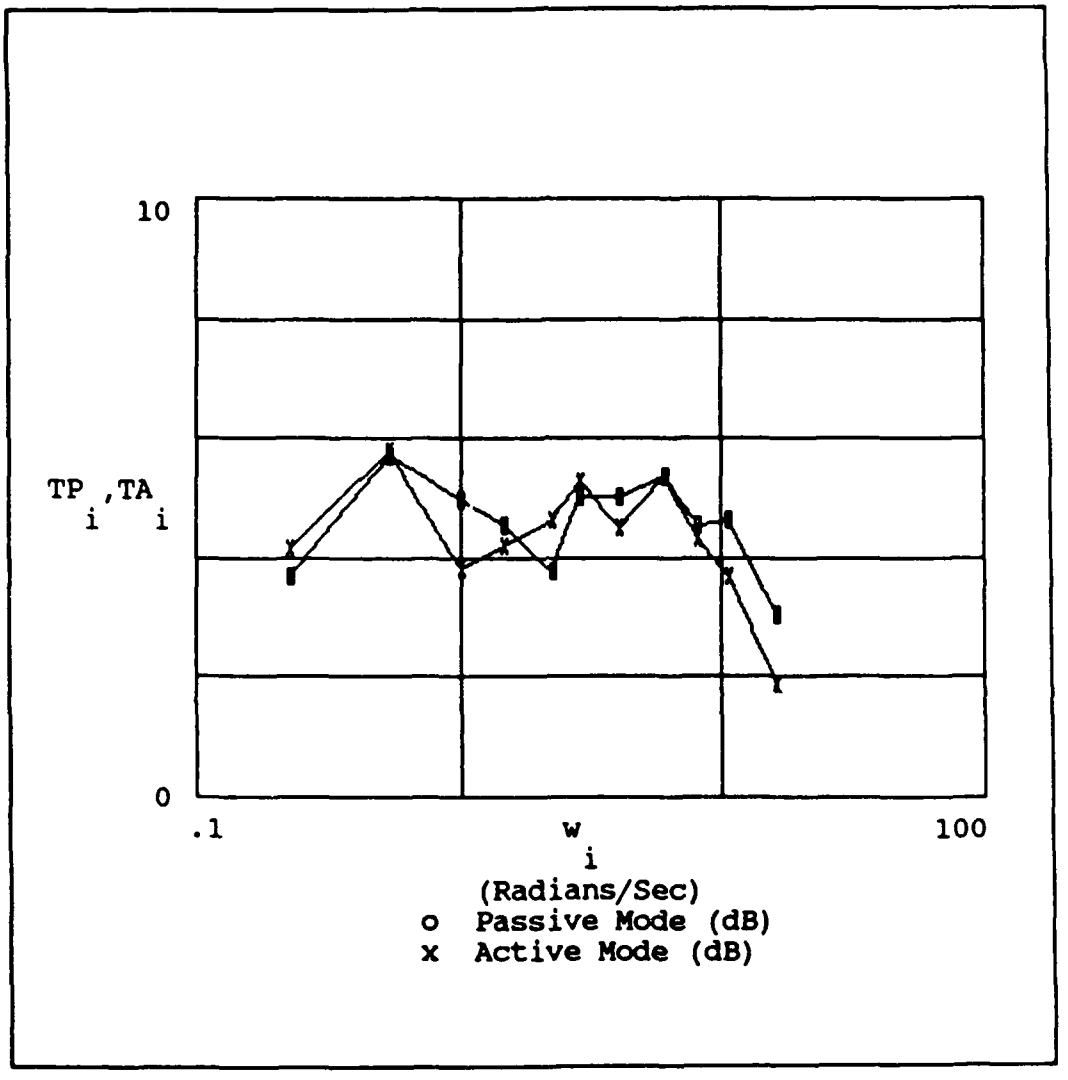

Figure C-6. Transinformation Rate (FF #2)

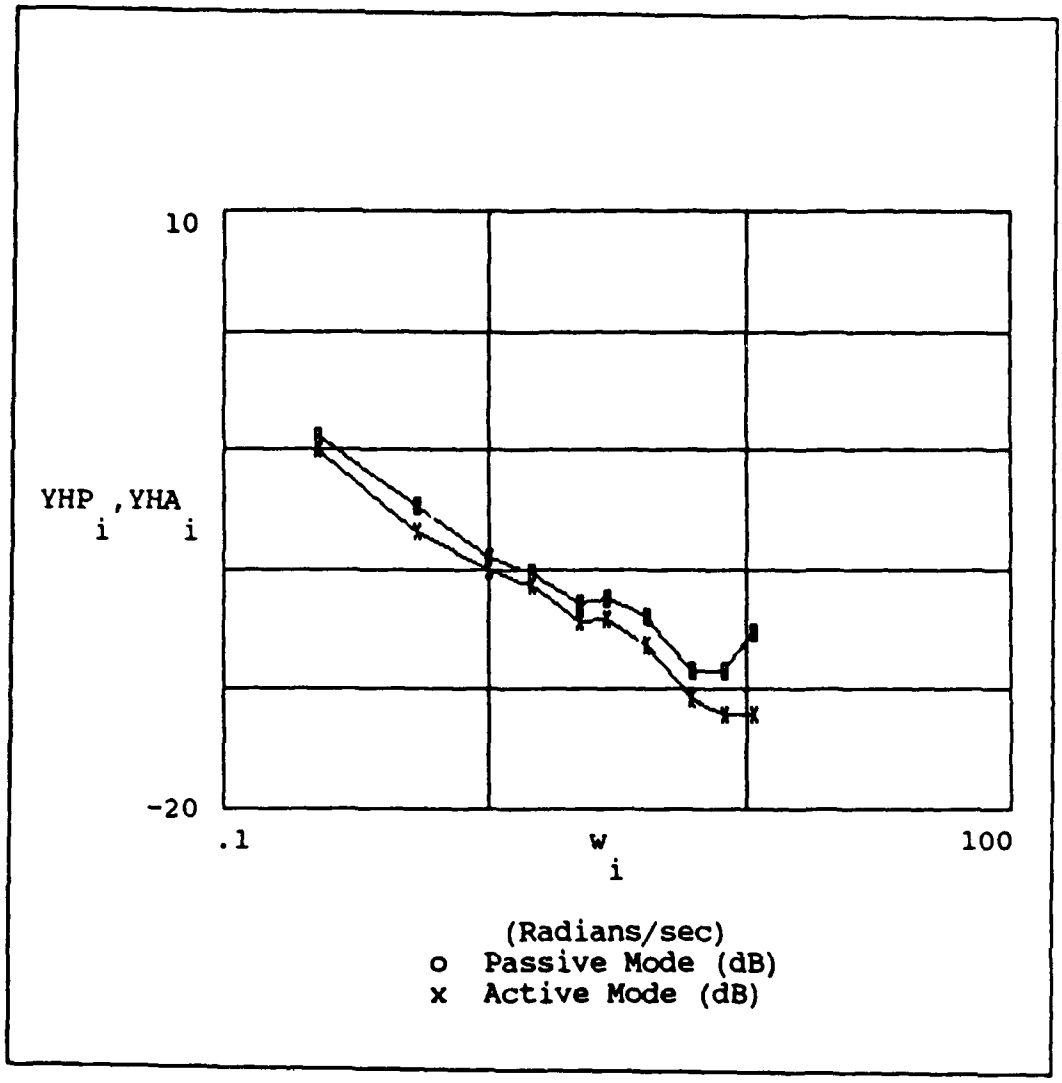

Figure C-7. Human Transfer Function (FF #3)

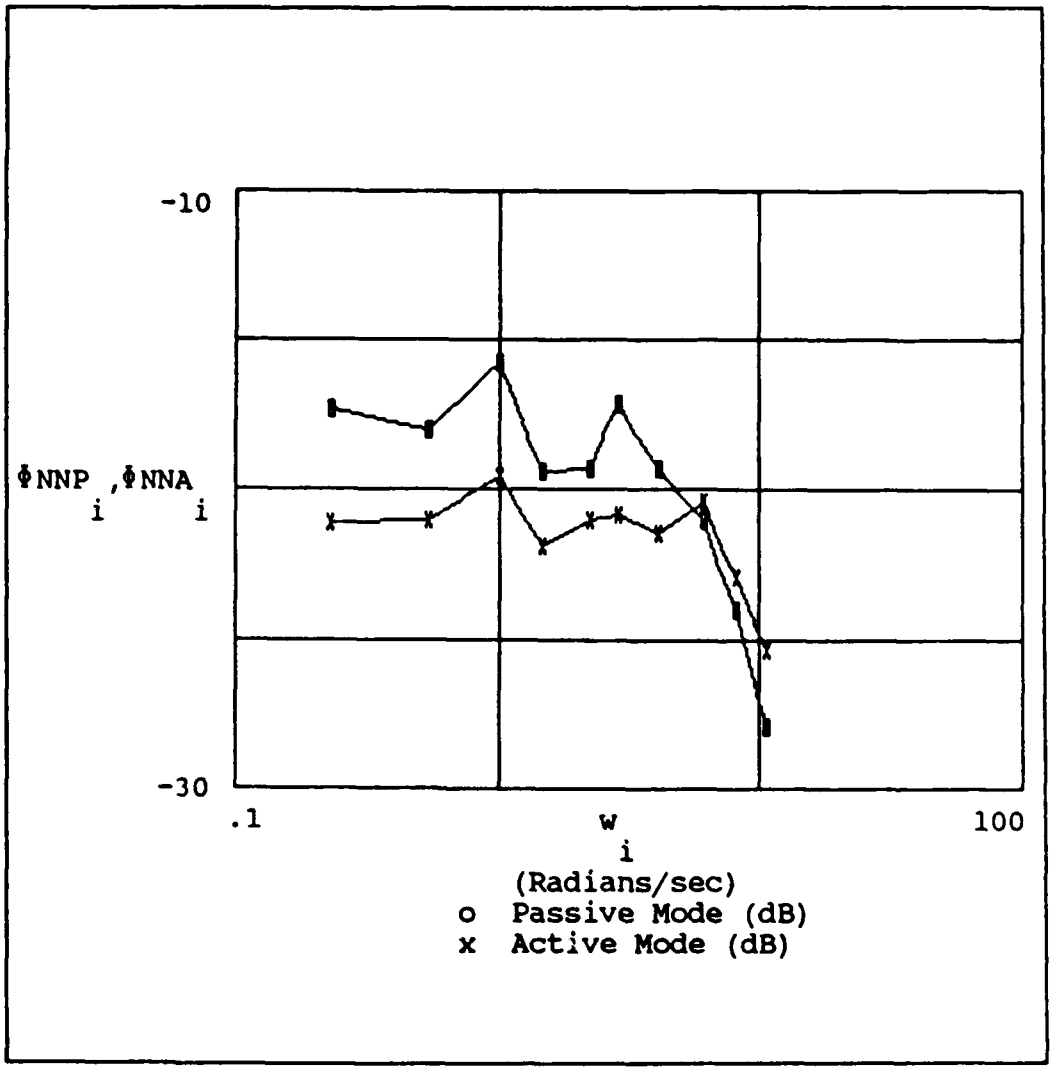

Figure C-8. Operator Noise (FF #3)

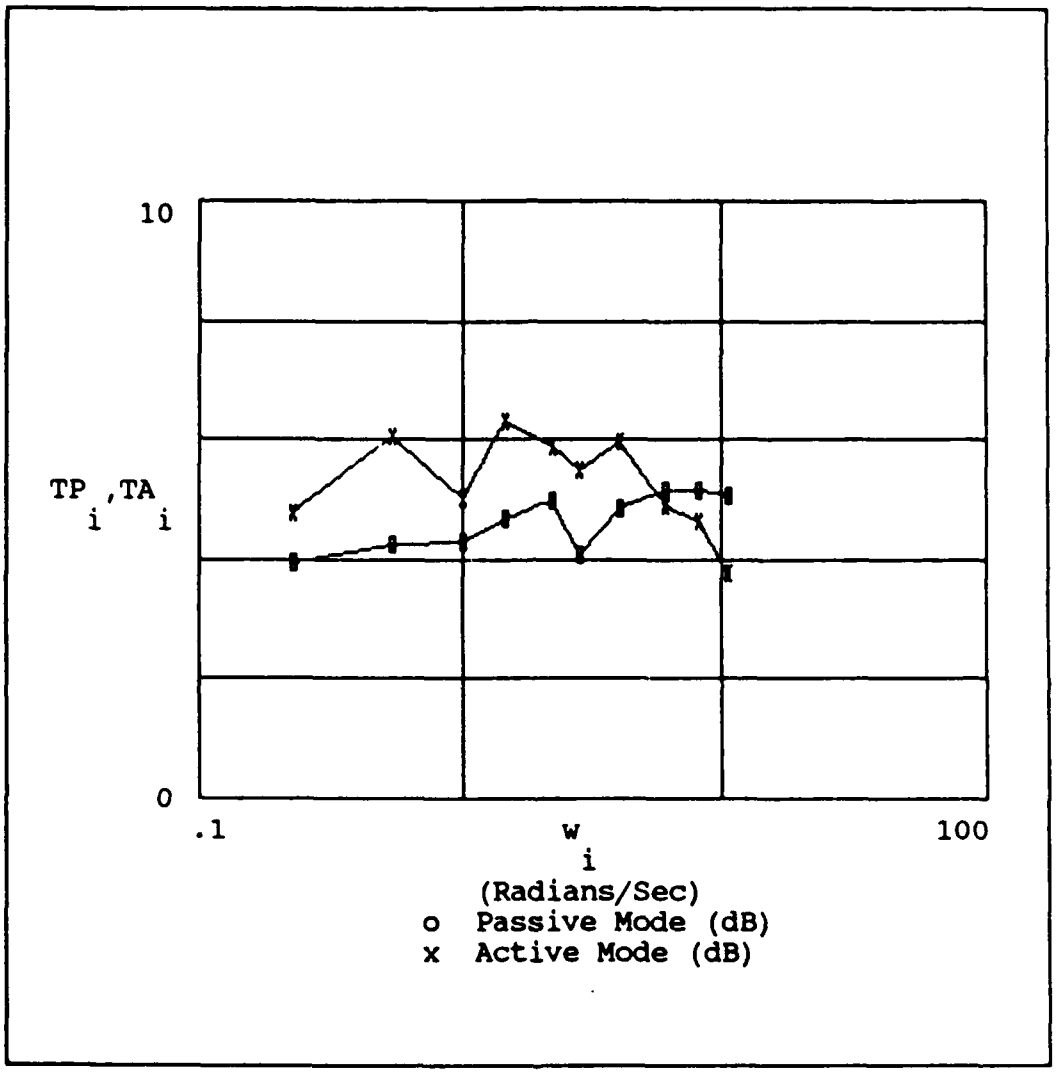

Figure C-9. Transinformation Rate (FF #3)

Appendix D. Graphical Representation of Experimental Results (Subject #5)

This appendix contains the experimental results obtained by testing subject #5. Each graph consists of a visual comparison of the active and passive modes of operation for the human transfer function, the noise remnant, and the transinformation rate for the three forcing functions.

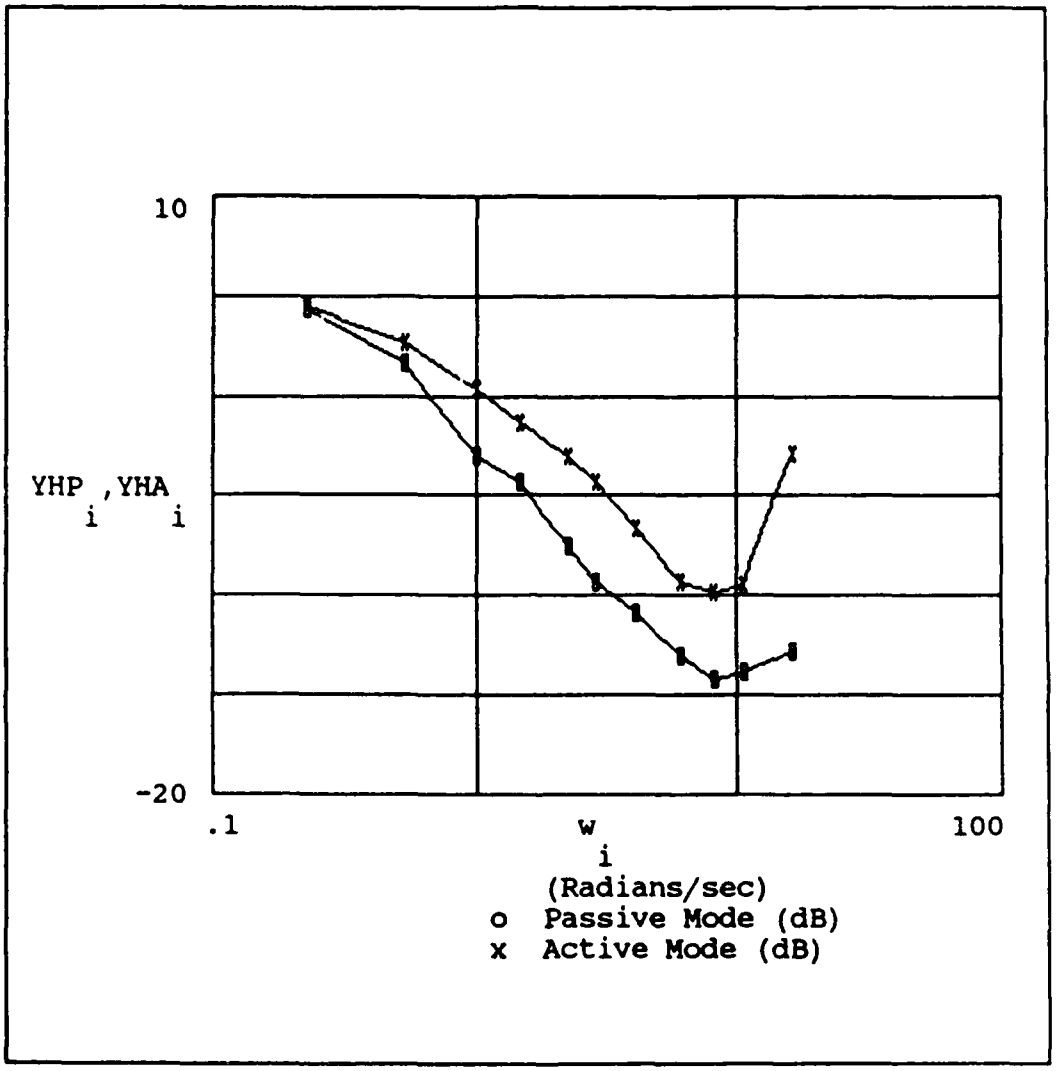

Figure D-1. Human Transfer Function (FF #1)

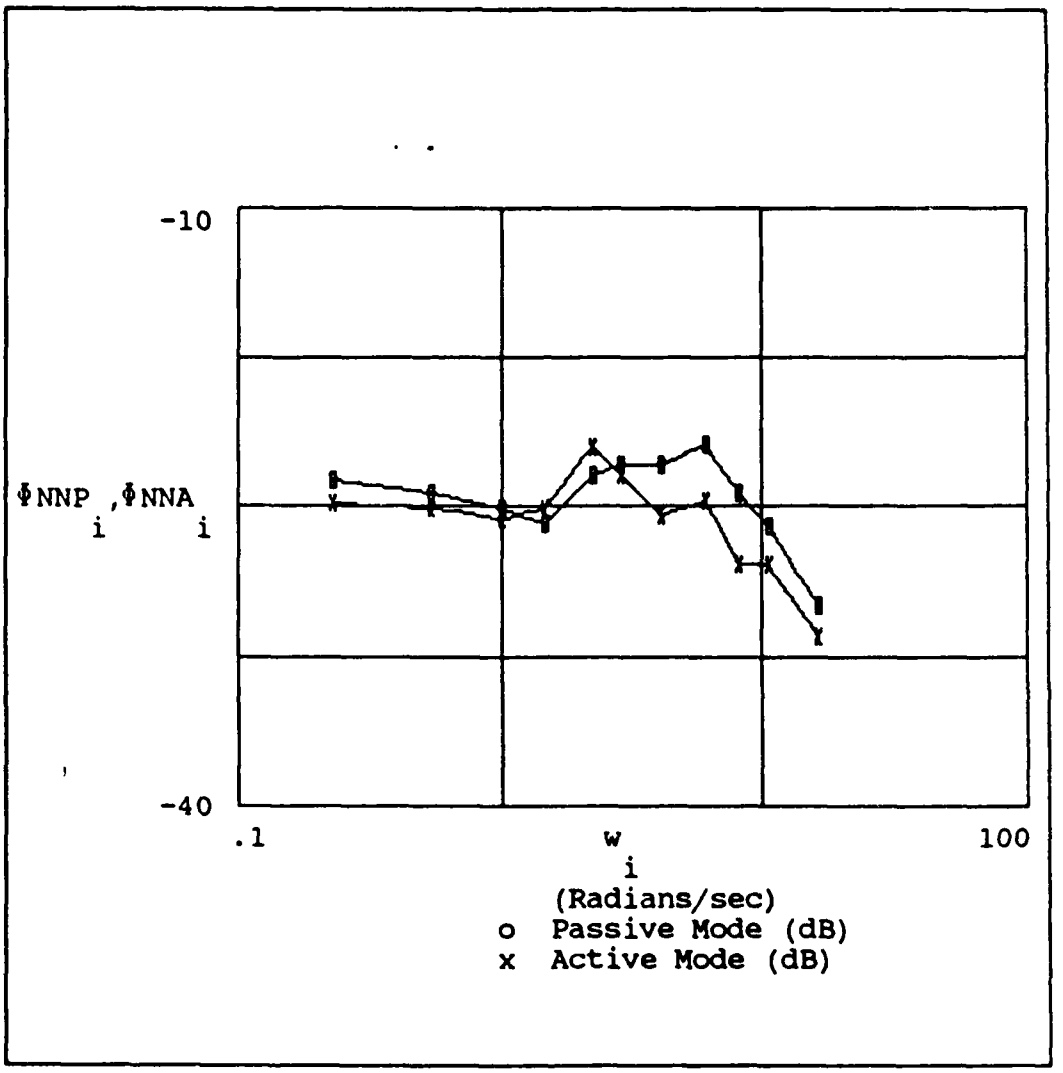

Figure D-2. Operator Noise (FF #1)

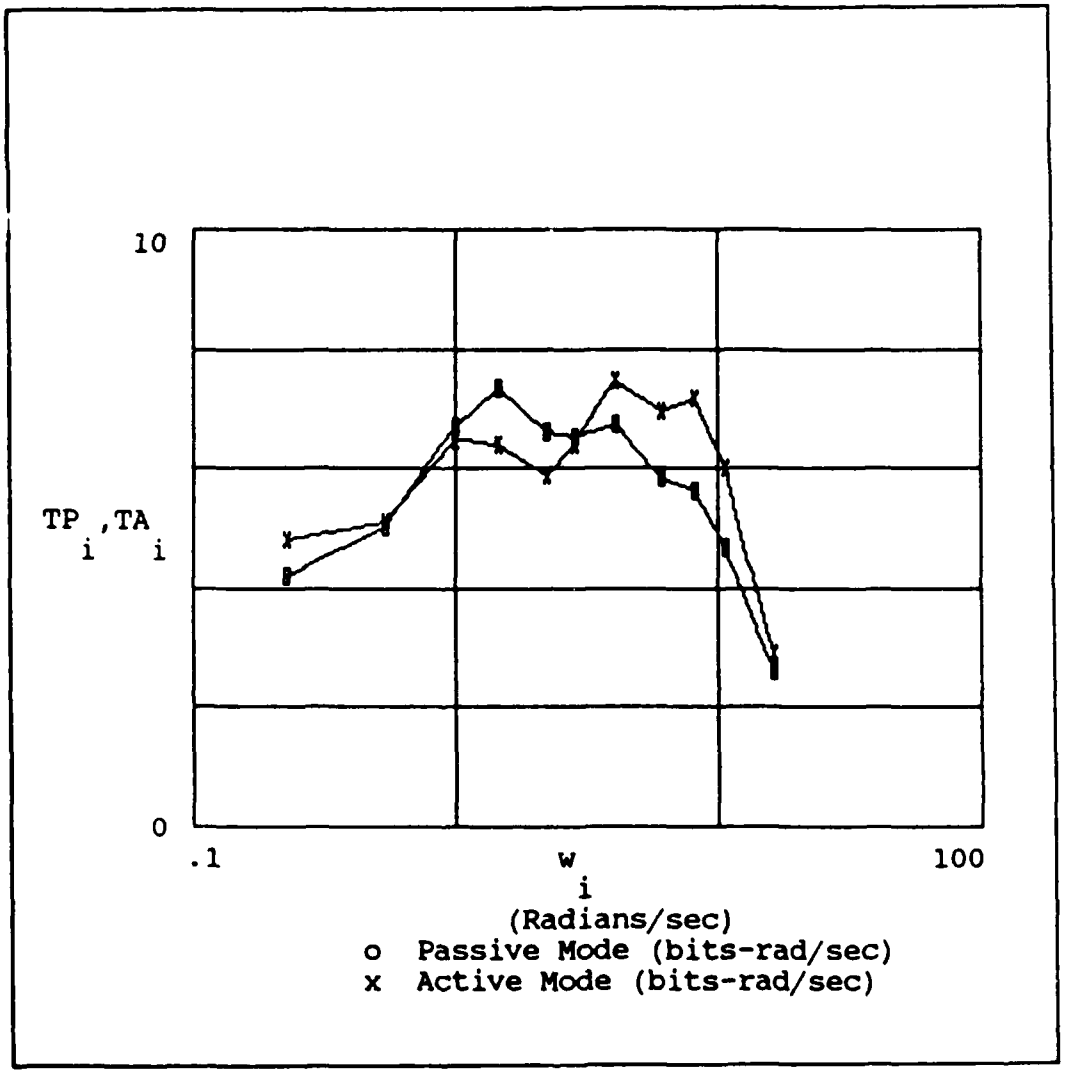

Figure D-3. Transinformation Rate (FF #1)

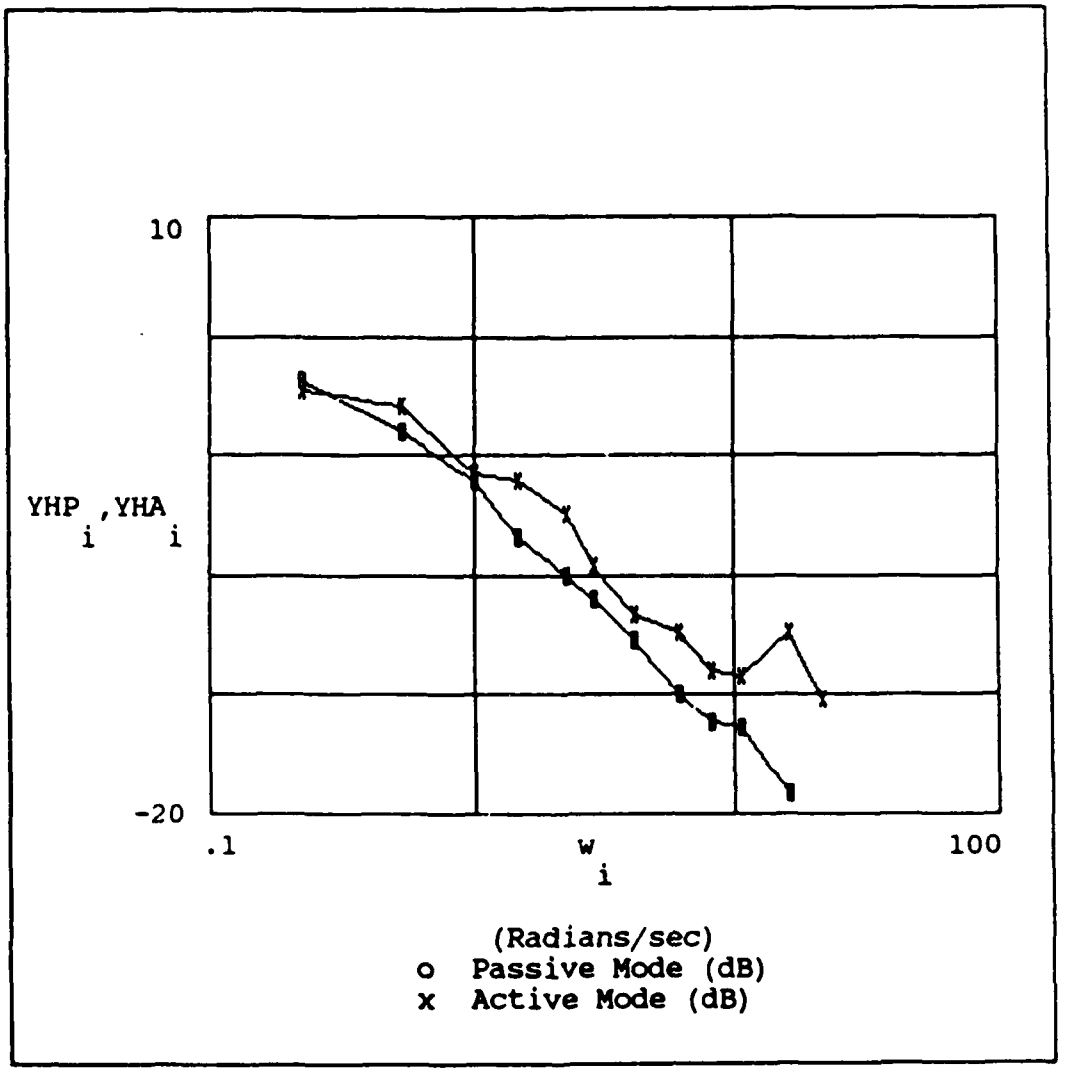

Figure D-4. Human Transfer Function (FF #2)

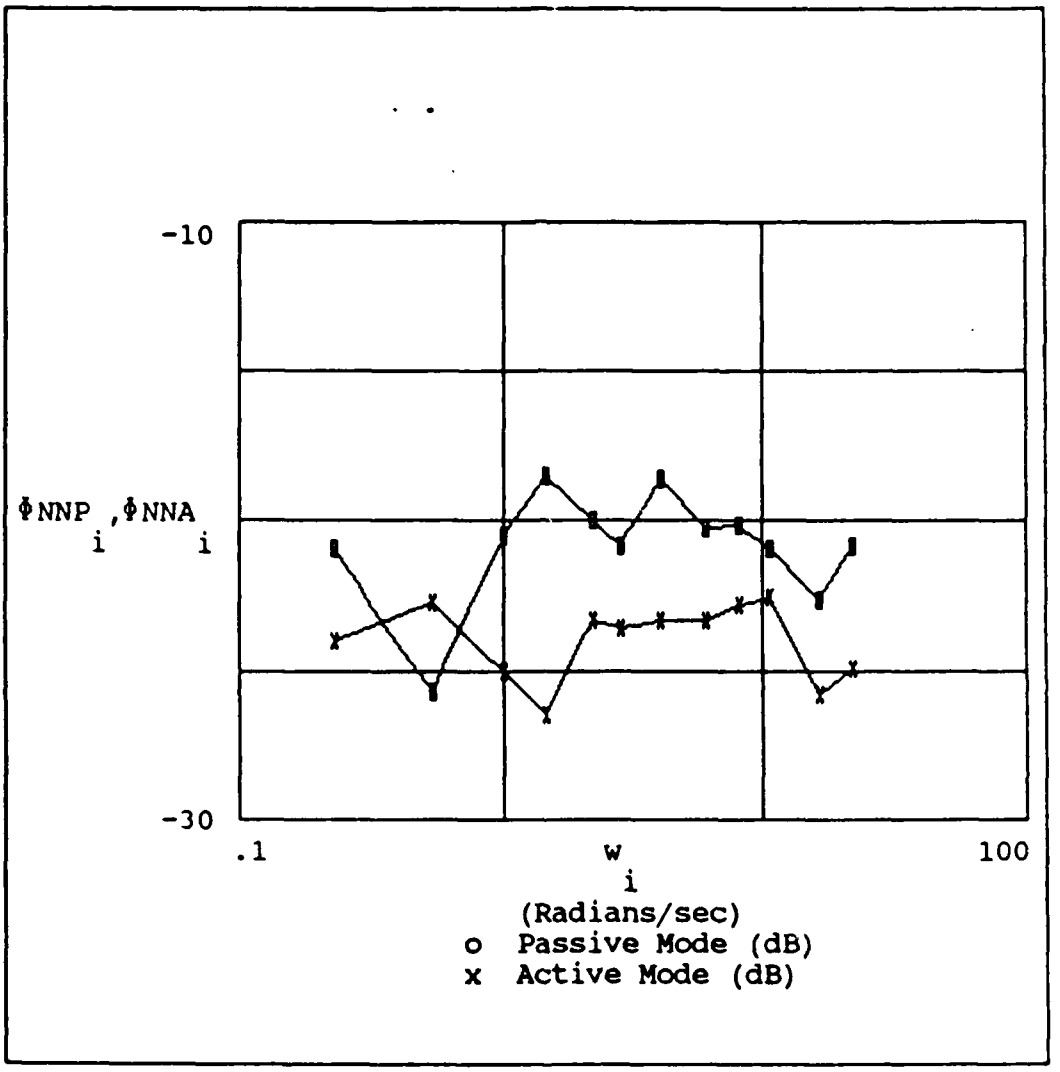

Figure D-5. Operator Noise (FF #2)

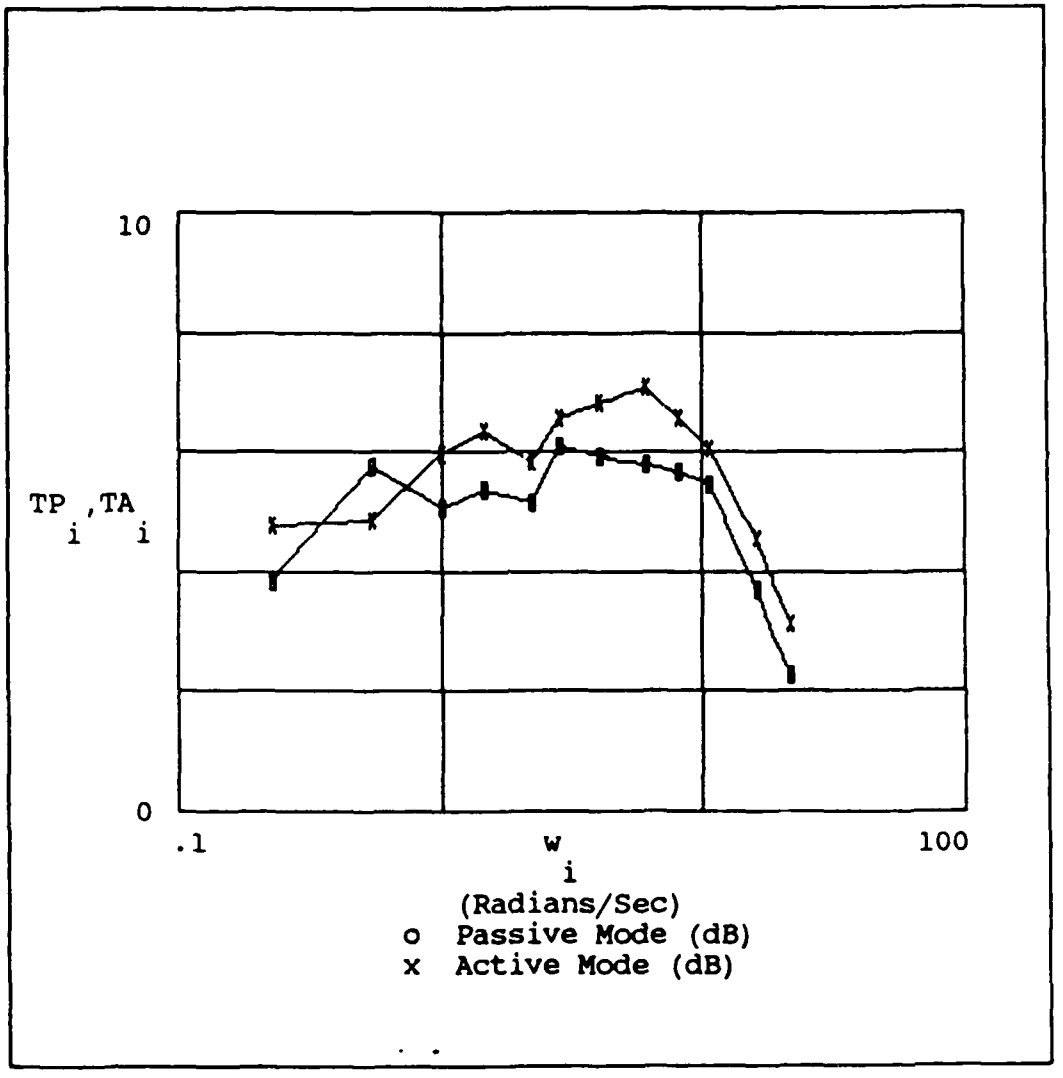

Figure D-6. Transinformation Rate (FF #2)

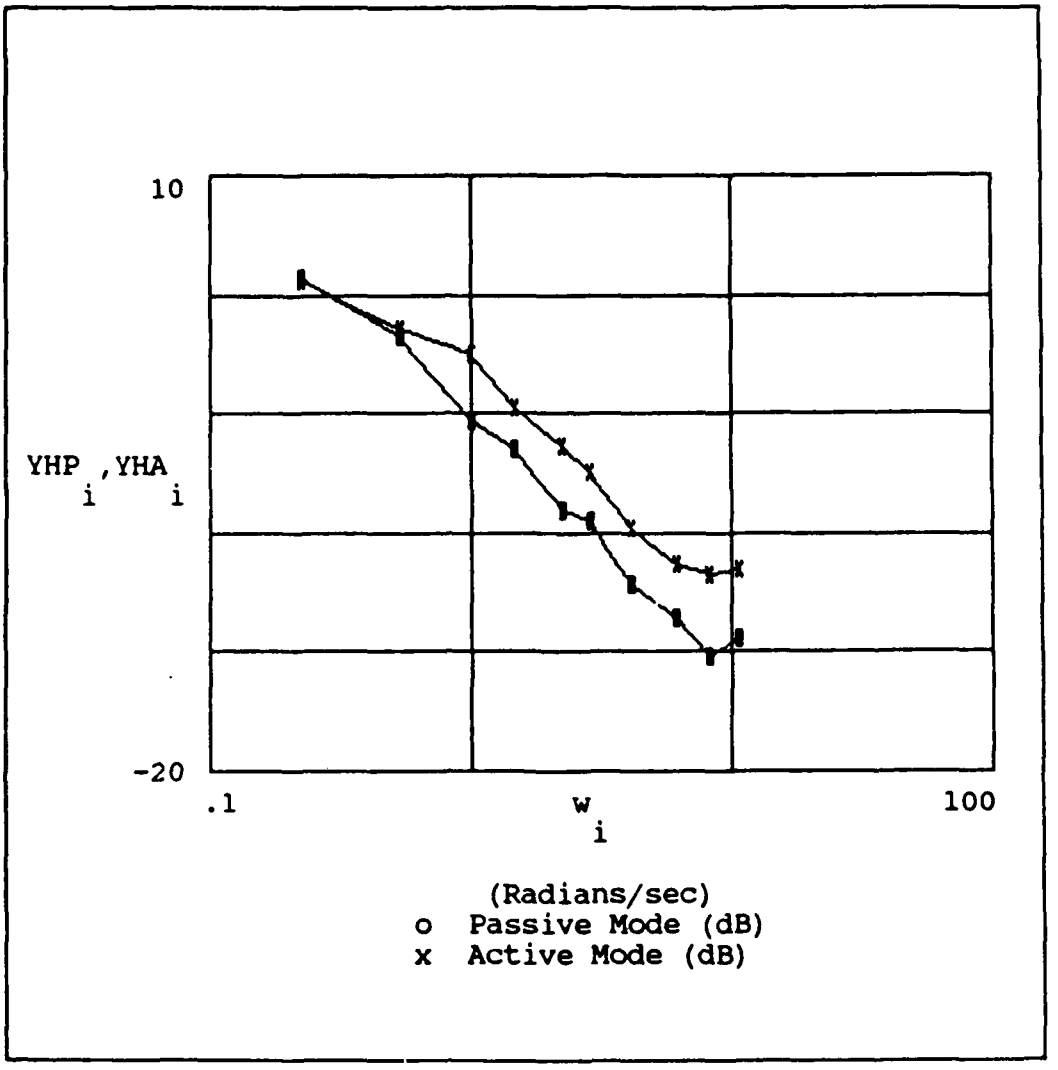

Figure D-7. Human Transfer Function (FF #3)

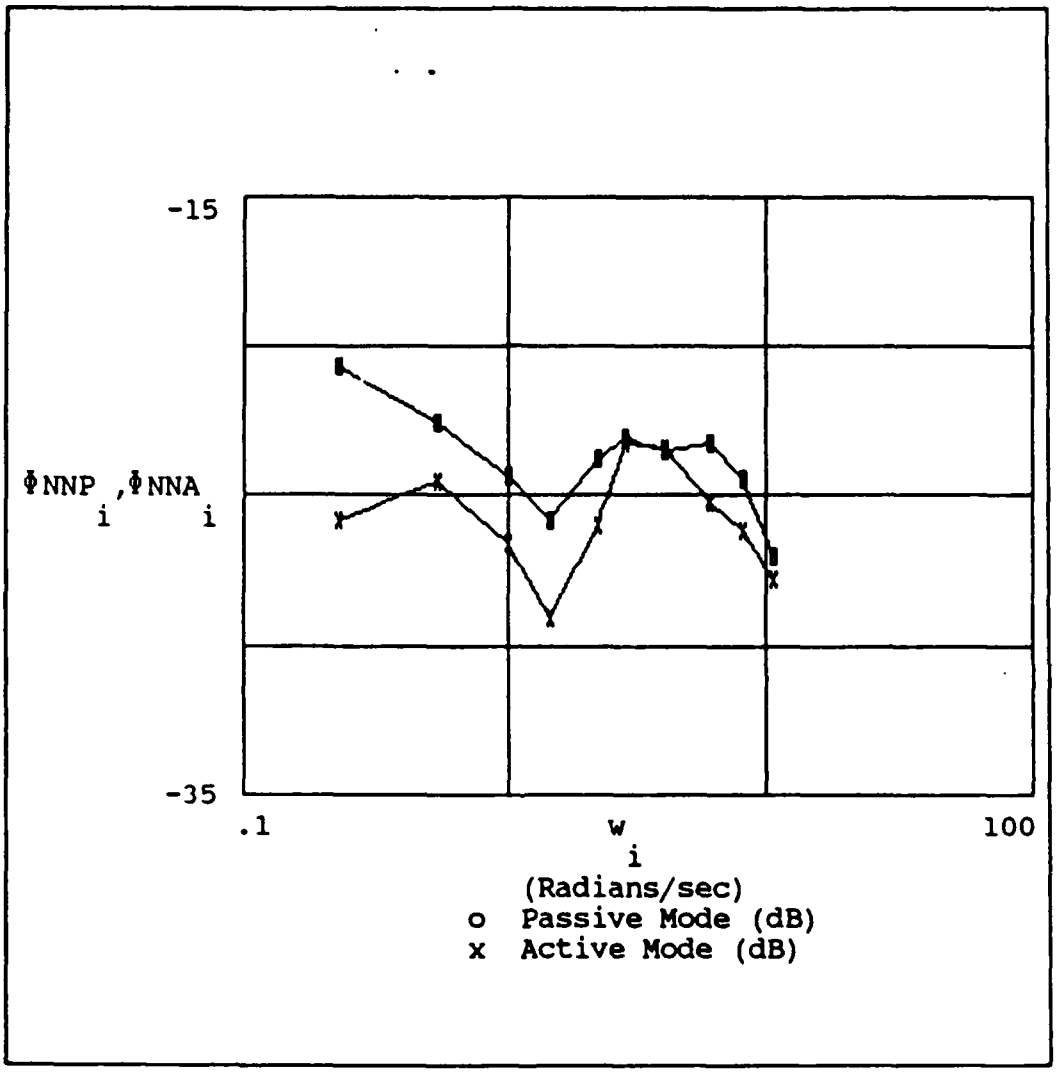

Figure D-8. Operator Noise (FF #3)

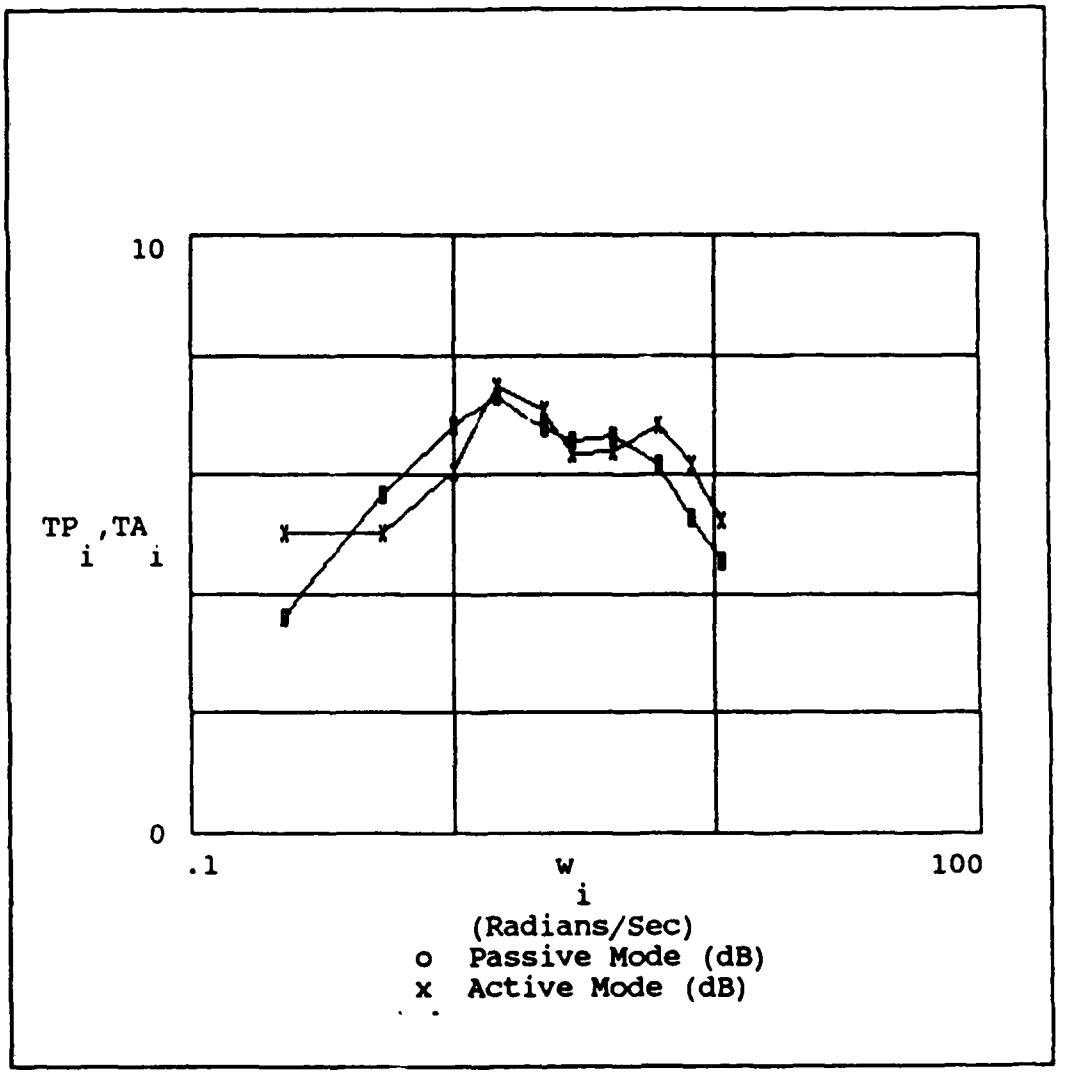

Figure D-9. Transinformation Rate (FF #3)

Appendix E. Graphical Representation of Experimental Results (Subject #6)

This appendix contains the experimental results obtained by testing subject #6. Each graph consists of a visual comparison of the active and passive modes of operation for the human transfer function, the noise remnant, and the transinformation rate for the three forcing functions.

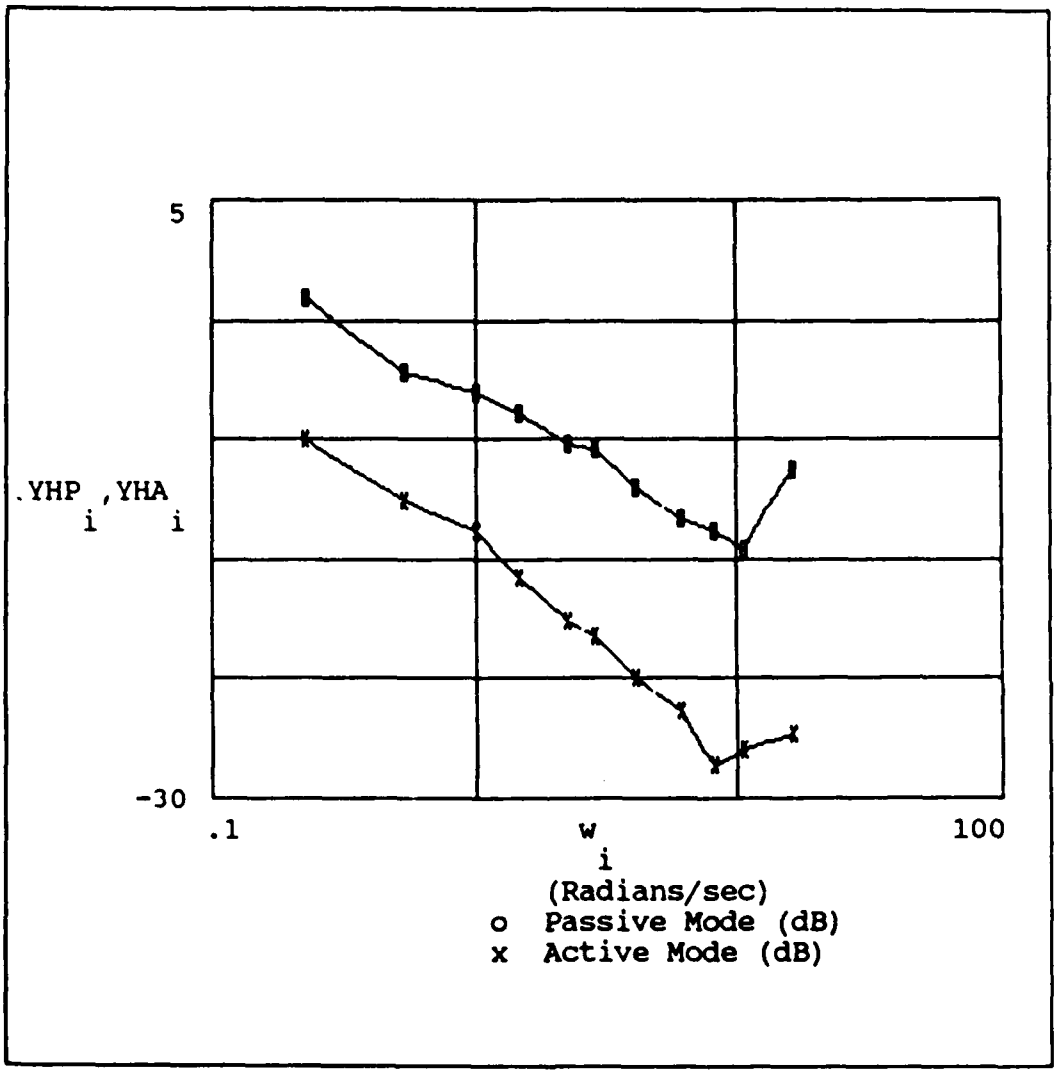

Figure E-1. Human Transfer Function (FF #1)

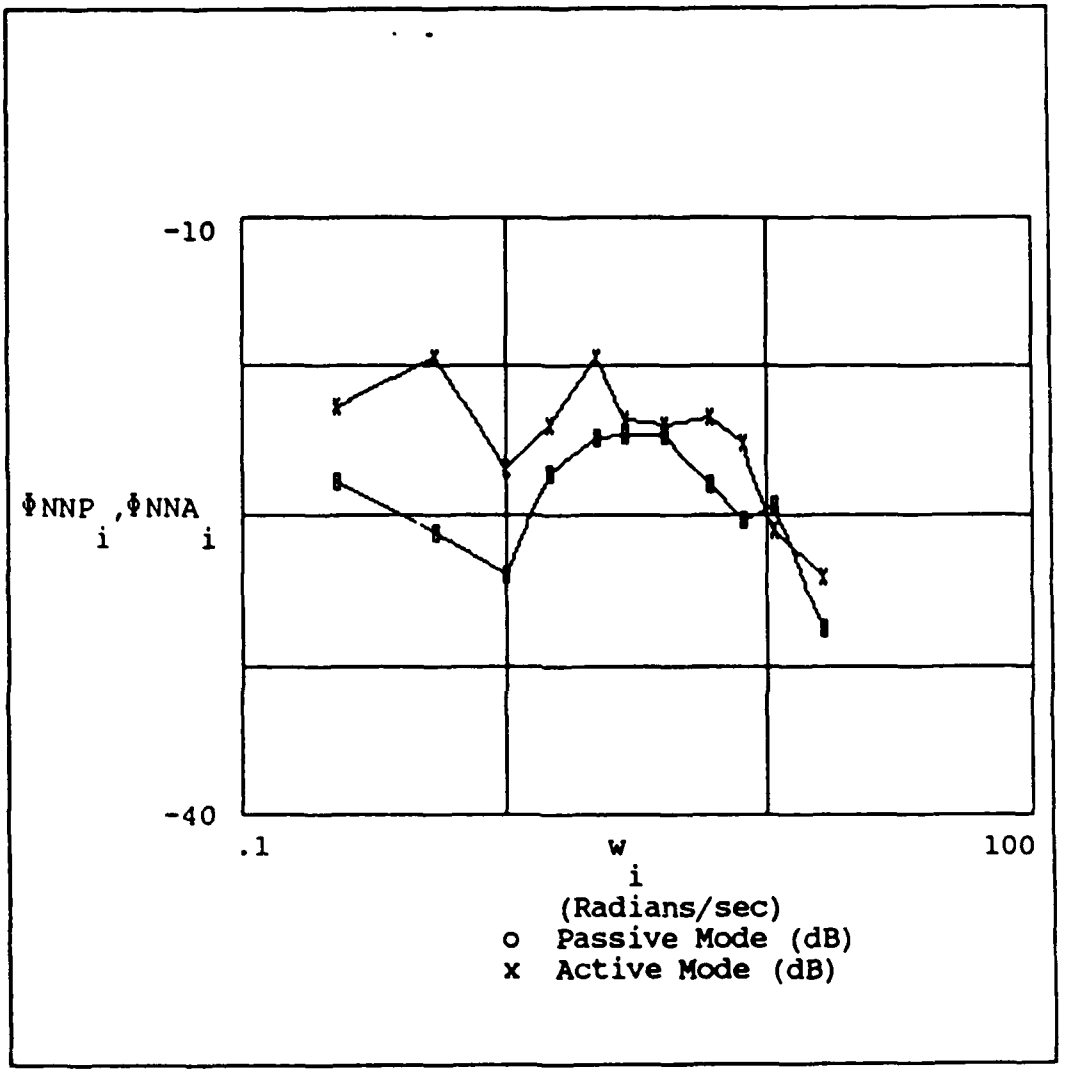

Figure E-2. Operator Noise (FF #1)

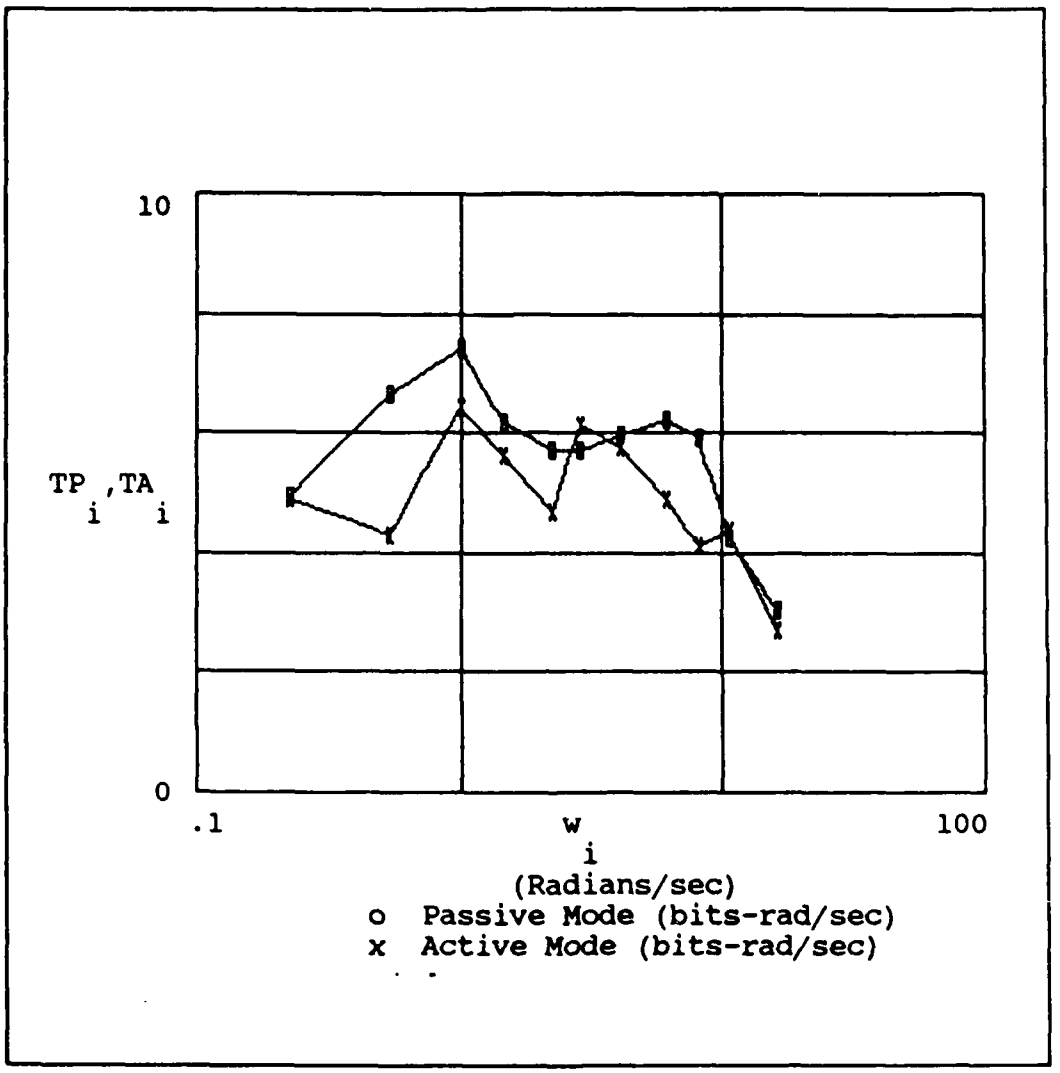

Figure E-3. Transinformation Rate (FF #1)

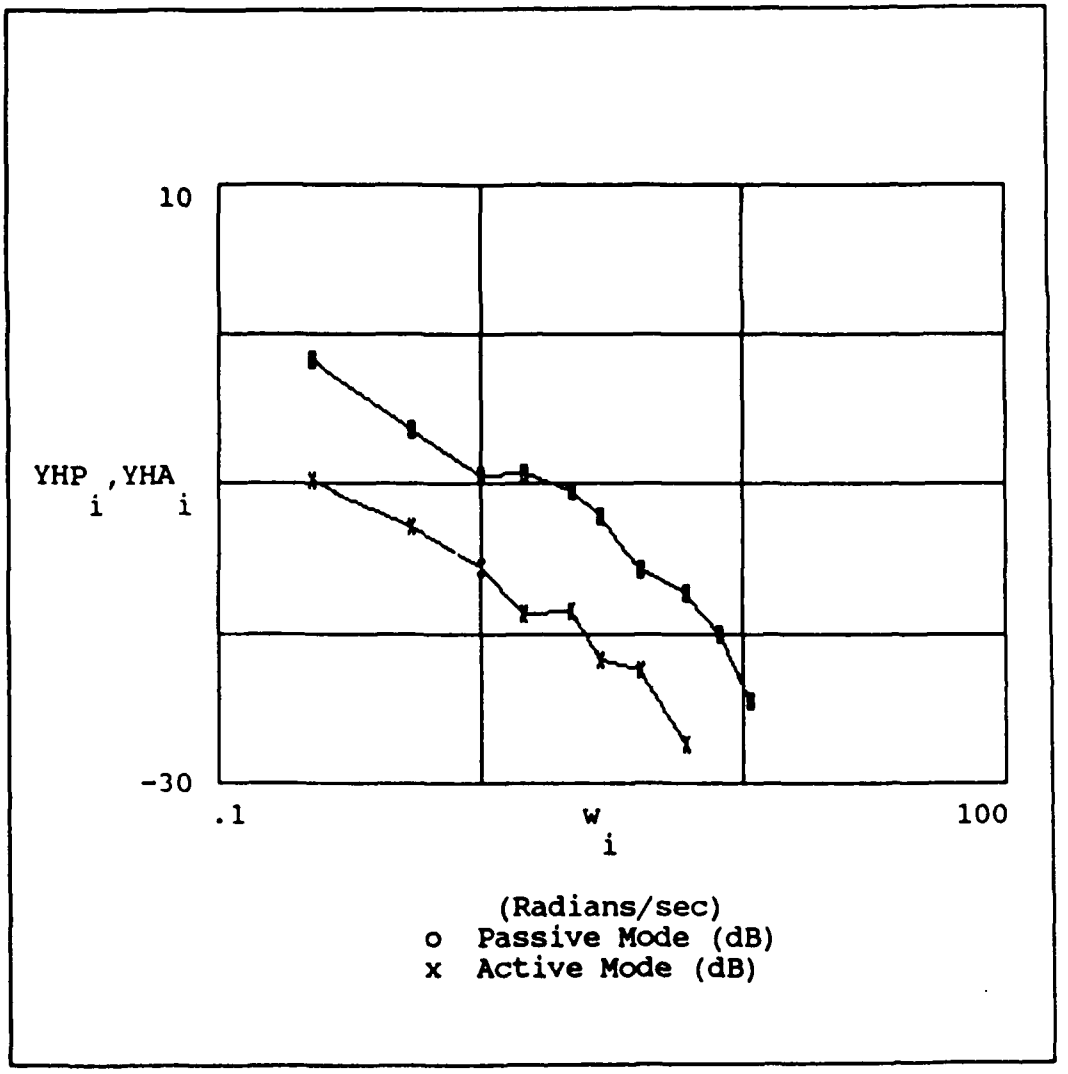

Figure E-4. Human Transfer Function (FF #2)

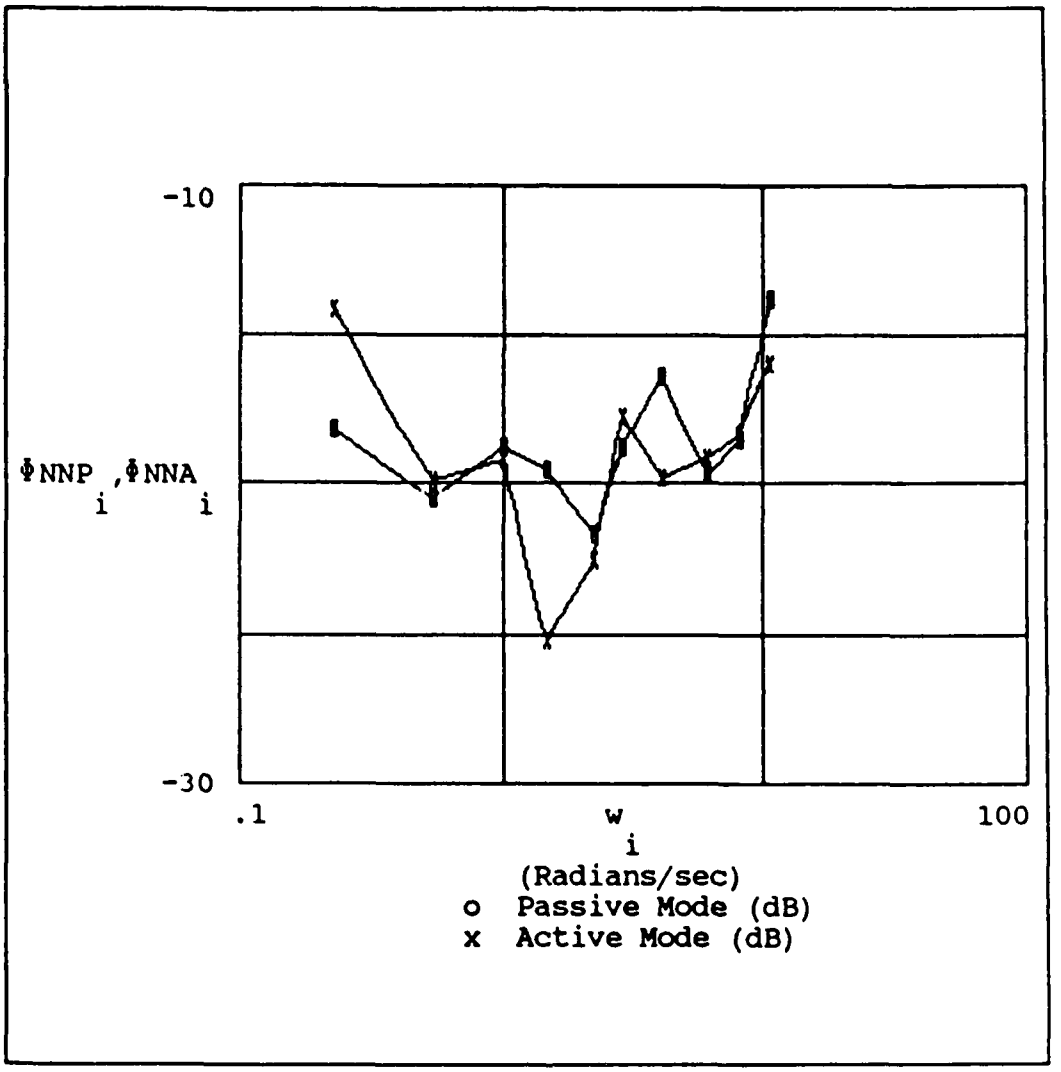

Figure E-5. Operator Noise (FF #2)

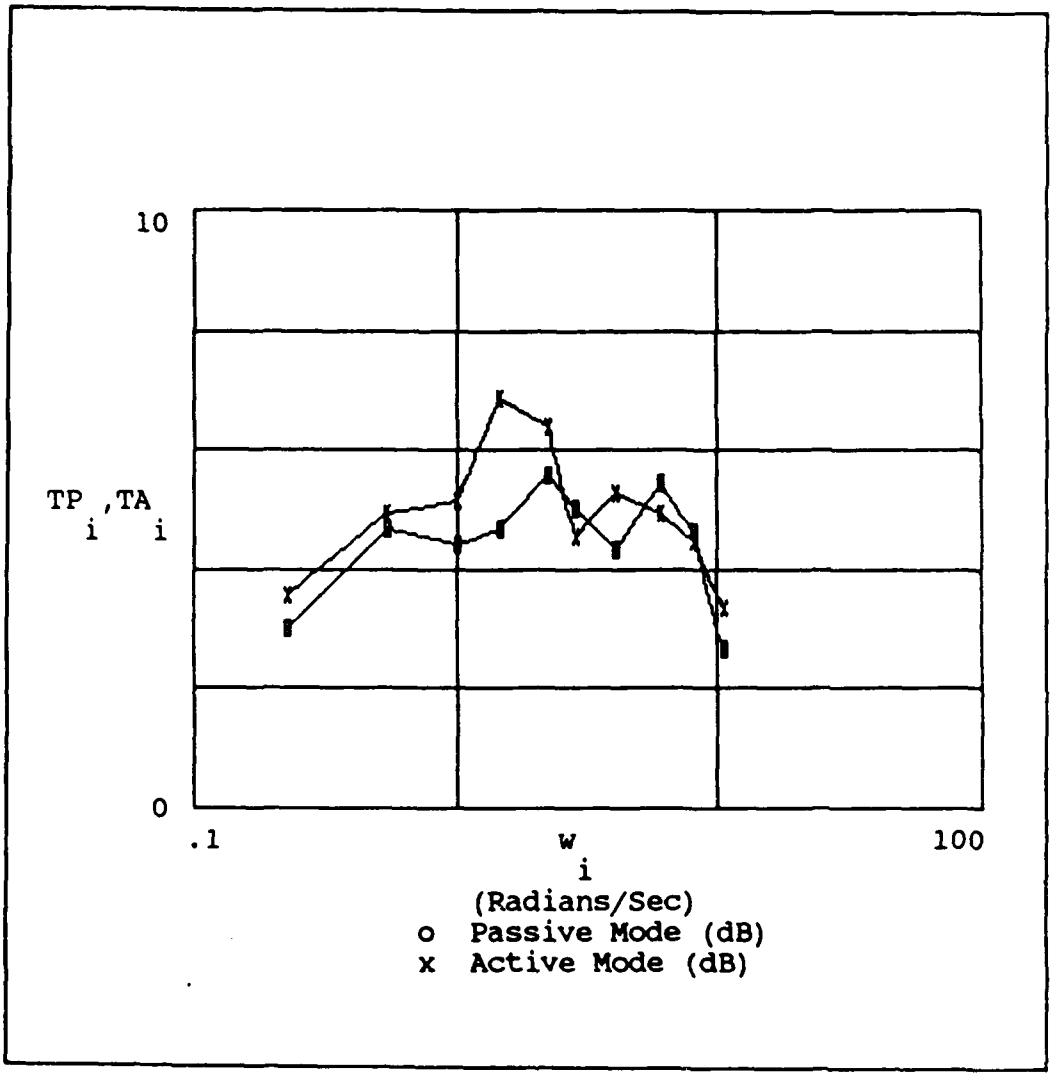

Figure E-6. Transinformation Rate (FF #2)

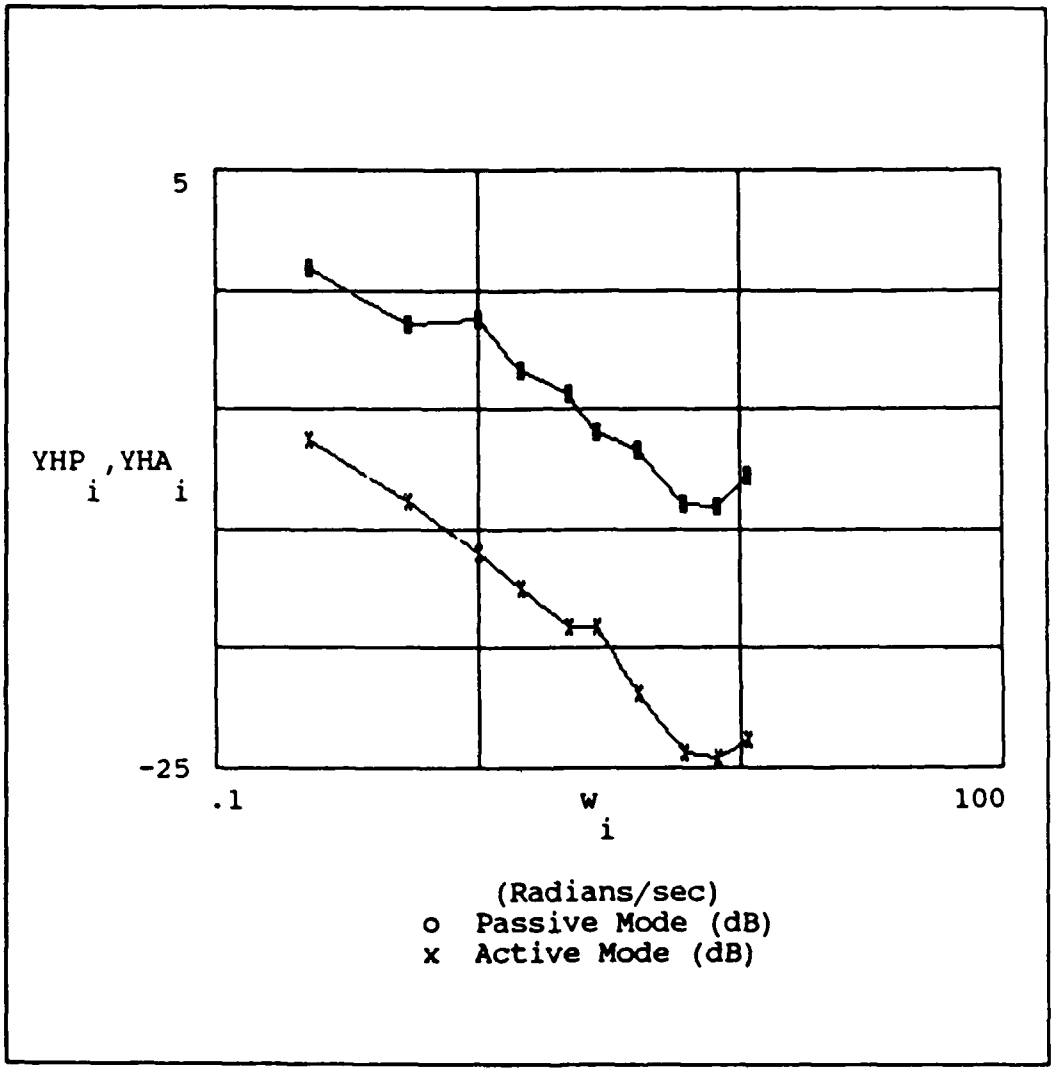

Figure E-7. Human Transfer Function (FF #3)

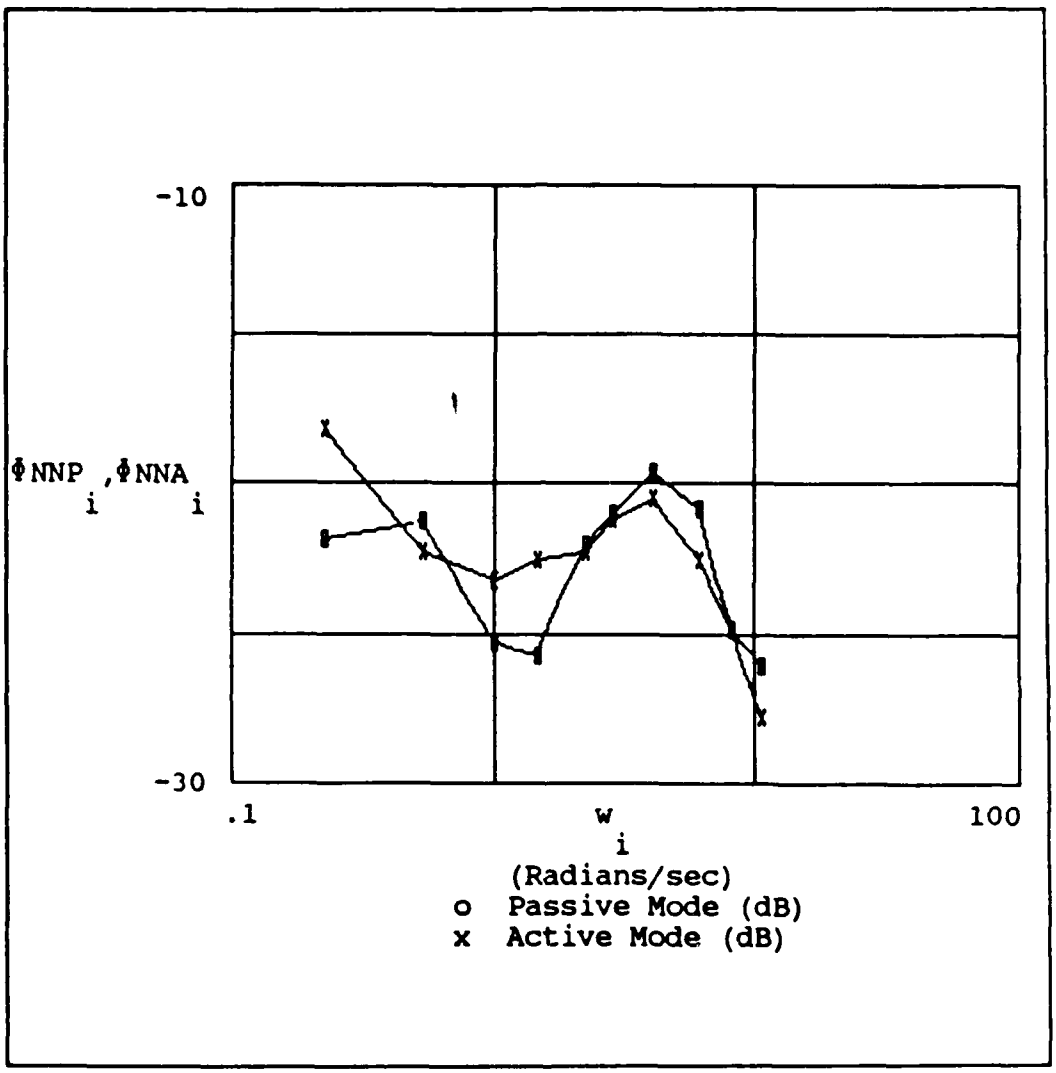

Figure E-8. Operator Noise (FF #3)

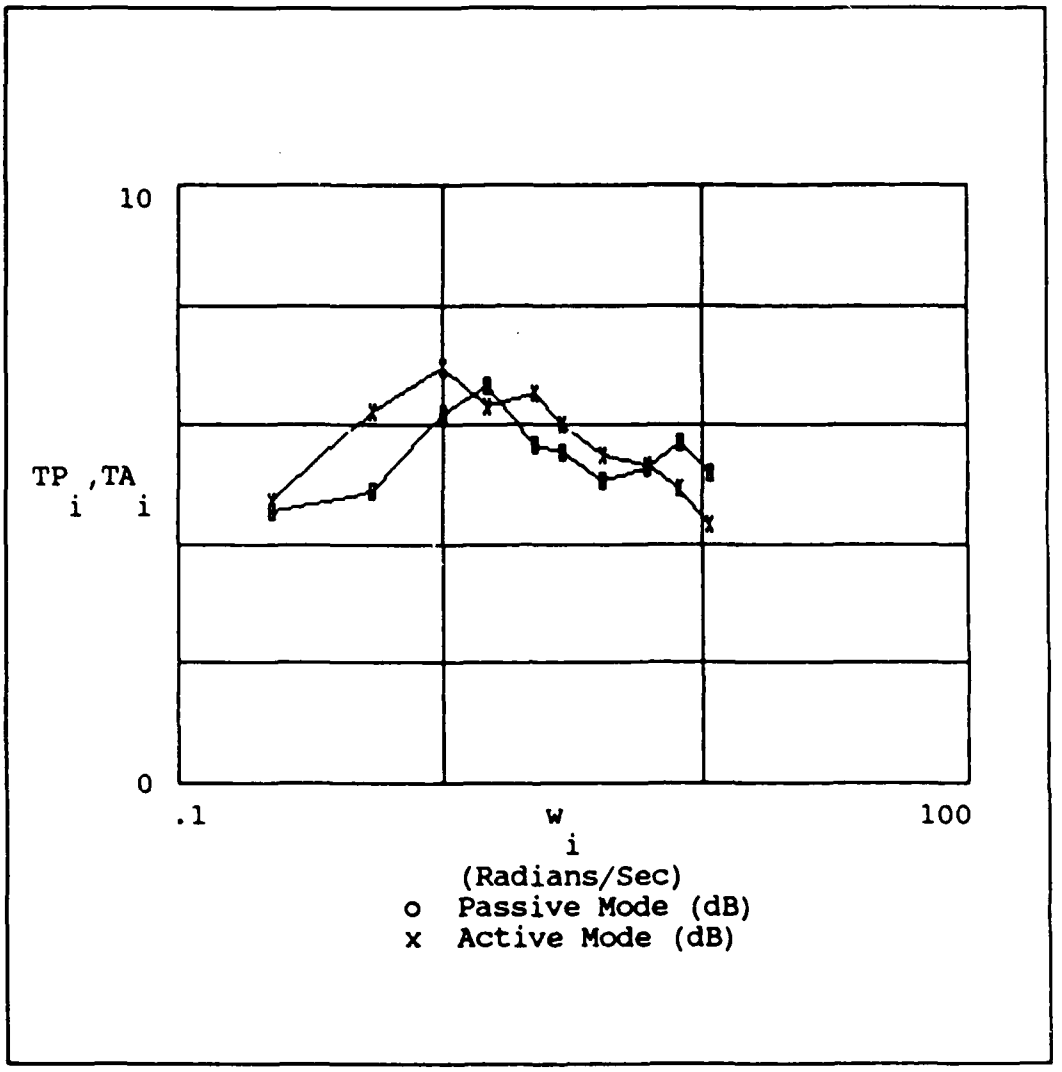

Figure E-9. Transinformation Rate (FF #3)

Bibliography

1. Blahut, Richard E. Principles and Practice of Information Theory. Reading, MA: Addison-Wesley Publishing Company, 1987.

2. Crossman, E.R.F.W. "The Information Capacity of Human Motor System in Pursuit Tracking", The Quarterly Journal of Experimental Psychology. Volume XII, Part I: 1-16 (1960).

3. Fitts, Paul M. and Posner, Michael I. Human Performance. Belmont, CA: Brooks/Cole Publishing Company, 1967.

4. Elkind, J.I. and Sprague,L.T. "Transmission of Information in Simple Manual Control Systems", IRE Transactions on Human Factors in Electronics, 58-60 (March 1961).

5. Levison, William H. et al. "A Model for Human Controller Remnant", IRE Transactions on Man-Machine Systems, 4: 101-108 (1969).

6. Levison, William H. Techniques for Data Analysis and Input Waveform Generation for Manual Control Research. Technical Memorandum CSD-75-2. Control Systems Department, Bolt Beranek and Newman, Inc, Cambridge, MA, January 1975.

7. McRuer, D.T. et al. Human Pilot Dynamics in Compensatory Systems: Theory, Models, and Experiments With Controlled-Element and Forcing Function Variations. AFFDL-TR-65-15. Wright-Patterson Air Force Base, OH, July 1965.

8. Repperger, D.W. and McCollor,D. "Active Sticks - A New Dimension in Controller Design", Proceedings of the 20th Annual Conference in Manual Control (June 1984).

9. Repperger, D.W. Controllers With Force and Position Prio-Prioceptive Feedback. Protocol 88-10, AAMRL, Wright-Patterson Air Force Base, OH (March 1988).

10. Sheridan, T.B. and Ferrell, W.R. Man-Machine Systems: Information, Control, and Decision Models of Human Performance. Cambridge, MA: MIT Press, 1974.

11. Wempe, T. and Baty, Y. "Usefulness of Transinformation as a Measure of Human Tracking Performance", Conference on Manual Control, pp 111-126 (circa 1966).

Vita

Adolfo Cozzone was born on [redacted] He graduated with great distinction from Lawrence High School, Lawrence, Massachusetts in 1974 and attended the University of Massachusetts from which he received a Bachelor in Physics and Mathematics in September 1978. He received a commission in the USAF from Officer Training School, Lackland AFB, Texas in May 1979. After completing the Communications Electronics course at Keesler AFB, Mississippi he was assigned to the 2152 Communications Squadron, Grand Forks AFB, North Dakota, as the Maintenance Control Officer. In June 1982 he was selected for assignment to the Air Force Institute of Technology, Civilian Institute Program and attended the Georgia Institute of Technology from which he received a Bachelor of Electrical Engineering in June 1984. Upon graduation, he was assigned to Headquarter Strategic Communication Division and served as Strategic Communication Engineer in the Technology Assessment Directorate until his assignment to the School of Engineering, Air Force Institute of Technology, in June 1987. He is a member of Sigma Pi Sigma.

[redacted]

UNCLASSIFIED
SECURITY CLASSIFICATION OF THIS PAGE

ADA202712

REPORT DOCUMENTATION PAGE

Form Approved
OMB No. 0704-0188

1a. REPORT SECURITY CLASSIFICATION UNCLASSIFIED	1b. RESTRICTIVE MARKINGS
2a. SECURITY CLASSIFICATION AUTHORITY	3. DISTRIBUTION/AVAILABILITY OF REPORT Approved for public release; Didtribution unlimited
2b. DECLASSIFICATION/DOWNGRADING SCHEDULE	
4. PERFORMING ORGANIZATION REPORT NUMBER(S) AFIT/GE/ENG/88D-7	5. MONITORING ORGANIZATION REPORT NUMBER(S)
6a. NAME OF PERFORMING ORGANIZATION School of Engineering 6b. OFFICE SYMBOL (If applicable) AFIT/ENG	7a. NAME OF MONITORING ORGANIZATION
6c. ADDRESS (City, State, and ZIP Code) Air Force Institute of Technology Wright-Patterson AFB OH 45433-6583	7b. ADDRESS (City, State, and ZIP Code)
8a. NAME OF FUNDING/SPONSORING ORGANIZATION 8b. OFFICE SYMBOL (If applicable)	9. PROCUREMENT INSTRUMENT IDENTIFICATION NUMBER
8c. ADDRESS (City, State, and ZIP Code)	10. SOURCE OF FUNDING NUMBERS PROGRAM ELEMENT NO. / PROJECT NO. / TASK NO / WORK UNIT ACCESSION NO.
11. TITLE (Include Security Classification) See item 19	
12. PERSONAL AUTHOR(S) Adolfo Cozzone, B.E.E., Captain, USAF	
13a. TYPE OF REPORT MS Thesis 13b. TIME COVERED FROM _____ TO _____	14. DATE OF REPORT (Year, Month, Day) 15. PAGE COUNT 140
16. SUPPLEMENTARY NOTATION	

17. COSATI CODES		
FIELD	GROUP	SUB-GROUP
23	02	
12	09	

18. SUBJECT TERMS (Continue on reverse if necessary and identify by block number)
Capacity, Transinformation, Control Stick, Control System Information Theory, Control Theory, Performance (Human)

19. ABSTRACT (Continue on reverse if necessary and identify by block number)

CAPACITY OF HUMAN OPERATOR

USING

SMART STICK CONTROLLER

Thesis Chairman: David M. Norman, Major, USAF

20. DISTRIBUTION/AVAILABILITY OF ABSTRACT ☒ UNCLASSIFIED/UNLIMITED ☐ SAME AS RPT. ☐ DTIC USERS	21. ABSTRACT SECURITY CLASSIFICATION
22a. NAME OF RESPONSIBLE INDIVIDUAL David M. Norman, Major, USAF	22b. TELEPHONE (Include Area Code) (513) 255-3576 22c. OFFICE SYMBOL AFIT/ENG

DD Form 1473, JUN 86 *Previous editions are obsolete.*

SECURITY CLASSIFICATION OF THIS PAGE
UNCLASSIFIED

This research provides an analysis of transinformation rate and capacity for six subjects using the smart stick controller. The subjects were tested in both a passive and active stick mode using three different forcing functions. The smart stick controller is an aircraft stick actively controlled by an algorithm developed by the Armstrong Aerospace Medical Research Laboratory (AAMRL) at Wright-Patterson AFB, OH to improve pilot tracking performance. In the passive mode, the stick behaves as any other stick used to control aircraft. However, in the active mode, the stick exerts a force in the direction opposite to the desired motion.

This thesis reviews the literature, develops and analyzes a compensatory tracking task using classical control theory, and applies information theory results to the human quasi-linear model to determine the transinformation rate and capacity of the human operator. Finally, the results for both the active and passive mode are compared. Power spectral densities of the forcing functions, display error, and human response are used to calculate the human transfer function, noise remnant, transinformation rate and capacity. Initial results indicate that there is an increase in the capacity of the operator between passive and active stick mode. The results indicate that, for four of the six subjects, the capacity increases under all three forcing functions. The highest capacity achieved was 11.34 bits/sec using the stick in the active mode. When information on capacity is used in conjunction with noise remnant, and human transfer function, it is evident that a significant change in performance occurs when the stick is operated in the active mode.